

**Understanding Tree Water Use Across the Snow-Rain Transition in Idaho's  
Mountain Watersheds: Interactions Between Stream Networks, Transpiration, and  
Basin Geomorphology**

by

John Whiting

A thesis

Submitted in partial fulfillment

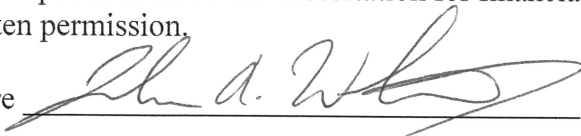
of the requirements for the degree of

Master of Science in the Department of Geosciences

Idaho State University

Summer 2015

In presenting this dissertation in partial fulfillment of the requirements for an advanced degree at Idaho State University, I agree that the Library shall make it freely available for inspection. I further state that permission to download and/or print my dissertation for scholarly purposes may be granted by the Dean of the Graduate School, Dean of my academic division, or by the University Librarian. It is understood that any copying or publication of this dissertation for financial gain shall not be allowed without my written permission.

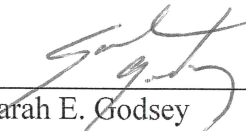
Signature 


Date 9/1/2015

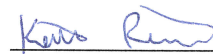
## Committee Approval

To the Graduate Faculty:

The members of the committee appointed to examine the thesis of JOHN ANTONELLI WHITING find it satisfactory and recommend that it be accepted.

  
\_\_\_\_\_  
Sarah E. Godsey  
Major Advisor

  
\_\_\_\_\_  
Glenn D. Thackray  
Committee Member

  
\_\_\_\_\_  
Keith Reinhardt  
Graduate Faculty Representative

## Acknowledgments

I would first like to thank Dr. Sarah Godsey for granting me the opportunity to work on this incredible project in the Frank Church-River of No Return Wilderness. Without Sarah's advice, support, and persistence, this project would not have been possible. Dr. Keith Reinhardt provided essential expertise on sap flow sensors and subsequent analysis. I also appreciated Dr. Glenn Thackray's knowledge of Idaho glaciations and hydrology.

In addition to my committee, this project was possible due to the efforts of numerous lab and field assistants. Tess Gardner, Kim Archibald, and Dylan Refaey became expert Granier sensor builders. Nate Tillotson, Jesse Bennet, and Bryan Tikalsky risked life and limb to build our sap flow monitoring infrastructure in the wilderness. Chris Connors, Arte Rosales, and Kate Wilcox also became familiar with the rigors of sap flow fieldwork on subsequent maintenance undertakings.

I relied on the humor and wisdom from the 2014-2015 ISU Geosciences cohort, especially those in the Galena Pod; my housemates, Holly Young, Amie Staley, and Doug MacLeod; the Reinhardt Lab; and the Godsey Lab, especially Chris Tennant and Caitlin Rushlow; and my parents, Ken and Loretta Whiting. Pete, Meg, and Tehya Gäg, the University of Idaho's Taylor Wilderness Research Station managers, supported this research enormously, but I am most grateful for their familial care and embrace throughout my time in the wilderness. I could not have asked for a more inspirational group to spend a Taylor Ranch summer with than the 2014 Big Creek 'branch' of the Baxter Stream Ecology Team, Dr. Colden Baxter, Dr. G. Wayne Minshall, Matt Schenk, Adam "Lunchbox" Eckersell, and Mirjam Scharer; the Idaho Fish and Game screw trap technicians, Bryce Oldemeyer and Chris Pike; and the Taylor Ranch Summer Interns, Sarah Rose, Dakotah Smith, Arte Rosales, Landon Schofield, Erik Robertson, Kate Wilcox, and their associated faculty and mentors.

I would like to thank the financial sponsors of this project: Sigma Xi, The Geslin Fund, NSF EPSCoR WRCC, Idaho State University, and the DeVlieg Foundation. The Frank Church-River of No Return Wilderness is an immense although elusive resource in every academic, spiritual, and physical sense. I am especially grateful to Taylor Ranch and the DeVlieg Foundation's commitment to introducing students to this special place in Idaho and encouraging a complete appreciation of wilderness.

## Table of Contents

List of Figures .....	viii
List of Tables .....	x
Abstract.....	xi
Chapter 1 Introduction .....	1
1.1 Problem Statement.....	1
1.2 Watershed Storage Background.....	1
1.2.1 Semi-arid Watersheds of the Intermountain West.....	1
1.2.2 Transpiration.....	2
1.2.3 Stream Networks.....	5
1.2.4 Streamflow Recession and Catchment Storage .....	7
1.3 Study Area and Methods.....	10
1.3.1 Big Creek Watershed .....	10
1.3.2 Quantifying Transpiration with Sap Flow .....	12
1.3.3 Measuring Stream Discharge.....	13
1.3.4 Surface Network Mapping.....	13
1.4 Thesis Organization and Objectives .....	13
References.....	15
Chapter 2 Understanding plant water use across the snow-rain transition, Salmon River Basin, Idaho .....	21
Abstract.....	21
2.1 Introduction.....	21

2.2	Study Area and Methods.....	24
2.2.1	Big Creek Watershed .....	24
2.2.2	Using Sap Flow to Quantify Transpiration.....	26
2.2.2.1	Sap Flow Uncertainties .....	28
2.2.2.2	Sap Flow Sites .....	30
2.2.2.3	Normalization .....	32
2.3	Results and Discussion .....	34
2.3.1	Vapor Pressure Deficit and Sap Flow.....	34
2.3.2	Soil Moisture and Sap Flow.....	39
2.3.3	Sap Flow Between Elevation Bands.....	44
2.4	Conclusion .....	47
	References.....	50
	Chapter 3 Discontinuous mountain headwater stream networks with stable flowheads, Salmon River Basin, Idaho. ....	54
	Abstract.....	54
3.1	Introduction.....	55
3.2	Study Area and Methods.....	57
3.2.1	Big Creek Watershed .....	57
3.2.2	Surface network mapping.....	59
3.2.2.1	Partitioning Active Stream Length Fluctuation .....	61
3.2.2.2	Flowhead Stability .....	61
3.2.3	Measuring discharge.....	62
3.3	Results and Discussion .....	64

3.3.1	Stream length to discharge relationships .....	64
3.3.2	Geologic and Geomorphic Influence on Surface Flow Extent .....	70
3.3.2.1	Geology and Springs.....	70
3.3.2.2	Flowhead Stability and Accumulation Area .....	72
3.3.2.3	Elevation and Aspect and Flowhead Stability .....	76
3.3.2.4	Geology and Stream Length Fluctuations.....	80
3.3.2.5	Local Hillslope Geomorphology and Flowhead Stability .....	82
3.3.3	Streamflow recession .....	85
3.4	Conclusions.....	86
	References.....	89
Chapter 4	Conclusions .....	93
4.1	Summary of Thesis Work .....	93
4.1.1	Sap Flow Across the Snow-Rain Transition.....	93
4.1.2	Active Drainage Network Summer Recession Dynamics .....	94
4.2	The Relationship between Trees and Streams .....	96
4.3	Opportunities for Future Work .....	101
	References.....	104
Appendix A	Suggestions for Similar Research .....	106
A.1	Quantifying Transpiration with Sap Flow .....	106
A.2	Measuring Stream Discharge.....	107
A.3	Surface Network Mapping.....	109
Appendix B	Granier-Style Thermal Dissipation Probes Assembly Protocol .....	111

## List of Figures

Figure 2.1: Pioneer Watershed Sap Flow Study Area Map.....	33
Figure 2.2: Vapor Pressure Deficit and Precipitation Time Series.....	37
Figure 2.3: Vapor Pressure Deficit versus Sap Flow Plots.....	38
Figure 2.4: 7/1/2014 Vapor Pressure Deficit Time Series.....	39
Figure 2.5: Soil Moisture and Sap Flow Diel Signals.....	42
Figure 2.6: Normalized Soil Water Content Time Series.....	43
Figure 2.7: Soil Water Content versus Sap Flow Plots.....	44
Figure 2.8: Sap Flow and Precipitation Time Series.....	46
Figure 2.9: Sap Flow versus Sap Flow Plots.....	47
Figure 3.1: High versus Low Flow Survey Active Drainage Network Map.....	67
Figure 3.2: Active Stream Length versus Runoff Plot.....	68
Figure 3.3: $\beta$ Histogram.....	69
Figure 3.4: Bedrock Geology of Lower Big Creek.....	71
Figure 3.5: Stream Stability End-Member Control Longitudinal Profiles.....	72
Figure 3.6: Flowhead Stability Diagrams.....	74
Figure 3.7: Fractional Gain in Flowhead Accumulation Area versus High Flow Initiation Accumulation Area Plot.....	75
Figure 3.8: Flowhead Stability and Topographic Map.....	79
Figure 3.9: Metasedimentary and Granodiorite Longitudinal Weathering Profiles.....	82
Figure 3.10: Fractional Gain in Flowhead Accumulation Area versus High Flow Flowhead Plan Curvature Plot.....	84
Figure 3.11: Pioneer Creek Hydrograph.....	86



Figure 4.1: Sap Flow and Stream Discharge Time Series. ....	100
Figure 4.2: Streamflow versus Sap Flow Plots. ....	101

## **List of Tables**

Table 3.1: Correction factors for the Pioneer Creek multiple linear regression model. ...	64
Table 3.2: Lower Big Creek tributary characteristics. ....	66

## Abstract

Warming climate is decreasing mountain snowpacks and melting these snowpacks earlier, which is causing lower peak streamflows and the earlier arrival of summer low flows. Warmer temperatures, less snow, and earlier melt also influence the timing and quantity of water availability for transpiration, which in turn impacts the watershed water balance. I assessed discharge, the spatial distribution of surface flow (i.e., active drainage network), and hillslope Douglas fir (*Pseudotsuga menziesii*) transpiration across rain and snow-dominated elevations within the lower Big Creek basin during the 2014 field season. In addition to using digital elevation models, meteorological data, and soil moisture data, I sought to determine if transpiration was different across the snow-rain transition, what controlled differences or similarities of transpiration across elevation, how the active drainage network responded to decreasing discharge, and if the spatial distribution of transpiration influenced spatial fluctuations of the active drainage network. I observed relatively little contraction of the active drainage network with decreasing discharge, and similar temporal patterns of transpiration across all elevations. The presented data suggests a weak connection between streamflow and Douglas fir transpiration. Discharge peaked during late May and rapidly declined, suggesting a seasonal hydrograph dominated by snowmelt, and stable active drainage networks suggest deep, bedrock-controlled supporting groundwater flowpaths. Douglas fir transpiration peaked around the same times as discharge although decreased at a much slower rate, and with surprisingly few differences across elevation, suggesting the primary influence of spring and summer rain events instead snowpack size and timing of melt.

## **Chapter 1 Introduction**

### **1.1 Problem Statement**

Warming and changing hydroclimate are expected to reduce mountain snow pack, increase evapotranspiration, and thus diminish the sometimes-limited water supplies of many streams and rivers in the Intermountain West (Stewart *et al.*, 2004; Barnett *et al.*, 2008). It remains uncertain how the timing and quantity of transpiration differ between snow-dominated and rain-dominated elevations, and how alterations in transpiration in these regions affect surface water flow in mountain stream networks.

### **1.2 Watershed Storage Background**

#### **1.2.1 Semi-arid Watersheds of the Intermountain West**

The Intermountain West of North America is characterized by rugged topography, complex geology, and an arid to semi-arid climate. Winters are cool and wet whereas summers are warm and dry, resulting in streamflows that are largely driven by spring and summer snowmelt from higher elevation mountain catchments (Knowles *et al.*, 2006; Stewart *et al.*, 2004). Vegetation assemblages are controlled by available water, nutrients, and energy, however in semi-arid climates vegetation communities primarily reflect water availability. Sagebrush steppe at warmer and drier low elevations contrasts with the cooler and higher elevation forested slopes of Ponderosa pine (*Pinus ponderosa*), Douglas fir (*Pseudotsuga menziesii*), Subalpine fir (*Abies lasiocarpa*) and Engelmann spruce (*Picea engelmannii*) that receive more rain and snow.

Warmer temperatures are expected to reduce the mountain snow packs critical to the water supplies of many intermountain communities and ecosystems (Knowles *et al.*,

2006; Tague and Grant, 2009). Hydrographs have already begun to shift as snow melts earlier in the spring and snowlines rise in elevation because more winter precipitation is falling as rain instead of snow (Barnett *et al.*, 2008; Stewart *et al.*, 2004). These changes in climate and hydrology influence freshwater aquatic and riparian ecosystems (Larned *et al.*, 2010), as well as wildfire frequency (Westerling *et al.*, 2006), which further impacts hillslope and aquatic ecosystems (Jackson *et al.*, 2012).

### **1.2.2 Transpiration**

Transpiration plays a critical role in catchment ecohydrology, with wide-ranging influence on streamflows (e.g., Graham *et al.*, 2013), spatial distribution of water storage (e.g., Godsey and Kirchner, 2014; Kirchner, 2009), ecosystem health and composition (e.g., Trujillo *et al.*, 2012), and wildfire susceptibility (e.g., Westerling *et al.*, 2006). Due to these motivations, numerous studies have attempted to measure and model watershed scale transpiration and to project changes in transpiration as a result of future climate change (e.g., Godsey *et al.*, 2013; Lundquist and Loheide, 2011; Tague *et al.*, 2009; Christensen *et al.*, 2008). Mountain watersheds of the western U.S. are of particular concern due to the importance of storage of winter precipitation in mountain snowpacks for the later release of meltwater during the warm and dry growing season (Stewart *et al.*, 2004; Knowles *et al.*, 2006). In this region, snowpacks and snowmelt drive the timing and quantity of water availability for plant water use as well as streamflow and groundwater infiltration (Stewart *et al.*, 2004; Barnett *et al.*, 2008), and the partitioning of snowmelt among these outlets is a central goal of recent models (Molotch *et al.*, 2009; Tague and Band, 2004).

Spatial heterogeneity of topography and climate within mountain watersheds result in variable snowpacks and transpiration that are difficult to accurately represent with distributed ecohydrologic models (Garcia *et al.*, 2013; Liston and Elder, 2006). Among these heterogeneities, elevation and temperature gradients are recognized as primary influences on snowpacks and transpiration (Goulden *et al.*, 2012; Trujillo *et al.*, 2012; Christensen *et al.*, 2008; McDowell *et al.*, 2008). At higher elevations, large persistent snowpacks lead to greater water availability for transpiration, however the cooler conditions that allow for snowpack accumulation also reduce potential transpiration. Thus, some models suggest transpiration should be greatest at intermediate elevations where temperatures are cool enough to permit snowpacks and greater water availability yet warm enough to maximize plant physiological activity (Lundquist and Loheide, 2011; Christensen *et al.*, 2008).

Intermediate elevations may also be the most susceptible to warming climate as snowpacks decrease and water limitations increase (Trujillo *et al.*, 2012). Trees at water-limited lower elevations have drought-resistant ecosystem structures, while energy-limited conditions at higher elevations may become increasingly favorable for transpiration and plant communities (Goulden *et al.*, 2012; Trujillo *et al.*, 2012). This conceptual model has implications for changes in catchment water balance, ecosystem composition and range (Goulden *et al.*, 2012). However, in many locations outside of the Sierra Nevada in California differences in transpiration across the snow-rain transition have yet to be confirmed in the field.

Shifts in transpiration may reduce or enhance the effects of earlier and reduced snowmelt on streamflow (Barnett *et al.*, 2005). A catchment-wide assessment of

transpiration is required for modeling effects on streamflow. Whether overall catchment transpiration increases or decreases with warming primarily depends on catchment hypsometry (Tennant *et al.*, 2015) and the relative timing of peak water availability and peak evaporative demand (Godsey *et al.*, 2013; Tague *et al.*, 2009). Furthermore, catchment ecohydrologic models should incorporate the hillslope and riparian flow dynamics that transmit the impacts of transpiration to the stream (Lundquist and Loheide, 2011; Emanuel *et al.*, 2010).

Transpiration influences streamflow, but the extent of influence is controversial. Diel cycles in streamflow with greater flow during periods of low potential evapotranspiration provide observational evidence of this link (Mutzner *et al.*, 2015; Graham *et al.*, 2013). By contrast, Brooks *et al.* (2010) observed seasonal patterns of water isotopes in soil and Douglas fir xylem and propose that in a Mediterranean climate, autumn rains refill small pore spaces in soils which trees access during the spring, following the primary drainage of winter precipitation. Infiltrating snowmelt and winter precipitation do not mix with waters in the small pore spaces filled by autumn rains. Instead winter precipitation leads to a short period of flow through large pores and preferential flow paths, which contributes heavily to streamflow but not transpiration (Brooks *et al.*, 2010).

Scaling tree transpiration up to watershed scales is also complicated because different species utilize different water sources within the unsaturated zone (Link *et al.*, 2014). Broadleaf species have deeper root networks than more shallow rooted needle-leaf species (Link *et al.*, 2014). Therefore, within the same watershed, or even stand, differing species composition likely mean variable water sources and hydrologic

processes supporting transpiration. Furthermore, within the same species, hydraulic redistribution of available water may maintain shallow soil moisture with sustained deeper water stores (Warren *et al.*, 2005; Meizner *et al.*, 2004).

Modeling work also suggests that decreasing late summer transpiration may maintain streamflows under a warming climate (Godsey *et al.*, 2013; Lundquist and Loheide, 2011; Tague *et al.*, 2009; Barnett *et al.*, 2005). However, modeling the effects of transpiration on streamflow is complicated. Flow dynamics during the relative timing of peak water availability and peak evaporative demand will determine the influence of transpiration on stream flow (Godsey *et al.*, 2013; Brooks *et al.*, 2010; Tague *et al.*, 2009). Transpiration will have little impact on flows if peak water availability and streamflow occur outside of the growing season, compared to when peak water availability coincides with peak evaporative demand and plants can utilize excess mobile water (Brooks *et al.*, 2010; Emanuel *et al.*, 2010). Thus, we must understand watershed storage characteristics that control streamflow dynamics in order to determine the susceptibility of streams to changes in transpiration.

### **1.2.3 Stream Networks**

As surficial expressions of groundwater conditions, streams provide accessible information regarding the spatiotemporal variability of subsurface storage (Biswal and Kumar, 2013; Bencala *et al.*, 2011; Kirchner, 2009). Headwater stream networks are particularly revealing as they expand and contract in response to individual precipitation events (Day, 1983 and 1978) and seasonal moisture conditions (Godsey and Kirchner, 2014; Roberts and Archibald, 1978; Blyth and Rodda, 1973; Roberts and Klingeman, 1972; Gregory and Walling, 1968). Each location where flow either surfaces or



infiltrates marks a point where flow matches the accommodation space of the subsurface. Thus, the expansion and contraction of the active stream network mirrors the spatial extent of subsurface water availability and flow characteristics (Godsey and Kirchner, 2014). We focus on the subsurface characteristics of the flow paths that support small, dynamic headwaters. Headwaters constitute most of the channel length of all stream networks (Bishop *et al.*, 2008; Leopold *et al.*, 1964), and thus are significant for managing water for human needs (e.g., Goyal *et al.*, 2015), riparian and terrestrial ecosystems (e.g., Jaeger *et al.*, 2014; Davis *et al.*, 2013), stream responses to wildfire (e.g., Wagner *et al.*, 2014), and other watershed ecosystem services.

In the research that follows, we focus on the ‘active drainage network,’ the dynamic network of flowing water visible at the surface. The extent and continuity of the active drainage network may fluctuate at any timescale depending on hydrological conditions, and may or may not coincide with the geomorphic channel network. Indeed, portions of flow may extend beyond the geomorphic channel. The geomorphic channel network constitutes the branched system of topographic features resulting from the erosion and deposition of channelized water, and therefore is related to the active drainage network. However, the geomorphic channel network is a stable landscape feature over the seasonal timescales during which we assess fluctuations in the active drainage network. Although the geomorphic channel network is stable during our study, channel initiation and maintenance require certain thresholds of flow to be surpassed (Montgomery *et al.*, 1997 and 2002; Montgomery and Dietrich, 1992). Channel networks allow the energy from these high flows to be efficiently dissipated (Rinaldo *et al.*, 2014; Tucker and Hancock, 2010). Instead of focusing on these high channel-

forming flows, we ask how the shape and characteristics of the subsurface and geomorphic network influences hydrologic surface expression over a range of seasonal flows.

From higher flows in May to low summer flows in early August, we witnessed more stable active drainage networks in the Lower Big Creek watershed than in many past studies (see Table 2 in Godsey and Kirchner, 2014). We noticed numerous spring and seep locations throughout these watersheds, where hillslope flow initiation was spatially stable. The role of groundwater, bedrock fracture flow paths, and springs is becoming increasingly recognized as an important source of streamflow (e.g., Gannon *et al.*, 2014; Zimmer *et al.*, 2013; Manning *et al.*, 2012; Rademacher *et al.*, 2005; Montgomery *et al.*, 2002). Even on steeper hillslopes with shallow soil layers, vertical percolation into bedrock and slower flow paths may significantly influence streamflow travel times and chemistry (Mueller *et al.*, 2014; Gabrielli *et al.*, 2012). Stable springs and seeps present a possible challenge for determining contributing source areas if the bedrock features controlling flow do not generally parallel topography (Welch and Allen, 2014). The complexity of hydrogeologic structure underlying and supporting catchments will influence our ability to model dynamics of the active drainage network.

#### **1.2.4 Streamflow Recession and Catchment Storage**

Streamflow recession analysis has long been recognized as a way to assess the catchment hydrological processes and aquifer characteristics that support streams (e.g., Boussinesq, 1877; Maillet, 1905). The procedure proposed by Brutsaert and Nieber (1977) using  $dQ/dt$  v.  $Q$  recession plots (i.e., plotting the rate of change in discharge for a given discharge) allows recession parameters to be applied to aquifer properties that

correspond with Dupuit-Boussinesq Theory (Tallaksen, 1995; Troch *et al.*, 2013). Stemming from these foundational works, there are many methods for assessing and modeling recession data to account for the variety of catchments and potential hydrological processes acting within these catchments. For a complete review, see Hall (1968), Tallaksen (1995), and Smakhtin (2001). Here I focus on two issues emphasized within the Tallaksen review (1995): subjective graphical separation of recession characteristics and the formation of master recession curves. Graphical separation is the attempt to assign sections of hydrographs or recession plots to primary flow components; for example, surface, unsaturated and saturated flow. Many of the methods used for separation are subjective and limited in their ability to determine prominent flow paths (e.g., Anderson and Burt; 1980; Nash, 1966). Instead, isotopic and chemical techniques for hydrograph separation are less subjective and may provide more accurate results (e.g., Liu *et al.*, 2013; Frisbee *et al.*, 2011). The subjectivity associated with graphical separation can influence the development of master recession curves. Master recession curves can be defined using different techniques, including the matching strip and correlation methods. The matching strip method of master curve formation involves the segmentation of the hydrograph recession followed by subjectively shifting these segments until they overlap (Nathan and McMahon, 1990; Toebes and Strang, 1964). The correlation method of master recession formation requires creating  $dQ/dt$  v.  $Q$  recession plots, which removes the variable of time (Langbein, 1938). When all flow data is incorporated, the subjectivity of graphical separation can be avoided (Tallaksen, 1995). However, all of the flow data is often not included because flows during precipitation, snowmelt, or high evapotranspiration will obscure the relationship between

storage and discharge (e.g., Shaw *et al.*, 2013; Shaw and Riha, 2012; Biswal and Marani, 2010; Kirchner, 2009).

Recession analyses can help improve flow predictions. Two recent approaches to understanding recession and storage in watersheds build off this legacy of analysis, but make different critical assumptions about watershed function. Kirchner (2009) developed a model based on streamflow recession characteristics that permits precipitation and evapotranspiration estimates based on discharge data and vice versa. The model generates a version of the master recession curve based on four years of flow data during periods of minimal evapotranspiration and no precipitation. By assuming that discharge depends only on the water stored within the catchment, the recession characteristics are then based on one overall storage-discharge relationship that fits the composite effect of numerous storage and flow complexities within the catchment (Kirchner, 2009).

Biswal and Marani (2010) criticize Kirchner's (2009) because they show that the storage-discharge slopes determined from individual events are greater than the relationship derived from the master recession curve point cloud. Multiple slopes undermine the assumption that discharge is a single function of catchment-wide storage. Instead, Biswal and Marani (2010) propose that discharge is proportional to the total length of the active drainage network, and thus recession characteristics are dominated by changes in the length of the active drainage network and number of supporting flowheads. This geomorphology-based model assumes that discharge per unit length is identical throughout the active drainage network, and the active drainage network recedes at a constant rate. While it is intuitively odd to assume that discharge is identical

throughout a stream network, Biswal and Marani (2010) suggest that changes in the length of the stream network are of greater influence on the recession rate than changes in discharge. Both models require discharge to be dominated by drainage of the unconfined aquifer intersected by the channel network; thus a single storage-discharge relationship should pertain in either model (Kirchner, 2009; Biswal and Marani, 2010). The stable spring flow and discontinuous networks that we witness in the lower Big Creek watersheds do not fit these assumptions, but instead suggest the influence of multiple and complex aquifers. Therefore, because leading storage-discharge recession models differ on whether streamflow recession characteristics depend on catchment-wide storage, drainage from one or multiple aquifers, or changes in the drainage network, field validation of model applicability and accuracy is needed.

### **1.3 Study Area and Methods**

In this section, I introduce past research at Big Creek and methods, which will be summarized briefly in Chapters 2 and 3.

#### **1.3.1 Big Creek Watershed**

Big Creek flows through the largest designated wilderness in the contiguous United States, the Frank Church-River of No Return Wilderness. Although this region is considered to be minimally disturbed by humans, it has a rich history strongly linked to the economics, politics, and motives driving the development of Idaho and the American West. Before 1879, a subgroup of Northern Shoshone Indians known as the Tukudika, or Sheepeaters, inhabited this mountainous region (Minshall, 2014). Today, depressions along flat streamside terraces mark historic wickiup (i.e., dwelling) locations and pictographs on rock walls still communicate lessons and information from previous

generations of Native people. In 1879, the U.S. Army forcefully removed the majority of remaining Tukudika inhabitants from Big Creek after members of the Tukudika were accused of killing five prospectors on another tributary of the Middle Fork of the Salmon River (Minshall, 2014). The removal of the Tukudika and the 1862 Homestead Act encouraged white settlement of the Middle Fork region that continues to this day. Notably, the Caswell brothers began exploiting the region's gold reserves in 1894 (Minshall, 2012 and 2014), and Dave Lewis, having first visited Big Creek as a packer for the Army in 1879, patented a homestead in 1924 (Peek, 2004). The land developed by these early settlers passed through the ownership of a series of later homesteaders, "hard timers", and dude ranchers. In 1931, the Idaho Primitive Area was established, leading to wilderness designation in 1980 (Minshall, 2014). The former Caswell property now consists of a single cabin that houses summer Forest Service employees, and the former Lewis property is the University of Idaho's Taylor Wilderness Research Station (TWRS). For a more complete history of the Big Creek region, begin with Minshall's books *Wilderness Brothers, Prospecting, Horse Packing, & Homesteading on the Western Frontier* (2012) and *Cabin Creek Chronicle, The History of the Most Remote Ranch in America* (2014), as well as Peek's *Cougar Dave, Mountain Man of Idaho* (2004).

The history of settlement and activity within Big Creek transitioned to research based at 'Taylor Ranch' in the 1960s. Maurice Hornocker began research based at Taylor Ranch in 1965 on mountain lion behavior (Hornocker, 1969 and 1970). These works were not only critical for removing mountain lions as bounty animals, but also led to the purchase of Taylor Ranch by the University of Idaho in 1970. Since then, TWRS

continues to support wildlife research on numerous species including bighorn sheep, wolverine, salmon, and wolves (e.g., Hamann *et al.*, 2014; Peek, 2010; Holecek *et al.*, 2009; Wagner and Peek, 2006; Copeland *et al.*, 2007). Wildfire plays an important role in ecosystems of the Intermountain West, and due to the lack of additional human impacts, TWRS has become an ideal setting for studying the impacts and recovery from wildfires, especially in stream and riparian ecosystems (Davis *et al.*, 2013; Malison and Baxter; 2010; Minshall *et al.*, 2001a and b; Royer and Minshall, 1997). With the emphasis on stream ecology in Big Creek growing since the 1990's, the need for measuring hydrologic and geomorphic processes influencing streams has also grown. Olson (2010) assessed controls on discharge within Big Creek and its tributaries through gaging and modeling. Tennant *et al.* (2015) continued those efforts through the assessment of catchment hypsometry on streamflow susceptibility to climate change throughout the Salmon River Basin (of which Big Creek is a part). The geomorphic and geologic histories underlying the ecology and hydrology of Big Creek are also the focus of recent publications by Lifton *et al.* (2009), Stewart *et al.* (2013), and Link *et al.* (2014), respectively. Managers and researchers, past and present, also know many things not yet recorded in publications; a lengthy visit to TWRS will improve any future research. I share many tips for successful research similar to what I completed in Appendix A.

### **1.3.2 Quantifying Transpiration with Sap Flow**

I used dual-probe heat dissipation sensors to measure sap flow in Douglas fir. I measured three sets of trees at approximately 1220 m, 2000 m, and 2370 m. For more details, please see Section 2.2.2, and Appendix A.1 and B.

### **1.3.3 Measuring Stream Discharge**

I used a Flowtracker ADV and a series of pressure transducers to gage Pioneer, Cougar, Goat and Dunce Creeks. For more details, please see Section 3.2.3 and Appendix A.2.

### **1.3.4 Surface Network Mapping**

I used a Trimble GeoXH GPS to map the extent of surface flow throughout Pioneer, Cougar, Goat and Dunce watersheds during three periods throughout the spring and summer of 2014. For more details, please see Section 3.2.2 and Appendix A.3.

## **1.4 Thesis Organization and Objectives**

To understand the spatiotemporal relationships of transpiration, I measured Douglas fir water use across the snow-rain transition line/elevation in the Pioneer Creek watershed of Idaho's Frank Church River of No Return Wilderness in 2014. I also recorded stream discharge and monitored the active drainage network (i.e., surface flow areal extent) from May through August 2014 in order to assess potential storage characteristics throughout four mountainous headwater catchments. The resulting thesis is organized into the following three chapters. In Chapter 2, I assess the results of the Pioneer Creek watershed sap flow study and discuss differences in water and energy limitations that drive transpiration characteristics of Douglas fir across the snow-rain transition. In Chapter 3, I present the field data documenting the retraction and disconnection of active drainage networks and discuss potential geologic, geomorphic, and climatic controls on catchment storage. Chapter 4 summarizes the conclusions of the previous two chapters and discusses the influence of transpiration of streamflow based on the observations and findings from the sap flow and active drainage network studies.



Finally, I propose future work to test remaining questions to advance the understanding of the spatiotemporal relationships of transpiration and streamflow in mountainous watersheds.

## References

- Anderson, M.G., & Burt, T.P. (1980). Interpretation of recession flow. *Journal of Hydrology*, 46: 89-101.
- Barnett, T. P., Adam, J. C., & Lettenmaier, D. P. (2005). Potential impacts of a warming climate on water availability in snow-dominated regions. *Nature*, 438(7066), 303-309.
- Barnett, T. P., Pierce, D. W., Hidalgo, H. G., Bonfils, C., Santer, B. D., Das, T., Wood, A. W., Nozawa, T., Mirin, A. W., Cayan, D. R., Dettinger, M. D. (2008). Human induced changes in the hydrology of the western United States. *Science (New York, N.Y.)*, 319(5866), 1080–1083.
- Bencala, K. E., Gooseff, M. N., & Kimball, B. A. (2011). Rethinking hyporheic flow and transient storage to advance understanding of stream-catchment connections. *Water Resources Research*, 47(3).
- Bishop, K., Buffam, I., Erlandsson, M., Fölster, J., Laudon, H., Seibert, J., & Temnerud, J. (2008). Aqua Incognita: the unknown headwaters. *Hydrological Processes*, 22(8), 1239–1242.
- Biswal, B., & Marani, M. (2010). Geomorphological origin of recession curves. *Geophysical Research Letters*, 37(24).
- Biswal, B., & Nagesh Kumar, D. (2013). A general geomorphological recession flow model for river basins. *Water Resources Research*, 49(8), 4900–4906.
- Blyth, K., & Rodda, J. (1973). A Stream Length Study. *Water Resources Research*, 9(5): 1454–1461.
- Boussinseq, J. (1877). Essai sur la théorie des eaux courantes. *Mémoires présentés par divers savants à l'Académie des Sciences de l'Institut National de France*, Tome XXIII, No. 1.
- Brooks, J.R., Barnard, H. R., Coulombe, R., & McDonnell, J. J. (2010). Ecohydrologic separation of water between trees and streams in a Mediterranean climate. *Nature Geoscience*. 2, 100-104.
- Christensen, L., Tague, C. L., & Baron, J. S. (2008). Spatial patterns of simulated transpiration response to climate variability in a snow dominated mountain ecosystem. *Hydrological Processes*, 22(18), 3576–3588.
- Copeland, J. P., Peek, J. M., Groves, C. R., Melquist, W. E., McKelvey, K. S., McDaniel, G. W., Long, C. D., Harris, C. E., & Melquist, N. E. (2007). Seasonal Habitat Associations of the Wolverine in Central Idaho. *Journal of Wildlife Management*, 71(7), 2201.
- Davis, J. M., Baxter, C. V., Minshall, G. W., Olson, N. F., Tang, C., & Crosby, B. T. (2013). Climate-induced shift in hydrological regime alters basal resource dynamics in a wilderness river ecosystem. *Freshwater Biology*, 58(2), 306–319.
- Day, D. (1978). Drainage density changes during rainfall. *Earth Surface Processes & Landforms*, 3, 319–326.
- Day, D. G. (1983). Drainage density variability and drainage basin outputs (New South Wales, Australia). *Journal of Hydrology: New Zealand*, 22, 3–17.
- Emanuel, R. E., Epstein, H. E., McGlynn, B. L., Welsch, D. L., Muth, D. J., & D'Odorico, P. (2010). Spatial and temporal controls on watershed ecohydrology in the northern Rocky Mountains. *Water Resources Research*, 46, 1–14.

- Frisbee, M. D., Phillips, F. M., Campbell, A. R., Liu, F., & Sanchez, S. A. (2011). Streamflow generation in a large, alpine watershed in the southern Rocky Mountains of Colorado: Is streamflow generation simply the aggregation of hillslope runoff responses? *Water Resources Research*, 47(6).
- Gabrielli, C. P., McDonnell, J. J., & Jarvis, W. T. (2012). The role of bedrock groundwater in rainfall-runoff response at hillslope and catchment scales. *Journal of Hydrology*, 450-451, 117–133.
- Gannon, J., Bailey, S., & McGuire, K. (2014). Organizing groundwater regimes and response thresholds by soils: a framework for understanding runoff generation in a headwater catchment. *Water Resources Research*, 8403–8419.
- Garcia, E. S., Tague, C. L., & Choate, J. S. (2013). Influence of spatial temperature estimation method in ecohydrologic modeling in the Western Oregon Cascades. *Water Resources Research*, 49(3), 1611–1624.
- Godsey, S. E., & Kirchner, J. W. (2014). Dynamic, discontinuous stream networks: hydrologically driven variations in active drainage density, flowing channels and stream order. *Hydrological Processes*, 28(23), 5791–5803.
- Godsey, S. E., Kirchner, J. W., & Tague, C. L. (2013). Effects of changes in winter snowpacks on summer low flows: case studies in the Sierra Nevada, California, USA. *Hydrological Processes*, 28(19), 5048-5064.
- Goulden, M. L., Anderson, R. G., Bales, R. C., Kelly, A. E., Meadows, M., & Winston, G. C. (2012). Evapotranspiration along an elevation gradient in California's Sierra Nevada. *Journal of Geophysical Research: Biogeosciences*, 117(3).
- Goyal, M. K., Madramootoo, C. A., & Richards, J. F. (2015) Simulation of the Streamflow for the Rio Nuevo Watershed of Jamaica for Use in Agriculture Water Scarcity Planning. *Journal of Irrigation and Drainage Engineering*, 141(3).
- Graham, C. B., Barnard, H. R., Kavanagh, K. L., & McNamara, J. P. (2013). Catchment scale controls the temporal connection of transpiration and diel fluctuations in streamflow. *Hydrological Processes*, 27(18), 2541–2556.
- Granier, A. (1985). Une nouvelle méthode pour la mesure du flux de sève brute dans le tronc des arbres. *Annales des Sciences Forestières*.
- Gregory, K. J., & Walling, D. E. (1968). The Variation of Drainage Density within a Catchment. *International Association of Scientific Hydrology Bulletin*, 13(2), 61–68.
- Hall, F.R., (1968). Base flow recessions – a review. *Water Resources Research*, 4(5): 973-983.
- Hamann, E.J., Kennedy B.P., Whited, D.C., Stanford, J.A. (2014). Spatial variability in spawning habitat selection by Chinook Salmon (*Oncorhynchus tshawytscha*) in a wilderness river. *River Research and Applications*, 30(9), 1099-1109.
- Holecek, D. E., Cromwell, K. J., & Kennedy, B. P. (2009). Juvenile Chinook Salmon Summer Microhabitat Availability, Use, and Selection in a Central Idaho Wilderness Stream. *Transactions of the American Fisheries Society*, 138(3), 633-644.
- Hornocker, M.G. (1969). Winter Territoriality in Mountain Lions. *The Journal of Wildlife Management*, 3(3), 457-464.

- Hornocker, M.G. (1970). An Analysis of Mountain Lion Predation upon Mule Deer and Elk in the Idaho Primitive Area. *Wildlife Monographs*, 21, 3-39.
- Jackson, B. K., Sullivan, S. M. P., & Malison, R. L. (2012). Wildfire severity mediates fluxes of plant material and terrestrial invertebrates to mountain streams. *Forest Ecology and Management*, 278, 27–34.
- Jaeger, K. L., Olden, J. D., & Pelland, N. A. (2014). Climate change poised to threaten hydrologic connectivity and endemic fishes in dryland streams. *Proceedings of the National Academy of Sciences of the United States of America*, 1–6.
- Kirchner, J. W. (2009). Catchments as simple dynamical systems: Catchment characterization, rainfall-runoff modeling, and doing hydrology backward. *Water Resources Research*, 45(2), 1–34.
- Knowles, N., Dettinger, M., & Cayan, D. (2006). Trends in snowfall versus rainfall in the western United States. *Journal of Climate*, 4545–4560.
- Larned, S. T., Datry, T., Arscott, D. B., & Tockner, K. (2010). Emerging concepts in temporary river ecology. *Freshwater Biology*, 55(4), 717–738.
- Langbein, W.B., (1938). Some channel storage studies and their application to the determination of infiltration. *Transactions of the American Geophysical Union*, 19, 435 – 445.
- Leopold, L. B., Wolman, M. G., & Miller, J. P. (1964). *Fluvial processes in geomorphology*. W.H. Freeman and Company: San Francisco; 522.
- Link, P. K., Crosby, B. T., Lifton, Z. M., Eversole, E. A., & Rittenour, T. M. (2014). The late Pleistocene ( 17 ka ) Soldier Bar landslide and Big Creek Lake, Frank Church-River of No Return Wilderness , central Idaho, U.S.A. *Rocky Mountain Geology*, 4(1), 17–31.
- Link, P., Simonin, K., Maness, H., Oshun, J., Dawson, T., & Fung, I. (2014). Species differences in the seasonality of evergreen tree transpiration in a Mediterranean climate: Analysis of multiyear, half-hourly sap flow observations. *Water Resources Research*, 50(3), 1869-1894.
- Lifton, Z. M., Thackray, G. D., Van Kirk, R., & Glenn, N. F. (2009). Influence of rock strength on the valley morphometry of Big Creek, central Idaho, USA. *Geomorphology*, 111(3-4), 173–181.
- Liston, G. E., & Elder, K. (2006). A Meteorological Distribution System for High Resolution Terrestrial Modeling (MicroMet). *Journal of Hydrometeorology*. 7(2), 217-234.
- Liu, F., Hunsaker, C., & Bales, R. C. (2013). Controls of streamflow generation in small catchments across the snow-rain transition in the Southern Sierra Nevada, California. *Hydrological Processes*, 27(14), 1959–1972.
- Lundquist, J. D., & Loheide, S. P. (2011). How evaporative water losses vary between wet and dry water years as a function of elevation in the Sierra Nevada, California, and critical factors for modeling. *Water Resources Research*, 47, 1–13.
- Maillet, E. (1905). *Essai d'hydraulique souterraine et fluviale*. Librairie Sci., A. Herman, Paris.
- Malison, R. L., & Baxter, C. V. (2010). Effects of wildfire of varying severity on benthic stream insect assemblages and emergence. *Journal of the North American Benthological Society*.

- Manning, A. H., Clark, J. F., Diaz, S. H., Rademacher, L. K., Earman, S., & Niel Plummer, L. (2012). Evolution of groundwater age in a mountain watershed over a period of thirteen years. *Journal of Hydrology*, 460-461, 13–28.
- McDowell, N., White, S., & Pockman, W. (2008). Transpiration and stomatal conductance across a steep climate gradient in the southern Rocky Mountains. *Ecohydrology*, 204, 193–204.
- Meinzer, F. C., Brooks, J. R., Bucci, S., Goldstein, G., Scholz, F. G., & Warren, J. M. (2004). Converging patterns of uptake and hydraulic redistribution of soil water in contrasting woody vegetation types. *Tree Physiology*, 24, 919–928.
- Minshall, G. W., Brock, J. T., Andrews, D. A., & Robinson, C. T. (2001a). Water quality, substratum and biotic responses of five central Idaho (USA) streams during the first year following the Mortar Creek fire. *International Journal of Wildland Fire*, 10(2), 185–199.
- Minshall, G.W. (2012). Wilderness Brothers, Prospecting, Horse Packing, & Homesteading on the Western Frontier. *Streamside Scribe Press*, Inkom, ID.
- Minshall, G.W. (2014). Cabin Creek Chronicle, The history of the most remote ranch in America. *Streamside Scribe Press*, Inkom ID.
- Minshall, G. W., Robinson, C. T., Lawrence, D. E., Andrews, D. A., & Brock, J. T. (2001). Benthic macroinvertebrate assemblages in five central Idaho (USA) streams over a 10 year period following disturbance by wildfire. *International Journal Of Wildland Fire*, 10, 201–213.
- Molotch, N., Brooks, P., & Burns, S. (2009). Ecohydrological controls on snowmelt partitioning in mixed-conifer sub-alpine forests. *Ecohydrology*, 142(May), 129–142.
- Montgomery, D. R., & Dietrich, W. E. (1992). Channel initiation and the problem of landscape scale. *Science (New York, N.Y.)*, 255(5046), 826–830.
- Montgomery, D. R., Dietrich, W. E., Torres, R., Anderson, S. P., Heffner, J. T., & Loague, K. (1997). Hydrologic response of a steep, unchanneled valley to natural and applied rainfall. *Water Resources Research*, 33(1), 91.
- Montgomery, D. R., & Dietrich, W. E. (2002). Runoff generation in a steep, soil-mantled landscape. *Water Resources Research*, 38(9), 1–8.
- Mueller, M. H., Alaoui, A., Kuells, C., Leistert, H., Meusburger, K., Stumpp, C., Weiler, M., & Alewell, C. (2014). Tracking water pathways in steep hillslopes by  $\delta^{18}\text{O}$  depth profiles of soil water. *Journal of Hydrology*, 519, 340–352.
- Mutzner, R., Weijs, S. V., Tarolli, P., Calaf, M., Oldroyd, H. J., & Parlange, M. B. (2015). Controls on the diurnal streamflow cycles in two subbasins of an alpine headwater catchment. *Water Resources Research*, 51(5), 3403–3418.
- Nash, J.E. (1966). Applied flood hydrology. In: River Engineering and Water Conservation Works, Thorn, R.B. (eds.), Butterworths, London, 63-110.
- Nathan, R.J., & McMahon, T.A. (1990). Evaluation Of Automated Techniques For Base flow And Recession Analyses. *Water Resources Research*, 26, 1465–1473.
- Olson, N. F. (2010). Hydrology of Big Creek, Idaho: Spatial and temporal heterogeneity of runoff in a snow-dominated wilderness mountain watershed, [M.S. Thesis], Idaho State University, 116.
- Onishi, N. & Wollan, M. (2014). Severe Drought Grows Worse in California. *The New York Times*. January 17.

- Peek, P.C., (2004). Cougar Dave, Mountain Man of Idaho. Ninebark Publications, 240.
- Peek, J.M. (2010). Pattern of Herbivory, Nitrogen Content, and Biomass of Bluebunch Wheatgrass on a Mountain Sheep Habitat in Central Idaho. *Northwest Science*, 84(4), 386-393.
- Rademacher, L. K., Clark, J. F., Clow, D. W., & Hudson, G. B. (2005). Old groundwater influence on stream hydrochemistry and catchment response times in a small Sierra Nevada catchment: Sagehen Creek, California. *Water Resources Research*, 41(2), 1–10.
- Rinaldo, A., Rigon, R., Banavar, J. R., Maritan, A., & Rodriguez-Iturbe, I. (2014). Evolution and selection of river networks: statics, dynamics, and complexity. *Proceedings of the National Academy of Sciences of the United States of America*, 111(7), 2417–24.
- Roberts MC, Archibold OW. (1978). Variation of drainage density in a small British Columbia watershed. *AWRA Water Resources Bulletin* 14(2), 470–476.
- Roberts M, Klingeman P. (1972). The relationship between drainage net fluctuation and discharge. International Geography, Proceedings of the 22nd International Geographical Congress, Canada, Adams and Helleiner (eds.), University of Toronto Press, 189–191.
- Roos, M. (1987). Possible Changes in California Snowmelt Patterns, *Proc., 4<sup>th</sup> Pacific Climate Change Workshop*, Pacific Grove, California, 22-31.
- Royer, T. V, & Minshall, G. W. (1997). Temperature patterns in small streams following wildfire. *Archiv Fur Hydrobiologie*, 140(2), 237–242.
- Shaw, S. B., McHardy, T. M., & Riha, S. J. (2013). Evaluating the influence of watershed moisture storage on variations in base flow recession rates during prolonged rain-free periods in medium-sized catchments in New York and Illinois, USA. *Water Resources Research*, 49(9), 6022–6028.
- Shaw, S. B., & Riha, S. J. (2012). Examining individual recession events instead of a data cloud: Using a modified interpretation of  $dQ/dt-Q$  streamflow recession in glaciated watersheds to better inform models of low flow. *Journal of Hydrology*, 434-435, 46–54.
- Smakhtin, V. U. (2001). Low flow hydrology: A review. *Journal of Hydrology*, 240(3-4), 147-186.
- Stewart, D. E., Lewis, R. S., Stewart, E. D., & Link, P. K. (2013). Geologic map of the central and lower Big Creek drainage, central Idaho: Idaho Geological Survey Digital Web Map DWM-161, scale 1:75,000.
- Stewart, I., Cayan, D., & Dettinger, M. (2004). Changes in snowmelt runoff timing in Western North America under a “business as usual” climate change scenario. *Climatic Change*, 217–232.
- Tague, C. L., & Band, L. E. (2004). RHESSys: Regional Hydro-Ecologic Simulation System An Object-Oriented Approach to Spatially Distributed Modeling of Carbon, Water, and Nutrient Cycling. *Earth Interactions*, 8(19), 1–42.
- Tague, C., & Grant, G. E. (2009). Groundwater dynamics mediate low-flow response to global warming in snow-dominated alpine regions. *Water Resources Research*, 45(7), 1–12.
- Tallaksen, L. (1995). A review of baseflow recession analysis. *Journal of Hydrology*, 165(1-4), 349–370.

- Tennant, C. J., Crosby, B. T., Godsey, S. E., VanKirk, R. W., & Derryberry, D. R. (2015). A simple framework for assessing the sensitivity of mountain watersheds to warming driven snowpack loss. *Geophysical Research Letters*, 42(8), 2814–2822.
- Toebes, C. and Strang, D.D., 1964. On recession curves, 1 – Recession equations. *Journal of Hydrology NZ*, 3(2): 2- 15.
- Troch, P. a., Berne, A., Bogaart, P., Harman, C., Hilberts, A. G. J., Lyon, S. W., Paniconi, C., Pauwels, V. R. N., Rupp, D. E., Selker, J. S., Teuling, A. J., Uijlenhoet, R., & Verhoest, N. E. C. (2013). The importance of hydraulic groundwater theory in catchment hydrology: The legacy of Wilfried Brutsaert and Jean-Yves Parlange. *Water Resources Research*, 49(9), 5099–5116.
- Trujillo, E., Molotch, N. P., Goulden, M. L., Kelly, A. E., & Bales, R. C. (2012). Elevation-dependent influence of snow accumulation on forest greening. *Nature Geoscience*, 5(10), 705–709.
- Tucker, G. E., & Hancock, G. R. (2010). Modelling landscape evolution. *Earth Surface Processes and Landforms*, 35(1), 28–50.
- Wagner, M. J., Bladon, K. D., Silins, U., Williams, C. H. S., Martens, A. M., Boon, S., ... Anderson, A. (2014). Catchment-scale stream temperature response to land disturbance by wildfire governed by surface-subsurface energy exchange and atmospheric controls. *Journal of Hydrology*, 517, 328–338.
- Wagner, G. D., & Peek, J. M. (2006). Bighorn sheep diet selection and forage quality in central Idaho. *Northwest Science*, 80(4), 246–258.
- Warren, J. M., Meinzer, F. C., Brooks, J. R., & Domec, J. C. (2005). Vertical stratification of soil water storage and release dynamics in Pacific Northwest coniferous forests. *Agricultural and Forest Meteorology*, 130(1-2), 39–58.
- Welch, L. A., & Allen, D. M. (2014). Hydraulic conductivity characteristics in mountains and implications for conceptualizing bedrock groundwater flow. *Hydrogeology Journal*, 22(August 2013), 1003–1026.
- Westerling, A. L., Hidalgo, H. G., Cayan, D. R., & Swetnam, T. W. (2006). Warming and earlier spring increase western U.S. forest wildfire activity. *Science (New York, N.Y.)*, 313(5789), 940–943.
- Zimmer, M. A., Bailey, S. W., Mcguire, K. J., & Bullen, T. D. (2013). Fine scale variations of surface water chemistry in an ephemeral to perennial drainage network. *Hydrological Processes*, 27(24), 3438–3451.

## **Chapter 2    Understanding plant water use across the snow-rain transition, Salmon River Basin, Idaho**

### **Abstract**

Decreasing mountain snowpacks and rising snowlines due to a warming climate are known to be directly impacting streamflow across the American West. The change in timing and quantity of liquid water availability to streams due to less snow accumulation and earlier melt is also likely influencing transpiration patterns. However, the relationships between snowpack characteristics and transpiration have not been widely studied in the field, especially in the Intermountain West. Here we investigated the differences in temporal patterns of Douglas fir transpiration using sap flow sensors at three sites spanning the snow-rain transition. Using additional vapor pressure deficit and soil moisture data from these sites, we assessed the primary controls on transpiration, i.e., evaporative demand and water availability, and interpreted the influence of snowmelt. The results from the May – November 2014 study period reveal surprisingly similar patterns in transpiration at all elevations with peak-recorded sap flow occurring at the beginning of the field season in May and early June. Decreasing sensitivity of sap flow to vapor pressure deficit, likely due to decreasing water availability, also occurs at approximately the same time at all elevations. The observed similarities in sap flow across all elevations during the study period suggests that periodic rainfall may be more influential than snowmelt on determining Douglas fir transpiration.

### **2.1 Introduction**

Transpiration influences catchment ecohydrology, with wide-ranging influence on streamflows (e.g., Graham *et al.*, 2013), spatial distribution of storage (e.g., Godsey *et al.*,



2013; Kirchner, 2009; Emanuel *et al.*, 2010), ecosystem health and composition (e.g., Trujillo *et al.*, 2012), and wildfire susceptibility (e.g., Westerling *et al.*, 2006). Because of these influences, numerous studies attempt to model watershed scale transpiration and project changes in transpiration due to climate change (e.g., Godsey *et al.*, 2013; Lundquist and Loheide, 2011; Tague *et al.*, 2009; Christensen *et al.*, 2008).

Transpiration in sensitive mountain regions may depend on snowpack accumulation, melting rates and timing (Stewart *et al.*, 2004). Streamflow and snowpack dynamics in these regions are already shifting towards earlier melt and earlier summer low flows (Stewart *et al.*, 2004; Knowles *et al.*, 2006). In semi-arid regions, mountain snowpacks and snowmelt drive the timing and quantity of water availability for plant water use as well as streamflow and groundwater infiltration (Stewart *et al.*, 2004; Barnett *et al.*, 2008). Thus, determining how snowmelt is portioned between transpiration and streamflow is important for determining the allocation of water throughout a watershed and the susceptibility of respective ecosystems to diminishing snowpacks (Molotch *et al.*, 2009; Tague and Band, 2004).

Even though elevation and temperature gradients are widely recognized as primary controls on snowpacks and transpiration (Garcia *et al.*, 2013; Liston and Elder, 2006), the spatial heterogeneity of these gradients within mountain watersheds still leads to poor transpiration and snowpack estimates in ecohydrologic models (Goulden and Bales, 2014; Goulden *et al.*, 2012; Trujillo *et al.*, 2012; Christensen *et al.*, 2008; McDowell *et al.*, 2008). At higher elevations, larger and more persistent snowpacks increase water availability for transpiration while atmospheric evaporative demand, which drives transpiration, decreases at higher elevations. Thus, at intermediate elevations, some

models suggest transpiration should be greatest due to temperatures being cool enough to permit substantive snowpacks and greater water availability, yet warm enough for a longer growing season (Lundquist and Loheide, 2011; Christensen *et al.*, 2008). In turn, some speculate that intermediate elevations may also be the most susceptible to warming climate as snowpacks decrease and water limitations increase (Trujillo *et al.*, 2012). Meanwhile, plants are less susceptible to drought at low elevations, where plants are more drought-resistant, and at high elevations, where thermal limitations to transpiration may be ameliorated by warming (Goulden *et al.*, 2012; Trujillo *et al.*, 2012).

The role of snowmelt for supplying water for transpiration is controversial. For a site with small intermittent snowpacks and little transpiration during the autumn and winter, Brooks *et al.* (2010) showed that autumn rains refill small pore spaces in soils, which trees then access during the spring, following the primary drainage of winter precipitation. Infiltrating snowmelt and winter precipitation do not mix with the small pore spaces filled by autumn rains; instead, winter precipitation leads to a short period of flow through large pores and preferential flow paths, which contributes heavily to streamflow but not to transpiration (Brooks *et al.*, 2010). Different species utilize different water sources within the unsaturated zone. In the northern California Coast Range, broadleaf species access more sustained water sources with deeper root networks and a physiology more resistant to hydraulic failure, while needle-leaf species exhibit shallower root networks and increased vulnerability to hydraulic failure (Link *et al.*, 2014, Oshun *et al.*, 2012). Therefore, within the same watershed, or even stand, differing species compositions likely rely on different water sources. Furthermore, within the same species, hydraulic redistribution of available water may maintain shallow soil

moisture with sustained deeper water stores (Warren *et al.*, 2005; Meizner *et al.*, 2004). Thus, the relationship between environmental limitations and plant hydraulics that contribute to transpiration characteristics are complex and dynamic within and between species. Current models may not accurately account for these complexities, and thus field validation is required.

In this study, we aim to assess differences in water and energy limitations that drive differences and similarities in transpiration of Douglas fir across the snow-rain transition in the Salmon River Basin of Idaho. We compare sap flow trends to quantify whole-tree transpiration at rain-dominated, mixed precipitation, and snow-dominated sites within a 16 km<sup>2</sup> watershed. The relationships between sap flow, soil moisture and vapor pressure at these sites allow us to interpret the primary controls of transpiration. Contrary to our initial hypothesis that water availability and transpiration patterns would differ across the snow-rain transition, we present similar temporal relationships between sap flow, atmospheric conditions, and water availability across all elevations during the 2014 study period. While previous modeling work suggests snowpacks may primarily influence water availability and thus seasonal patterns in transpiration, our findings suggest the periodicity and intensity of spring and summer rain events may be more influential to Douglas fir transpiration trends throughout the watersheds of the Salmon River Basin.

## **2.2 Study Area and Methods**

### **2.2.1 Big Creek Watershed**

Big Creek is a major tributary of the Middle Fork of the Salmon River in central Idaho and flows through the Frank Church-River of No Return Wilderness. Big Creek watershed is 1540 km<sup>2</sup>, with an elevation range from 1030 m to 2900 m (USGS, 2014).

The large elevation range of this watershed is ideal for assessing transpiration relationships between snow-dominated (> 2500 m) versus rain-dominated terrain (1030 – 1500 m) (Tennant *et al.*, 2014). Basin-wide mean annual precipitation is 70 cm, which primarily falls as snow in wet winter months, resulting in peak runoff from late spring to midsummer (USGS, 2014; Knowles *et al.*, 2006; Stewart *et al.*, 2004). Baseflow conditions extend from late summer through winter.

Due to semi-arid conditions and wildfire activity, lower elevation hillslopes have patchy forest cover of primarily Douglas fir (*Pseudotsuga menziesii* var. *glauca*) and ponderosa pine (*Pinus ponderosa*) with interspersed bunchgrasses, wildflowers, and sparse big sagebrush (*Artemisia tridentata*). Higher elevation slopes are forested with Douglas fir, and subalpine fir (*Abies lasiocarpa*) at the highest elevations. Stands of Lodgepole pine (*Pinus contorta* var. *latifolia*) dominate some slopes recovering from wildfires.

The bedrock geology includes rocks of the Mesoproterozoic Lemhi and Neoproterozoic Windermere Supergroup, the Eocene Challis Volcanic Group, and Neoproterozoic, Cretaceous, and Eocene intrusive rocks (Stewart *et al.*, 2013). Primarily northeast-southwest normal faulting is a result of Neoproterozoic, Cretaceous, and Eocene extension (Stewart *et al.*, 2013). Steep hillslopes and deeply incised river canyons are an effect of significant Neogene uplift (~10 Ma) and the related capture of the Salmon River drainage by the Snake River (~2-4 Ma) (Sweetkind and Blackwell, 1989; Meyer and Leidecker, 1999; Kirchner *et al.*, 2001). Steep slopes, averaging ~ 25 degrees, result in thin or absent soil cover, and erosion processes dominated by rock fall and debris flows initiated from deep-seated rotational slumps (Link *et al.*, 2014).

The Frank Church-River of No Return Wilderness is the largest designated wilderness in the contiguous United States that has undergone minimal human disturbance and thus provides an ideal setting to study catchment hydrology. Although its headwaters are remote, the Salmon River is a major tributary to the Snake and Columbia Rivers, which act together as a major waterway for inland transport of goods to the Pacific Northwest, as well as a significant source of water and electric power to the region. This research is based at Taylor Wilderness Research Station (“Taylor Ranch”), a small facility along Big Creek owned by the University of Idaho.

### **2.2.2 Using Sap Flow to Quantify Transpiration**

Within the study watersheds, the most widespread tree across both rain and snow dominated elevations is the Rocky Mountain Douglas fir (*Pseudotsuga menziesii* var. *glauca*). We measured transpiration of Douglas fir across the snow-rain transition in order to make an assessment of transpiration differences in rain-dominated versus snow-dominated terrains of central Idaho. Many studies of Douglas fir transpiration and water-use have utilized the same dual-probe sap flow sensor technique used for this project (e.g., Simpson, 2000; Domec *et al.*, 2006; Granier, 1985).

In the process of transpiration, water is drawn from the soil into the roots, and up through the xylem tissue in the roots, trunk, branches and finally needles of the tree, where it evaporates into the air. Water transport along this soil-plant-air continuum is driven largely by the vapor pressure deficit (VPD) (i.e., evaporative demand) of the atmosphere, which is a function of air temperature and humidity. The atmosphere’s VPD, approximately 0.1-6 kPa, is much greater than the saturated conditions within the leaf, so water is transported from the soil into the atmosphere via this driving gradient of

water from saturated to less saturated conditions. This theory of water movement through plants is referred to as the Cohesion-Tension theory described in Domec *et al.* (2006), through the Soil-Plant-Air Continuum (SPAC) (Kitajima *et al.*, 2013) and was described much earlier by Dixon (1914). The sapwood of Douglas fir is the region of the stem in which water transport occurs, and approximately 98% of water that moves through the xylem of a plant is escaping the plant via the atmosphere, i.e., there is essentially no storage of water in trees (Ördög & Zoltán, 2011). Therefore, by measuring rates of water flow through a cross-section of a Douglas fir trunk, we can estimate the water escaping all of the tree's needles via transpiration.

Dual-probe sap flow sensors were developed by Granier (1985), and have since been utilized in many plant physiology and hydrology studies. The dual-probe design provides reliable results, yet is simple in design and inexpensive to construct (Lu *et al.*, 2004). These sensors consist of two 2-cm probes with thermocouples; one of the probes also has a heating wire coiled around the needle providing a constant source of heat energy. Both probes are inserted into the tree sapwood, with the heated probe ~ 15 to 10 cm directly above the reference (non-heated) probe. A Campbell Scientific CR1000 data logger connected to the sensor registers the difference in voltage and thus temperature between the two probes. As sap flow increases, the temperature difference between the reference and heated probe decreases because more heat is being dissipated from the heated probe, thus lowering the temperature. We convert those temperature differences between the probes to sap flow velocity using Granier's (1985) empirically derived formula:

$$F_d = 118.99 \times 10^{-6} \left[ \frac{(\Delta T_{max} - \Delta T)}{\Delta T} \right]^{1.23} \quad \text{Equation 2.1}$$

where  $F_d$ , sap flow velocity, is a function of  $\Delta T_{max}$ , the maximum temperature differential between the probes, and the  $\Delta T$ , temperature differential. By assuming that sap flow is the same around the rest of the trunk's circumference and thickness, we use the sapwood area to determine the whole plant's sap flow. We assume that the sap and probes are in thermal equilibrium with each other.

### 2.2.2.1 Sap Flow Uncertainties

Although Granier's method is simple and accurate, in practice there are complexities worth addressing. The determination of  $\Delta T_{max}$  during periods of no sap flow is the primary challenge. Theoretically,  $\Delta T_{max}$  occurs at night during periods of no sap flow. However, this assumption may not always be true because in reality  $\Delta T_{max}$  often occurs when there is some, although minimal, sap flow (e.g., Pataki *et al.*, 2011; Kavanagh *et al.*, 2007; Lu *et al.*, 2004). To account for this, we adopted Kavanagh *et al.*'s (2007) VPD minimum threshold of a 0.1 kPa for nocturnal transpiration; that is, we assumed transpiration did not occur at night when the VPD was lower than 0.1 kPa. We set this threshold in Oren's BaseLiner program (accessible online: <http://c-h2oecology.env.duke.edu/software.html>), which aids in the process of establishing the no-flow  $\Delta T_{max}$  'baseline' throughout the dataset. We then converted the raw voltage differential data from the dual probe sensors to sap flow data using Granier's (1985)

formula. We manually adjusted the  $\Delta T_{max}$  no-flow baseline in instances where the  $\Delta T$  was greater than the automatic baseline set by the BaseLiner program.

All needles of a tree do not have the same exposure and same transpiration rates and thus not all sides or depths of the trunk sapwood maintain the same sap flow (Lu *et al.*, 2004). We accounted for differences in sap flow around the trunk by placing two sensors in each tree; one on the shaded north side of the tree, which will be least influenced by changes in exposure to sunlight, and the other sensor at another varying cardinal direction. We monitored three trees at each site where sap flow is being measured, and therefore transpiration of all the cardinal directions was monitored for a given ‘sap flow site’. We only measured the sap flow of the outer 2-cm of sapwood, and so differences in flow deeper than 2-cm will contribute to uncertainty in whole-tree transpiration estimates (Lu *et al.*, 2004). We maintained the 2-cm design despite often encountering thicker sapwood because a change from Granier’s original design would have required calibration (Lu *et al.*, 2004). Where sapwood thickness was greater than 2 cm, we applied Pataki *et al.*’s (2011) Gaussian equation for gymnosperms which accounts for the reduction of sapwood hydraulic conductivity with increasing sapwood depth:

$$\frac{J_i}{J_o} = 1.257 \times \exp \left[ -0.5 \left( \frac{x+0.3724}{0.6620} \right)^2 \right] \quad \text{Equation 2.2}$$

where  $J_i/J_o$  is the ratio of sap flow at depth  $i$  to the sap flow at the outer 2-cm of sapwood, and  $x$  is the ratio of depth  $i$  to total sapwood thickness. In the single instance where sapwood thickness was smaller than 2-cm, we use Clearwater’s (1999) equation:



$$\Delta T_{sw} = \frac{(\Delta T - b\Delta T_{max})}{a} \quad \text{Equation 2.3}$$

where  $\Delta T_{sw}$  is the temperature differential of the probe in sapwood,  $\Delta T$  is the temperature differential of the whole probe, and  $b$  and  $a$  are the proportions of the probe in inactive heartwood and sapwood, respectively. Lu *et al.* (2004) also outlines the impact of tree growth around the probe. Because this study is based on the season directly following installation, tree growth around the probes was of minimal concern.

We focused primarily on relative changes in sap flow relationships with evaporative demand and between the sap flow sites instead of the differences in absolute sap flow quantities (i.e., whole-tree water use). The differences in sap flow velocities may be due to several factors: sapwood thickness and the portion of sapwood accounted for by the 2 cm long sensor (Lu *et al.*, 2004), the tree age (Moore *et al.*, 2004), and past and present environmental factors that influence sapwood growth and hydraulic characteristics (Roderick and Berry, 2001). Although we attempt to control for these factors, it is possible that these differences may dominate transpiration patterns that we observe in trees across the snow-rain transition.

#### **2.2.2.2 Sap Flow Sites**

We measured sap flow along an elevation gradient to focus on the effects of precipitation phase (rain versus snow) on Douglas fir transpiration. Each of three sites was along the eastern ridge of the Pioneer Creek Watershed (Figure 2.1), a tributary of Big Creek, and consisted of two sensors in three Douglas firs. We monitored three trees at each site to account for site heterogeneity. We located one sap flow site within each of the snow-dominated, the mixed, and the rain-dominated elevation bands (2370 m, 2000 m, and 1210 m, respectively). The elevation bands were determined by Tennant *et al.*

(2014), using 2004 - 2011 precipitation data for the Salmon River Basin from the National Weather Service's Snow Data Assimilation System (SNODAS).

Because environmental controls on transpiration are more complex than the impact of cooler temperatures at higher elevations, we controlled for as many other factors as possible. Sites had similar hillside aspect, slope (grade), and contributing draining area, as these factors affect the solar energy reaching a site and the rate and quantity of water moving through the site. There are many other factors that may impact transpiration, but are more difficult to account for in the project design, such as soil permeability, bedrock geology, nutrient availability, and rooting depth. We accounted for differences in geology by investigating preliminary soil and bedrock descriptions, and monitoring soil-moisture (Decagon 5TM sensors) at a depth of 25 cm at the snow and rain-dominated sites. Nutrients and rooting depth are not incorporated into this analysis, although Douglas fir roots are known to penetrate several meters into weathered and coherent bedrock when soil cover is thin (Roering *et al.*, 2010). In addition to the sap flow sensors, we installed photosynthetically active radiation (PAR) sensors (LiCOR LI-190 Quantum Sensor), and temperature and relative humidity sensors (Onset HOBO Pro v2 U23-002) in order to assess the strength of correlations between these environmental factors and transpiration. We also relied on the light and VPD data from meteorological sensors at the sap flow sites and nearby Taylor Ranch remote automatic weather station (RAWS) to determine the  $\Delta T_{max}$  in the BaseLiner program. Vapor pressure deficit (VPD) is measured in units of pressure (kPa), and is the measure by which we quantify the evaporative demand pulling water into the atmosphere using the following equation:

$$\text{VPD(kPa)} = \left(0.611 \times 10^{\left(\frac{7.5T}{237.3+T}\right)}\right) \times \left(1 - \frac{RH}{100}\right) \quad \text{Equation 2.4}$$

where  $T$  is temperature ( $^{\circ}\text{C}$ ), and  $RH$  is relative humidity (%).

### 2.2.2.3 Normalization

For the analyses described below, we use normalized sap flow, VPD, and soil moisture values. Normalization allows for us to compare temporal relationships and environmental responses between sensors and sites along the elevation transect with different absolute values (Link *et al.*, 2014b). Absolute values of sap flow vary between trees and sites for reasons briefly discussed in Section 2.2.2.1. VPD absolute values will be greatest at lower elevations due to warmer and drier conditions. The absolute values reported by the soil moisture sensors are also not easily comparable without site-specific calibration, which was not conducted. We used the normalization equation below for all analyses at both daily and hourly timescales.

$$\frac{[(Data) - 0.5 \text{ Percentile}(Data)]}{[99.5 \text{ Percentile}(Data) - 0.5 \text{ Percentile}(Data)]} \quad \text{Equation 2.5}$$

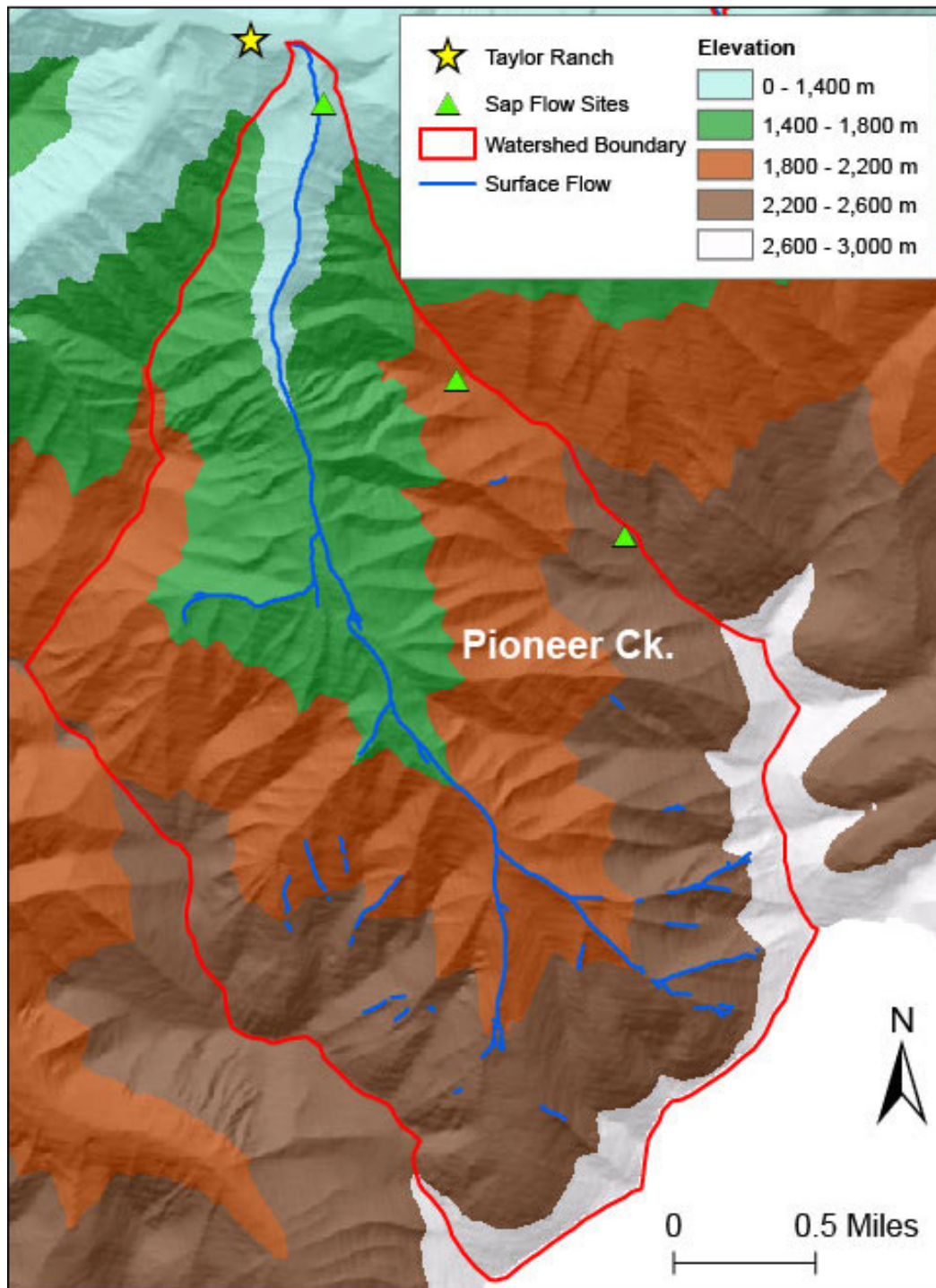


Figure 2.1: The three sap flow sites were located along the eastern ridge of the Pioneer Watershed. Surface flow was mapped at the end of May 2014.

## 2.3 Results and Discussion

### 2.3.1 Vapor Pressure Deficit and Sap Flow

During the 2014 season, seasonal VPD patterns were similar, although of different magnitudes, across the three elevation bands, with peak VPD values occurring at the beginning in July (Figure 2.2). VPD and sap flow had a moderate linear relationship at the rain, mixed, and snow dominated sites ( $R^2 = 0.48, 0.38, 0.54$ , respectively;  $p < 0.0001$ ), throughout the study period (Figure 2.3). Sap flow at all three sites was twice as sensitive to changes in VPD in the early season compared with later in the summer on approximately July 1<sup>st</sup> (Figure 2.3). This shift occurred during the onset of peak summer VPD values following two large precipitation events at the end of June. The early season normalized sap flow-VPD slopes are approximately 0.5, 0.8, and 1.3 ( $R^2 = 0.68, 0.76, 0.79$ ;  $p < 0.0001$ ) at the rain, mixed, and snow-dominated sites, respectively. That is, if VPD shifts by 10%, sap flow shifts by 5, 8, and 13%, respectively. By contrast, after July 1<sup>st</sup>, the slopes shallow to 0.2, 0.3, and 0.6 ( $R^2 = 0.76, 0.68, 0.68$ ;  $p < 0.0001$ ) at the rain, mixed, and snow-dominated sites, respectively (Figure 2.3). The slope of the sap flow to VPD relationships remained low until the end of October, when precipitation increased and VPD dropped. This late autumn increase was most prominent at the rain-dominated site, where changes in sap flow increase to 83% of the corresponding shift in VPD ( $R^2 = 0.61$ ;  $p < 0.0001$ ).

The abrupt shift in VPD - sap flow relationships at the beginning of July at all three elevation-bands may have been due to a shift in energy and water limitations at all three sites concurrently. We observe that late season sap flow is less responsive to changes in VPD, which potentially reflects a physiological shift within the Douglas fir

trees to reduce water consumption. However, it is surprising that the onset of water limitation would occur at the same time at all elevation bands. Snowmelt timing differs at the three sites, but two large rain events at the end of June may have obscured the snowmelt timing controls on soil moisture (Figure 2.2). It is possible the soil moisture and drainage conditions at rooting depths following these rain events were similar at all three sites. Our soil moisture data suggest similar drying conditions during this period (Section 2.3.2).

The July 1<sup>st</sup> shift in VPD – sap flow slopes also corresponds with a steep increase in VPD values at all elevations (Figure 2.2 and Figure 2.4). Although, VPD values are lower at higher elevations (Figure 2.4).

If there were a VPD-based physiological threshold controlling this shift to more reserved sap flows (i.e., transpiration) it would have to be more sensitive at higher elevations. Otherwise, the observed shift in the VPD – sap flow relationship would occur earlier at lower elevations. A significant difference in VPD thresholds within trees of the same species within a 3-km transect spanning 1200 m in elevation is a possibility, although it still remains unlikely that a VPD-related response would occur at the same time across the different elevations. Intraspecific variability in plant hydraulics has been documented within Douglas fir and other gymnosperms; however, the populations studied extend well beyond the 16-km<sup>2</sup>-watershed scale and are often across a broader regional to continental scale (Martínez-Vilalta *et al.*, 2008 and 2014; Anderegg, 2014; Bansal *et al.*, 2015).

The abrupt seasonal shifts in the relationship between sap flow and VPD (Figure 2.3) suggest water limitations to evapotranspiration, especially at the mixed and rain-

dominated elevations. The mixed precipitation site exhibits the greatest observed shift (~64%) in the sap flow to VPD relationship in July, suggesting the greatest water limitations (Figure 2.3B). One might expect water availability to be lowest at the rain-dominated site where VPD is higher and snowpacks are small and intermittent, but we do not observe this pattern. Although both locations have similar contributing areas (i.e., drainage area based on surface topography), the trees at the rain-dominated site are only approximately 35 m from the valley bottom and Pioneer Creek, and thus may have access to deep and sustained flow path from higher in the watershed, whereas the mid-elevation sites are much further (~ 620 m) from flowing surface water.

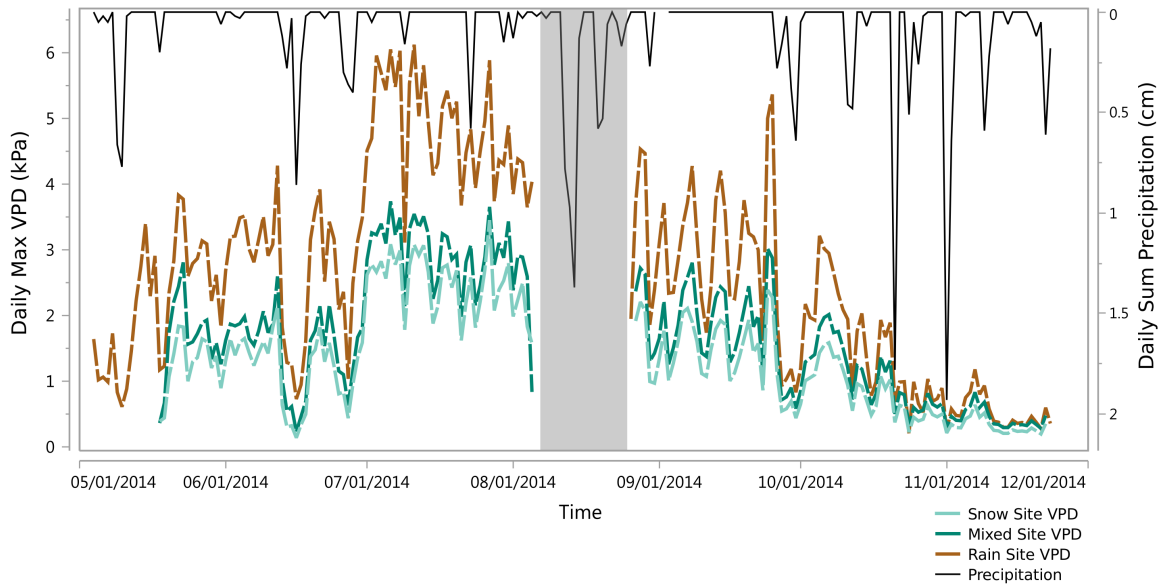


Figure 2.2: Seasonal patterns of VPD are similar across the three elevation-bands. Peak VPD values occur during early July at all three sites. VPD values are highest at the rain-dominated site where temperatures are also higher. VPD typically drops during precipitation events due to lower temperatures and higher humidity associated with storms. The gray box indicates a gap in data from sap flow site instrumentation failure.



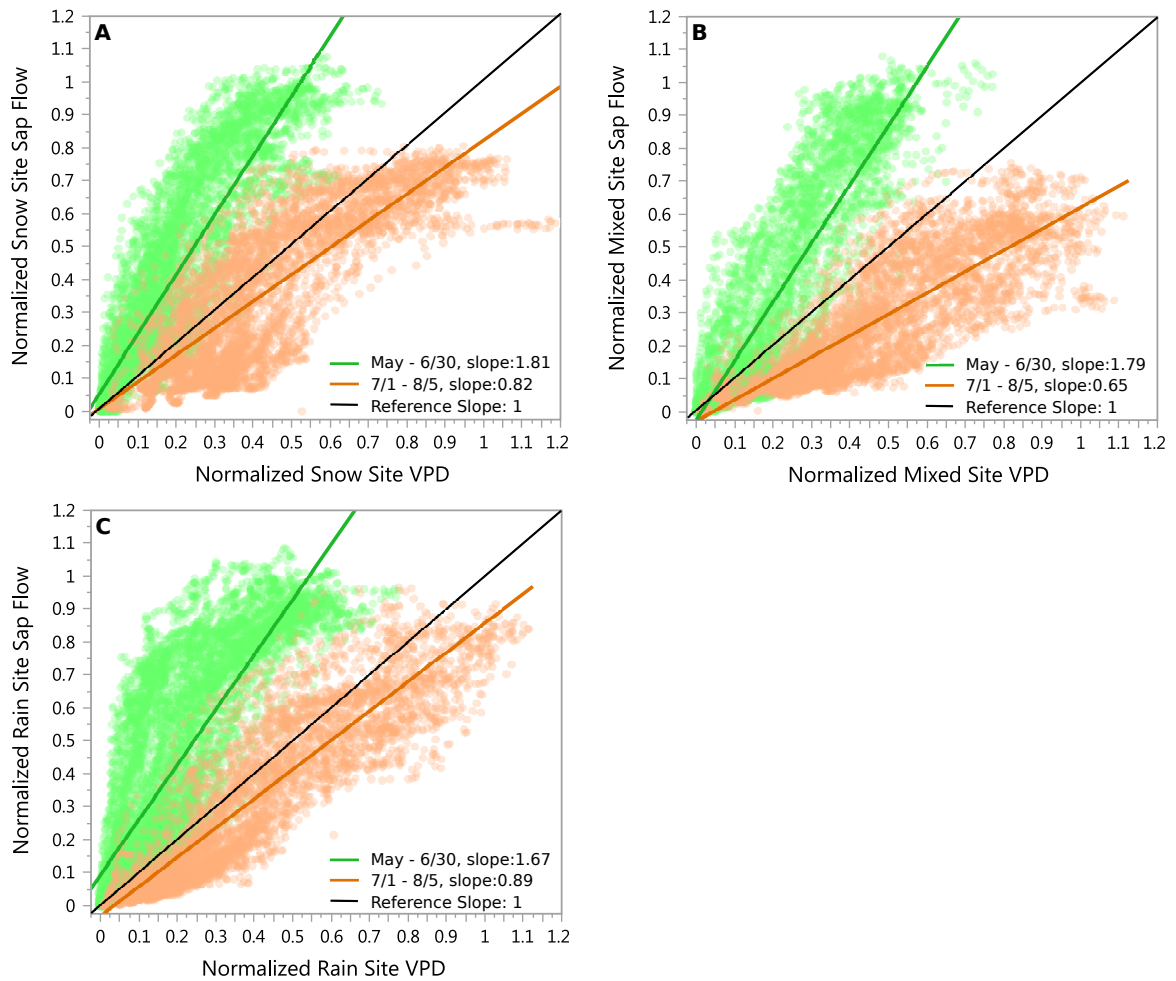


Figure 2.3: Hourly average sap flow and VPD are normalized by the 99.5 and 0.5 percentile values at each of the sap flow sites (Section 2.2.2.3). The green line and data points indicate values prior to 7/1/2014, while the orange represents values from 7/1/2014 – 8/5/2014. On approximately 7/1/2014, sap flow sensitivity to VPD drops at all sites. The slope of the sap flow to VPD relationship from 7/1/2014 to 8/5/2014 was 55%, 64% and 47% of the slope values from May to the end of June at the snow-dominated site (A), mixed precipitation site (B), and rain-dominated site (C), respectively. The largest shift in sensitivity at the mixed precipitation (B) site suggests the greater water limitations than at the other sap flow sites.

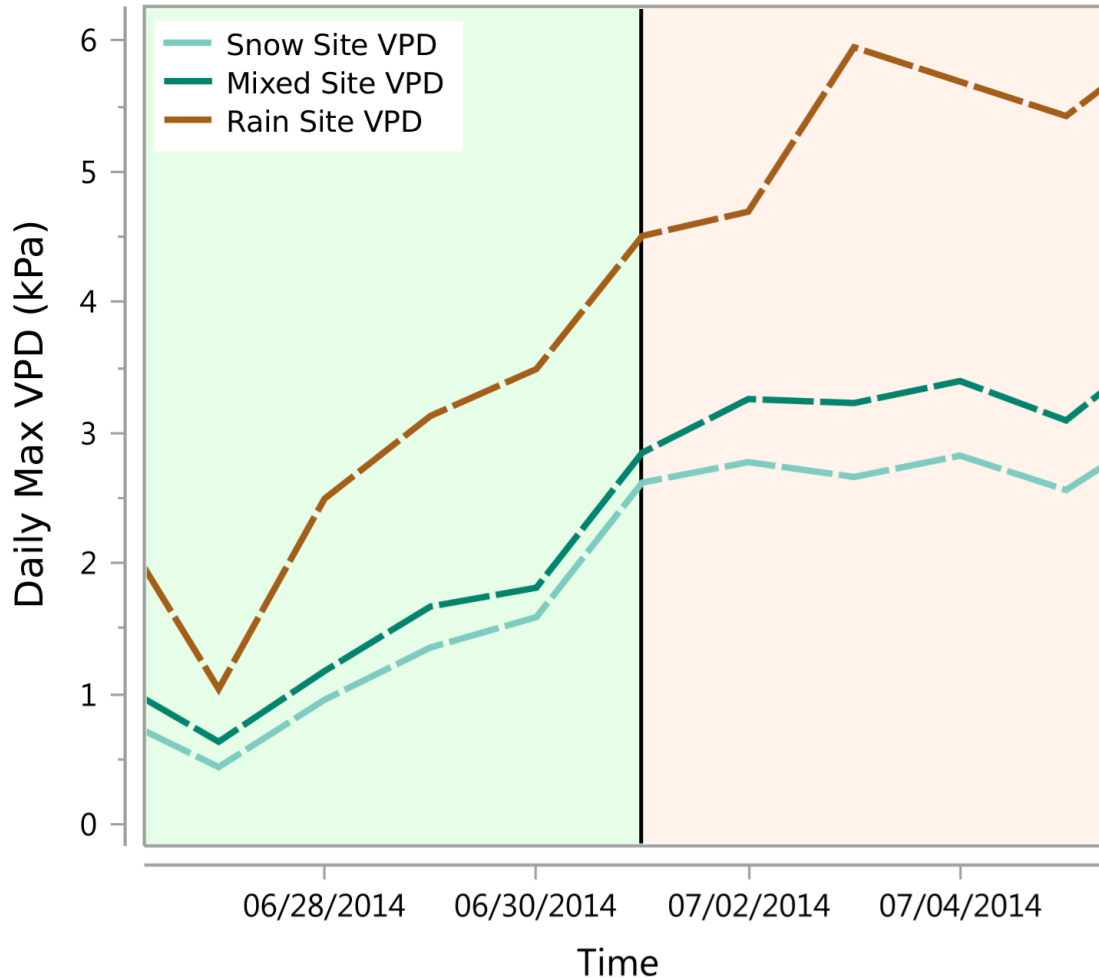


Figure 2.4: Daily max VPD values on 7/1/2014 are increasing at all three sites. VPD is also consistently much higher at lower elevations.

### 2.3.2 Soil Moisture and Sap Flow

Shallow soil layers contain the greatest fine root biomass (Warren *et al.*, 2005), although Douglas fir roots can extend several meters beneath the surface into bedrock (Roering *et al.*, 2010). Thus, soil moisture sensors at 25 cm indicate moisture available to shallow roots. We focus on the timing of soil moisture instead of soil moisture quantity because soil moisture probes were not calibrated to the individual soils at each site (Figure 2.6). Soil moisture data from the rain and snow-dominated sites exhibited

weak to moderate diel signals with peaks during the night and troughs during the day (Figure 2.5), which mirrors the expected effects of evapotranspiration (Moore *et al.*, 2011; Barnard *et al.*, 2010). Soil conditions at both the snow and rain-dominated sites show similar trends throughout the study period (Figure 2.6). Soils dry throughout the summer following snowmelt. Starting in October, soils begin to moisten due to more frequent precipitation events as well as cooler temperatures and lower VPD, which decrease evapotranspiration (Figure 2.6). Despite the overall autumn moistening trends, soils dry fairly rapidly following precipitation events because the shallow rocky soils are very well-drained.

Observed daily maximum soil moisture and sap flow do not show a strong relationship at either the snow or rain-dominated site ( $R^2 = 0.34$  and  $0.08$ ;  $p \approx 0.2$ ) (Figure 2.7). We suggest this relationship is weak in part because there is a short and variable lag in the response of sap flow to soil moisture associated with storm length. Precipitation events that increase soil moisture also lower VPD, which can impose a temporary energy limitation to transpiration. Following a precipitation event, soil moisture begins to decrease while VPD increases, thus allowing transpiration to increase rapidly until returning to a water-limited state.

Furthermore, around the beginning of October, soil moisture begins an overall increase while sap flow becomes increasingly variable. This helps explain additional weakness in the sap flow – soil moisture relationship (Figure 2.6 and Figure 2.8). We propose that cooler autumn temperatures impose energy-limitations at all elevations transpiration resulting in the decoupling of sap flow and soil moisture.

The relationship between daily maximum sap flow and daily average soil moisture is stronger when we ignore days with precipitation and isolate three different periods within the study period: (1) a late spring to early summer sap flow and soil moisture recession (5/4/14 to 8/5/14), a late summer to early autumn recession (8/26/14 to 9/29/14), and an autumn period (following 9/29/14) (Figure 2.6 and Figure 2.7). The soil moisture and sap flow relationships prior to 9/29/14 are slightly weaker at the snow-dominated site than at the rain-dominated site, which may reflect increased influence of cooler temperatures and lower VPD at higher elevations as observed in previous studies (Goulden *et al.*, 2012; Trujillo *et al.*, 2012) (Figure 2.7). The slope of the sap flow to soil moisture relationship following 9/29/14 is negative at the snow-dominated site and nearly absent at the rain-dominated site, which we propose is result of more frequent energy limitations at both sites in mid to late autumn (Figure 2.7). The negative relationship at the snow-dominated site may indicate greater temperature and energy limitations than at the rain-dominated site due to reduced transpiration and sap flow with dropping temperatures as soil moisture increases with increased storm frequency (Figure 2.6, Figure 2.7 and Figure 2.8).

Previous studies have reported the strong correlation between the onset of spring shallow soil desiccation and reduction in Douglas fir transpiration prior to the onset seasonal peak VPD (Link *et al.*, 2014b; Jassal *et al.*, 2009; Bond and Kavanagh, 1999; Granier, 1987). In support of these studies we observe a similar timing of peak soil moisture and sap flow (late May and June) versus peak VPD values in early July. Peak soil moisture earlier in the spring may correspond with snowmelt, and therefore timing and quantity of snowmelt may be influential to Douglas fir transpiration. However, in

Section 2.3.1 we discuss that a similar decrease in soil moisture at all three sites following two June precipitation events accounts for the abrupt drop in sap flow sensitivity to VPD observed at all sites on approximately July 1<sup>st</sup>. Therefore Douglas fir transpiration may be more dependent on the timing and quantity of spring rains than snow water equivalent and timing of melt. Supporting this hypothesis, we observe similarly decreasing trends in soil moisture at both snow and rain-dominated sites on July 1<sup>st</sup> (Figure 2.6).

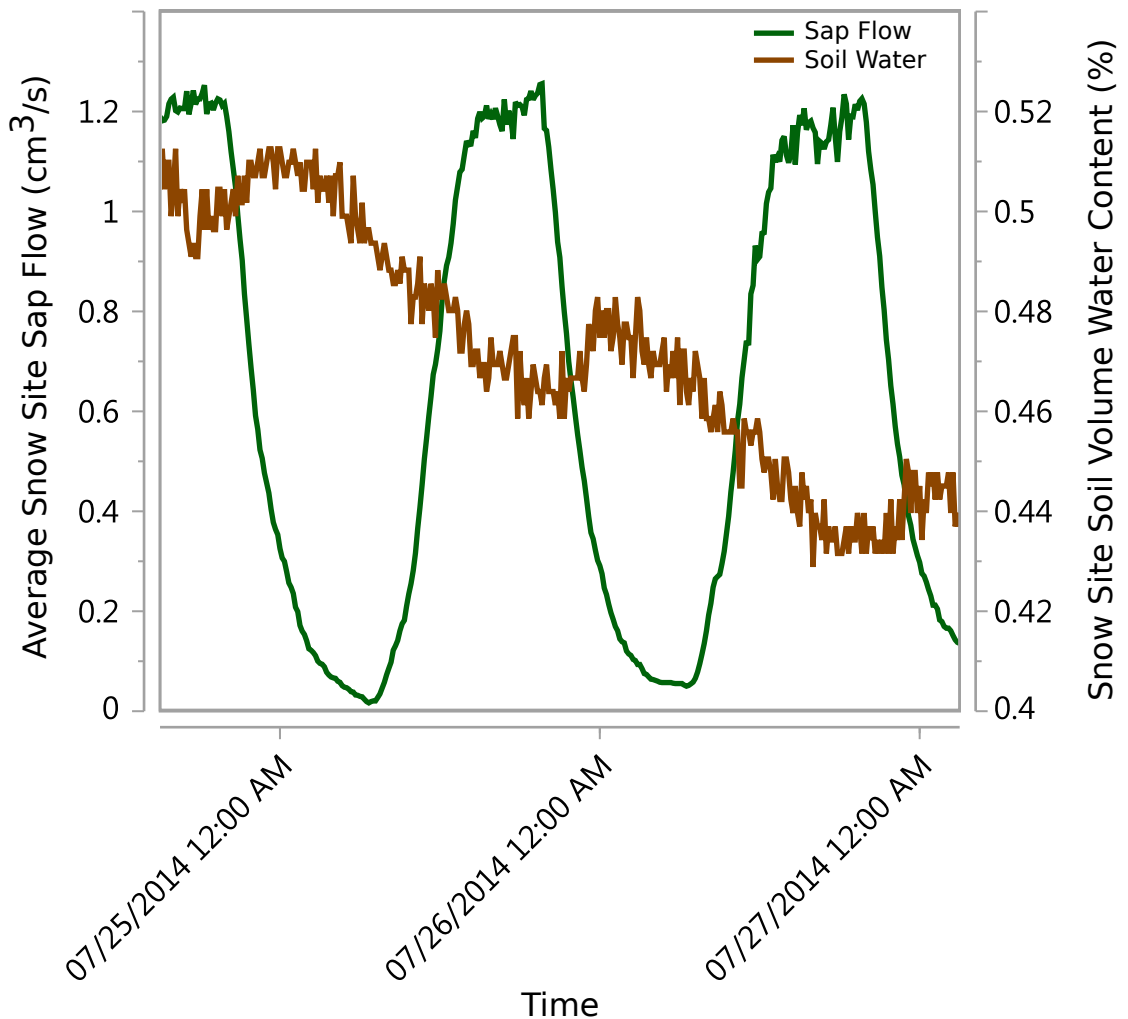


Figure 2.5: An example of diel signals of both sap flow and soil moisture at the snow-dominated site from 10 minute average values. While soil moisture exhibits an overall drying trend, daily peaks in soil moisture occur at night when sap flow is

lower.

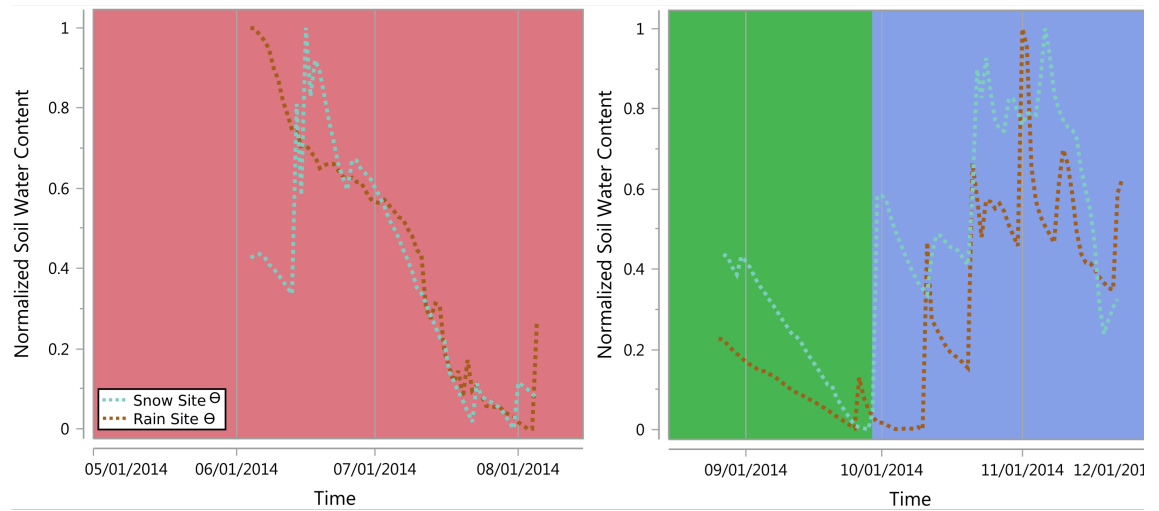


Figure 2.6: Soil water content normalized by maximum and minimum values recorded at the snow and rain-dominated sites from June to beginning of August, and the end of August to November. We separate the normalized data in order to highlight the similar seasonal patterns of soil moisture observed at the snow and rain-dominated sites. The background colors highlighting sections of the time series correspond with the sap flow – soil water content relationships in Figure 2.7.

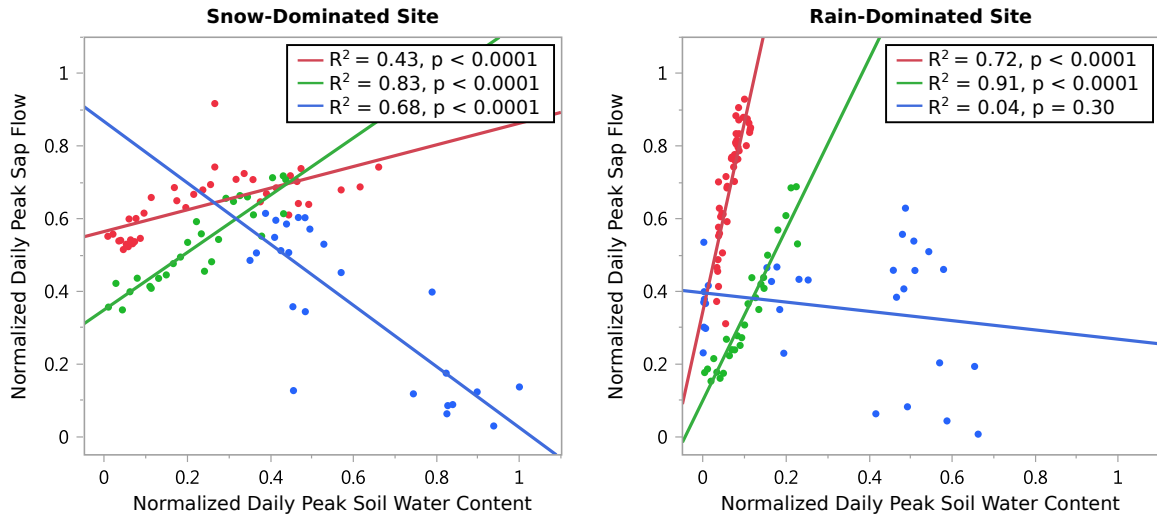


Figure 2.7: The colors of the data points and best-fit lines correspond with the background colors in Figure 2.6. At the snow-dominated sites, the sap flow – soil water content correlations during rain-free days from 8/26/14 to 9/29/14 (green) and 9/29/14 (blue) are stronger than during the earlier period, 5/4/14 to 8/5/14 (red). At the rain-dominated site, the sap flow – soil water content correlations are strongest earlier in the study period (red and green) and then become insignificant after 9/29/14 (blue). At both sites stronger correlations during 8/26/14 to 9/29/14 (green), suggest this period is characterized by the strongest water limitations to transpiration. The negative slope at the snow-dominated site and nearly absent relationship at the rain-dominated site after 9/29/14 (blue) are indicative of energy limitations to transpiration. Please note for the snow-dominated site, we also did not include outlying data prior to 6/12/2014, which may represent a settling period following installation of the sensor.

### 2.3.3 Sap Flow Between Elevation Bands

Sap flow shifts occur at similar times at each elevation band (Figure 2.8). Sap flow relationships between each of the three sites (i.e., sap flow at the rain-dominated site versus snow-dominated site, rain-dominated site versus mixed precipitation site, and snow-dominated versus mixed precipitation site) are linearly correlated throughout the study period ( $R^2 > 0.7$ ). However, there is a rain-free period from September 4 to 25 (Figure 2.8), during which we recognize differences in the sap flow relationships between sites (Figure 2.9). The relative sap flow responsiveness between sites is indicated by the

direction of the shift of the inter-site sap flow relationship slope in Figure 2.9. For example, in Figure 2.9A the relationship between sap flow at the mixed precipitation versus snow-dominated site shifts towards the snow-dominated site axis during the September rain-free period (purple), indicating sap flow becomes more responsive at the snow-dominated site relative to the mixed precipitation site. Overall, sap flows become most responsive at the snow-dominated site, followed by the rain-dominated and mixed precipitation sites during the September rain-free period. Because the shifts in the relationships of sap flow between each of the three sites occurs during a rain-free period, we suggest they reflect differences in water availability between the sites. Therefore, the snow-dominated site water availability remains highest, while water availability drops the most at the mixed precipitation site. The lower water availability at the mixed precipitation site is consistent with the shift in sap flow – VPD relationships on July 1<sup>st</sup> (section 2.3.1). The snow-dominated site water availability may remain highest because (1) the trees are larger and potentially have larger root networks for accessing soil moisture, (2) more precipitation falls at higher elevations, and (3) lower VPD at the snow-dominated site may result in more conservative transpiration rates.

These results emphasize the importance of occasional rain events on maintaining similar water availability and sap flow patterns between elevations. There were occasional precipitation events throughout the 2014 study period; however, if conditions were drier we would expect sap flow relationships between sites would be less stable.



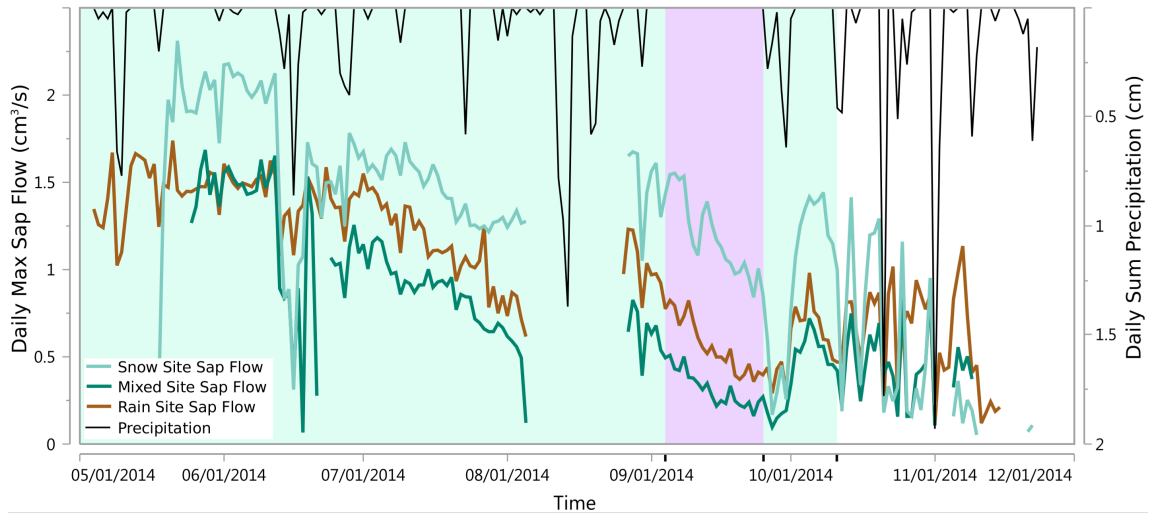


Figure 2.8: Sap flow is the averaged between the three trees monitored at each site. Seasonal trends are similar between each site with peak flows in May to early June. Sap flow drop during longer storm events due to low VPD and PAR values (i.e., energy-limited conditions). The same gap in data mentioned for Figure 2.2 pertains here. The turquoise background represents the period of data that constitutes the primary sap flow relationships between sites, while the purple background highlights the September dry period (Figure 2.9). After 10/11/2014, dropping VPD values (Figure 2.2) induce lower sap flow values at higher elevations and likely energy-limited conditions.

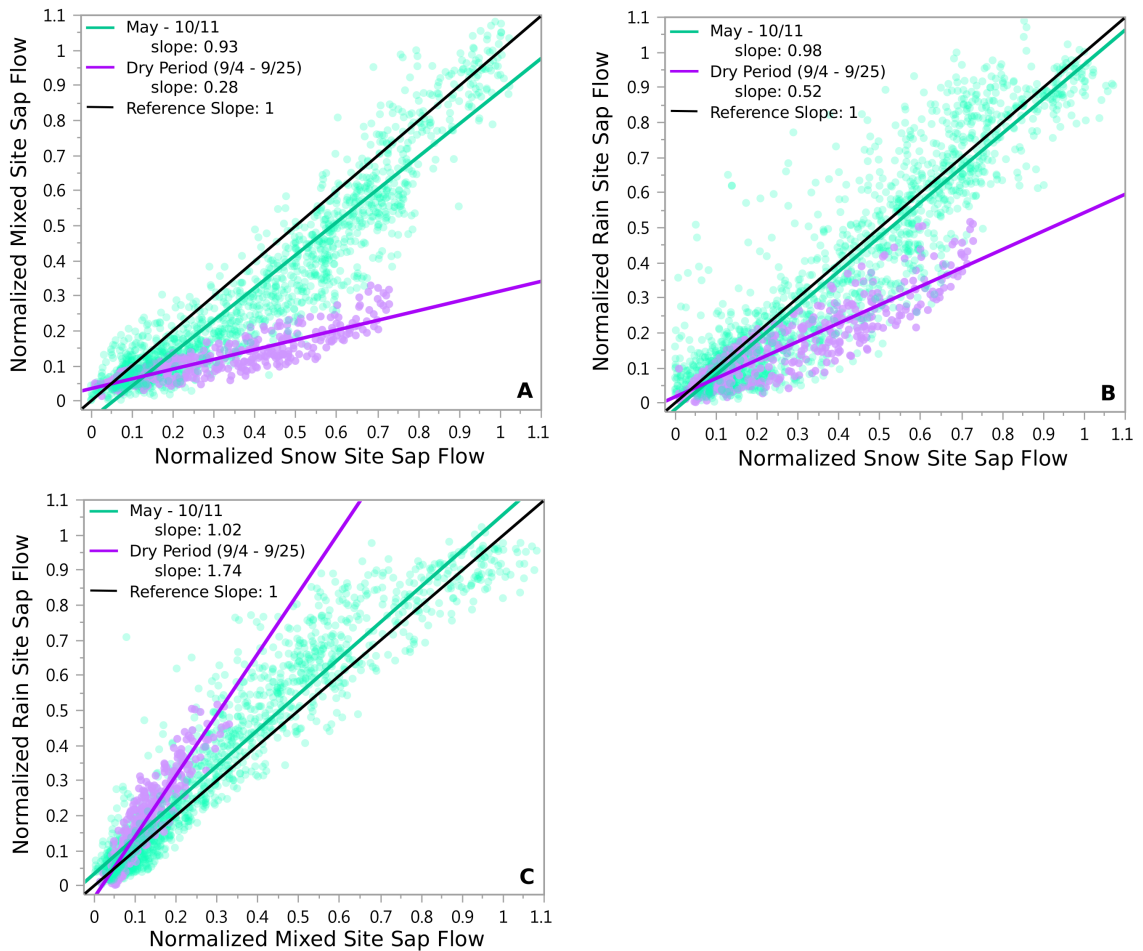


Figure 2.9: Hourly average sap flow points are from periods without precipitation in the previous 24 hours. Each graph plots normalized sap flow from one site against another site. The purple points and model represent the 21 day period in September without precipitation. Compared to the May – October models, during the dry period sap flow becomes 70% more responsive at the snow-dominated site than the mixed precipitation site (A), 40% more responsive at the snow-dominated site than the rain-dominated site (B), and 70% more responsive at the rain-dominated site than the mixed precipitation site (C). Therefore, we suggest sap flow is the most resistant to drought at the snow-dominated site and least resistant to drought at the mixed precipitation site.

## 2.4 Conclusion

During the 2014 study period, temporal sap flow patterns are largely consistent across all elevations, peaking around the same time in early June and reaching the lowest

flows at the end of the study period in November. In early July, sap flow responsiveness to changes in VPD markedly dropped, likely due to decreasing water availability as indicated by soil moisture data. We were surprised that this change in responsiveness occurred at approximately the same time across all elevations, because of differences in snow quantity and melt timing. We suggest that late spring rain events maintain similar soil moisture conditions throughout the watershed upon the onset of drier summer weather, thus allowing the similar timing in the reduction of Douglas fir transpiration across snowline. Similar soil drying trends observed at the snow and rain-dominated sites in early July support this hypothesis. Rising VPD is an unlikely cause for the change in the observed sap flow-VPD relationship because VPD values differ at each of the sites.

When occasional summer rain events temporarily ceased in early September, we observed differences in sap flow relationships between individual sites (e.g., sap flow at the snow-dominated site versus rain-dominated site) due to relative changes in water availability for transpiration between the sites. We initially expected water availability to increase with elevation; however, the observed change in sap flow relationships between sites suggests water availability dropped the most at the mixed-precipitation site and least at the snow-dominated site during the 21-day period of drought. Less water availability at the mixed precipitation site may be due to shallower and less extensive root networks of the smaller trees. Also, the closer proximity of the rain-dominated site to the valley bottom may result in access to deeper, more consistent flow paths from higher in the watershed. We suspect the snow-dominated site was most resilient to drought due to

larger trees with deeper and more extensive root networks, greater precipitation due to orographic enhancement, and lower evaporative demand (i.e., lower VPD values).

We propose spring and summer rain events, instead of snowpack size and persistence, control spatial patterns of soil moisture and thus transpiration. However, we cannot identify the source of water utilized for Douglas fir transpiration given our current dataset. Isotopic analysis of soil water and xylem sap, similar to Brooks *et al.* (2010), would help to reveal the age and source of water for transpiration (e.g., groundwater, rainwater, or snowmelt) within Pioneer watershed. In order to assess further the influence of snowpacks on transpiration it would be helpful to quantify the percentage of water transpired throughout a given year sourced from groundwater, rainwater, and snowmelt across the elevation transect. Also, our study focused on the environmental, but not physiological controls on transpiration patterns. An assessment of Douglas fir hydraulics (e.g., leaf and stem water potentials) across an elevation transect may aid in explaining the similar timing in the abrupt reduction of the sap flow response to VPD at all of our study sites.

We studied sap flow at sites with similar slope, aspect, and accumulation area so that we could isolate the effect of an elevation and temperature gradient on Douglas fir transpiration. Therefore, we did not account for the multitude of microclimates within the heterogeneous topography of Pioneer watershed as well as the variety of species. It is possible that snowmelt is increasingly important for transpiration in regions with greater accumulation area, or more north facing slopes with more persistent snowpacks. Therefore, future work should account for more intra-catchment variety.

## References

- Anderegg, W. R. L. (2015). Spatial and temporal variation in plant hydraulic traits and their relevance for climate change impacts on vegetation. *New Phytologist*, 205(3), 1008–1014.
- Barnard, H. R., Graham, C. B., Van Verseveld, W. J., Brooks, J. R., Bond, B. J., & McDonnell, J. J. (2010). Mechanistic assessment of hillslope transpiration controls of diel subsurface flow: A steady-state irrigation approach. *Ecohydrology*, 3(2), 133–142.
- Barnett, T. P., Pierce, D. W., Hidalgo, H. G., Bonfils, C., Santer, B. D., Das, T., Wood, A. W., Nozawa, T., Mirin, A. W., Cayan, D. R., Dettinger, M. D. (2008). Human induced changes in the hydrology of the western United States. *Science (New York, N.Y.)*, 319(5866), 1080–1083.
- Bansal, S., Harrington, C. A., Gould, P. J., & St.Clair, J. B. (2015). Climate-related genetic variation in drought-resistance of Douglas-fir (*Pseudotsuga menziesii*). *Global Change Biology*, 21(2), 947–958.
- Bond, B. J., & Kavanagh, K. L. (1999). Stomatal behaviour of four woody species in relation to leaf-specific hydraulic conductance and threshold water potential. *Tree Physiology*, 19, 503–510.
- Brooks, J.R., Barnard, H. R., Coulombe, R., & McDonnell, J. J. (2010). Ecohydrologic separation of water between trees and streams in a Mediterranean climate. *Nature Geoscience*. 2, 100-104.
- Christensen, L., Tague, C. L., & Baron, J. S. (2008). Spatial patterns of simulated transpiration response to climate variability in a snow dominated mountain ecosystem. *Hydrological Processes*, 22(18), 3576–3588.
- Clearwater, M. J., Meinzer, F. C., Andrade, J. L., Goldstein, G., & Holbrook, N. M. (1999). Potential errors in measurement of nonuniform sap flow using heat dissipation probes. *Tree Physiology*, 19(10), 681–687.
- Dixon, H.H. (1914). *Transpiration and the ascent of sap in plants*. Macmillan, London, 216.
- Domec, J.C., Meinzer, F. C., Gartner, B. L., & Woodruff, D. (2006). Transpiration-induced axial and radial tension gradients in trunks of Douglas-fir trees. *Tree Physiology*, 26(3), 275–84.
- Emanuel, R. E., Epstein, H. E., McGlynn, B. L., Welsch, D. L., Muth, D. J., & D’Odorico, P. (2010). Spatial and temporal controls on watershed ecohydrology in the northern Rocky Mountains. *Water Resources Research*, 46, 1–14.
- Garcia, E. S., Tague, C. L., & Choate, J. S. (2013). Influence of spatial temperature estimation method in ecohydrologic modeling in the Western Oregon Cascades. *Water Resources Research*, 49(3), 1611–1624.
- Godsey, S. E., Kirchner, J. W., & Tague, C. L. (2013). Effects of changes in winter snowpacks on summer low flows: case studies in the Sierra Nevada, California, USA. *Hydrological Processes*, 28(19), 5048-5064.
- Goulden, M. L., Anderson, R. G., Bales, R. C., Kelly, A. E., Meadows, M., & Winston, G. C. (2012). Evapotranspiration along an elevation gradient in California’s Sierra Nevada. *Journal of Geophysical Research: Biogeosciences*, 117(3).

- Goulden, M. L., & Bales, R. C. (2014). Mountain runoff vulnerability to increased evapotranspiration with vegetation expansion. *Proceedings of the National Academy of Sciences*, *111*(39), 14071–14075.
- Graham, C. B., Barnard, H. R., Kavanagh, K. L., & McNamara, J. P. (2013). Catchment scale controls the temporal connection of transpiration and diel fluctuations in streamflow. *Hydrological Processes*, *27*(18), 2541–2556.
- Granier, A. (1985). Une nouvelle méthode pour la mesure du flux de séve brute dans le tronc des arbres. *Annales des Sciences Forestieres*.
- Granier, A. (1987). Evaluation of transpiration in a Douglas-fir stand by means of sap flow measurements. *Tree Physiology*, *3*, 309–20.
- Jassal, R. S., Black, T. A., Spittlehouse, D. L., Brümmer, C., & Nesic, Z. (2009). Evapotranspiration and water use efficiency in different-aged Pacific Northwest Douglas fir stands. *Agricultural and Forest Meteorology*, *149*(6-7), 1168–1178.
- Kavanagh, K. L., Pangle, R., & Schotzko, A. D. (2007). Nocturnal transpiration causing disequilibrium between soil and stem predawn water potential in mixed conifer forests of Idaho. *Tree Physiology*, *27*(4), 621–629.
- Kirchner, J. W. (2009). Catchments as simple dynamical systems: Catchment characterization, rainfall-runoff modeling, and doing hydrology backward. *Water Resources Research*, *45*(2), 1–34.
- Kirchner, J. W., Finkel, R. C., Riebe, C. S., Granger, D. E., Clayton, J. L., King, J. G., & Megahan, W. F. (2001). Mountain erosion over 10 yr, 10 ky, and 10 my time scales. *Geology*, *29*(7), 591-594.
- Kitajima, K., Allen, M. F., & Goulden, M. L. (2013). Contribution of hydraulically lifted deep moisture to the water budget in a Southern California mixed forest. *Journal of Geophysical Research: Biogeosciences*, *118*(4), 1561–1572.
- Knowles, N., Dettinger, M., & Cayan, D. (2006). Trends in snowfall versus rainfall in the western United States. *Journal of Climate*, *19*, 4545–4560.
- Link, P. K., Crosby, B. T., Lifton, Z. M., Eversole, E. A., & Rittenour, T. M. (2014). The late Pleistocene (17 ka) Soldier Bar landslide and Big Creek Lake, Frank Church-River of No Return Wilderness, central Idaho, U.S.A. *Rocky Mountain Geology*, *4*(1), 17–31.
- Link, P., Simonin, K., Maness, H., Oshun, J., Dawson, T., & Fung, I. (2014b). Species differences in the seasonality of evergreen tree transpiration in a Mediterranean climate: Analysis of multiyear, half-hourly sap flow observations. *Water Resources Research*, *50*(3), 1869 -1894.
- Liston, G. E., & Elder, K. (2006). A Meteorological Distribution System for High Resolution Terrestrial Modeling (MicroMet). *Journal of Hydrometeorology*. *7*(2), 217-234.
- Lundquist, J. D., & Loheide, S. P. (2011). How evaporative water losses vary between wet and dry water years as a function of elevation in the Sierra Nevada, California, and critical factors for modeling. *Water Resources Research*, *47*, 1–13.
- Lu, P., Urban, L., & Zhao, P. (2004). Granier's Thermal Dissipation Probe (TDP) method for Measuring Sap Flow in Trees: Theory and Practice. *Acta Botanica Sinica*. *46*(6), 631-646.
- Martínez-Vilalta, J., Cochard, H., Mencuccini, M., Sterck, F., Herrero, A., Korhonen, J. F. J., Llorens, P., Nikinmaa E., Nolé, A., Poyatos, R., Ripullone, F., Sass

- Klaassen, U., Zweifel, R. (2009). Hydraulic adjustment of Scots pine across Europe. *New Phytologist*, 184(2), 353–364.
- Martínez-Vilalta, J., Poyatos, R., Aguadé, D., Retana, J., & Mencuccini, M. (2014). A new look at water transport regulation in plants. *New Phytologist*, 204(1), 105–115.
- McDowell, N., White, S., & Pockman, W. (2008). Transpiration and stomatal conductance across a steep climate gradient in the southern Rocky Mountains. *Ecohydrology*, 204, 193–204.
- Meinzer, F. C., Brooks, J. R., Bucci, S., Goldstein, G., Scholz, F. G., & Warren, J. M. (2004). Converging patterns of uptake and hydraulic redistribution of soil water in contrasting woody vegetation types. *Tree Physiology*, 24, 919–928.
- Meyer, G.A., & Leidecker, M.E. (1999). Fluvial Terraces along the Middle fork Salmon River, Idaho, and their Relation to Glaciation, Landslide Dams, and Incision Rates: A Preliminary Analysis and River-mile Guide: A preliminary analysis and river-mile guide. In Hughes, S.S., and Thackray, G.D., (eds.), *Guidebook to the Geology of Eastern Idaho: Pocatello, Idaho Museum of Natural History*, 219–235.
- Molotch, N., Brooks, P., & Burns, S. (2009). Ecohydrological controls on snowmelt partitioning in mixed-conifer sub-alpine forests. *Ecohydrology*, 142(May), 129–142.
- Moore, G. W., Bond, B. J., Jones, J. a, Phillips, N., & Meinzer, F. C. (2004). Structural and compositional controls on transpiration in 40- and 450-year-old riparian forests in western Oregon, USA. *Tree Physiology*, 24, 481–491.
- Moore, G. W., Jones, J. A., & Bond, B. J. (2011). How soil moisture mediates the influence of transpiration on streamflow at hourly to interannual scales in a forested catchment. *Hydrological Processes*, 25(24), 3701–3710.
- Ördög, V., & Zoltán, M. (2011). Water balance of plants. In *Plant Physiology*.
- Oshun, J., D. Rempe, P. Link, K. A. Simonin, W. E. Dietrich, T. E. Dawson, & I. Fung (2012). A look deep inside a hillslope reveals a structured heterogeneity of isotopic reservoirs and distinct water use strategies for adjacent trees. Abstract B33A-0498 presented at 2012 *Fall Meeting*, AGU, San Francisco, Calif.
- Pataki, D., McCarthy, H., Litvak, E., & Pincetl, S. (2011). Transpiration of urban forests in the Los Angeles metropolitan area. *Ecological Applications*, 21(3), 661–677.
- Simpson, D. (2000). Water use of interior Douglas-fir. *Canadian Journal of Forest Research*, 30, 534–547.
- Stewart, D.E., Lewis, R.S., Stewart, E.D., and Link, P.K. (2013). *Geologic map of the central and lower Big Creek drainage, central Idaho*: Idaho Geological Survey Digital Web Map, scale 1:75,000.
- Stewart, I., Cayan, D., & Dettinger, M. (2004). Changes in snowmelt runoff timing in Western North America under a “business as usual” climate change scenario. *Climatic Change*, 217–232.
- Sweetkind, D.S., & Blackwell, D.D. (1989). Fission-track evidence of the Cenozoic thermal history of the Idaho Batholith. *Tectonophysics*, 157, 241 – 250.
- Roderick, M. L., & Berry, S. L. (2001). Linking wood density with tree growth and environment: A theoretical analysis based on the motion of water. *New Phytologist*, 149(3), 473–485.

- Roering, J. J., Marshall, J., Booth, A. M., Mort, M., & Jin, Q. (2010). Evidence for biotic controls on topography and soil production. *Earth and Planetary Science Letters*, 298(12), 183–190.
- Tague, C. L., & Band, L. E. (2004). RHESSys: Regional Hydro-Ecologic Simulation System An Object-Oriented Approach to Spatially Distributed Modeling of Carbon, Water, and Nutrient Cycling. *Earth Interactions*, 8(19), 1–42.
- Tague, C., & Grant, G. E. (2009). Groundwater dynamics mediate low-flow response to global warming in snow-dominated alpine regions. *Water Resources Research*, 45(7), 1–12.
- Tennant, C. J., Crosby, B. T., & Godsey, S. E. (2014). Elevation-dependent responses of streamflow to climate warming. *Hydrological Processes*, 29(2015), 991-1001.
- Trujillo, E., Molotch, N. P., Goulden, M. L., Kelly, A. E., & Bales, R. C. (2012). Elevation-dependent influence of snow accumulation on forest greening. *Nature Geoscience*, 5(10), 705–709.
- U.S. Geological Survey (U.S.G.S), 2014, The StreamStats program for Idaho, online at <http://water.usgs.gov/osw/streamstats/idaho.html>.
- Warren, J. M., Meinzer, F. C., Brooks, J. R., & Domec, J. C. (2005). Vertical stratification of soil water storage and release dynamics in Pacific Northwest coniferous forests. *Agricultural and Forest Meteorology*, 130(1-2), 39–58.
- Westerling, A. L., Hidalgo, H. G., Cayan, D. R., & Swetnam, T. W. (2006). Warming and earlier spring increase western U.S. forest wildfire activity. *Science (New York, N.Y.)*, 313(5789), 940–943.



### **Chapter 3    Discontinuous mountain headwater stream networks with stable flowheads, Salmon River Basin, Idaho.**

#### **Abstract**

Headwater streams expand, contract, and disconnect in response to seasonal moisture conditions related to snowmelt as well as individual precipitation events. The fluctuation of the surface flow extent, or active drainage network, is known to have important impacts on stream ecology and influences some models interpreting catchment storage characteristics; however, the hydrological mechanisms which drive this phenomenon are still uncertain. Here we present field surveys of the active drainage networks of four headwater streams in Central Idaho's Frank Church-River of No Return Wilderness (7-21 km<sup>2</sup>) spanning the spring and summer months of 2014. The total length of the active drainage network varied as a power-law function of stream discharge with power-law exponents of  $\sim 0.11 \pm 0.03$  (range: 0.05 – 0.20). Generally, these active drainage networks were less responsive to changes in discharge than many streams in past studies. We observed that the locations where surface flow originates –known as flowheads– were often stable, and on average, approximately 64% of the change in active drainage network length was explained by downstream discontinuities. Most of the flowheads anchoring the active drainage networks below approximately 2200 m are associated with bedrock structural controls. At higher elevations, saturation of shallow and conductive soil and colluvium after snowmelt resulted in less stable flowhead locations. Therefore, the dynamics of active drainage networks can help illuminate the spatiotemporal structure of flowpaths supporting surface flow.

### 3.1 Introduction

As surficial expressions of groundwater conditions, streams provide accessible information regarding the spatiotemporal variability of subsurface storage (Biswal and Kumar, 2013; Bencala *et al.*, 2011; Kirchner, 2009). Headwater stream networks are particularly revealing as they expand and contract in response to individual precipitation events (Day, 1983 and 1978) and seasonal moisture conditions (Godsey and Kirchner, 2014; Roberts and Archibald, 1978; Blyth and Rodda, 1973; Roberts and Klingeman, 1972; Gregory and Walling, 1968). Each location where flow either surfaces or infiltrates marks a point where flow equals the ability of the subsurface to accommodate that flow, and the expansion and contraction of the active stream network potentially mirrors the spatial extent of subsurface water availability (Godsey and Kirchner, 2014). The dynamic headwaters of streams constitute most of the channel length of all stream networks (Bishop *et al.*, 2008; Leopold *et al.*, 1964), and significantly influence downstream systems.

Understanding catchment storage is important for managing water for human needs (e.g., Goyal *et al.*, 2015), evaluating riparian and terrestrial ecosystem impacts (e.g., Jaeger *et al.*, 2014; Davis *et al.*, 2013), managing stream responses to wildfire (e.g., Wagner *et al.*, 2014), and for comparing catchments (McNamara *et al.*, 2011). In order to explain drainage behavior and storage characteristics, models simplify complexities within natural watersheds and thus make important assumptions about natural systems. For example, Kirchner (2009) proposes a single-equation rainfall-runoff model based on the assumption that the drainage characteristics of a single aquifer, or a single storage-discharge relationship, can explain streamflow at the catchment-scale. Additionally,

Biswal and Marani (2010) propose a geomorphological recession flow model, which assumes drainage of an unconfined aquifer by an intersecting channel network. Furthermore, a given length of stream in this conceptualized network maintains the same discharge throughout the entire network, and the rate of stream length recession remains constant (Biswal and Marani, 2010; Biswal and Kumar, 2013). Such simplifying assumptions are a necessary and useful element in models; however, their field validation remains critical.

Quantifying watershed-scale storage characteristics is difficult, largely due to the distribution and heterogeneity of storage within snowpacks, vegetation, surface water, and especially soil moisture and groundwater (McNamara, 2011). In particular, flows between soils and bedrock at large scales are difficult to measure accurately (e.g., Gabrielli *et al.*, 2012). However, the active stream network provides a spatially extensive reflection of groundwater conditions and hydrological processes regulating surface flow throughout a catchment. Observations of the active stream network structure and fluctuations may therefore provide useful information such as whether networks fluctuate in a consistent and connected manner as required for Biswal and Marani's (2010) model, a dynamic and disconnected fashion as described by Godsey and Kirchner (2014), or fluctuate in some other manner.

Here we present field data documenting the contraction and disconnection of active drainage networks from May through August 2014 in four mountainous headwater catchments. In contrast to Godsey and Kirchner (2014), these data show more stable active drainage network dynamics with simultaneous reductions in outlet discharge. We discuss potential geologic, geomorphic, and climatic controls resulting in more stable

active drainage configurations. We also assess potential controls of individual flowhead stability. Due to the general stability of the observed active drainage networks, we consider the role of groundwater, bedrock fracture flow paths, and springs as an important source of streamflow.

## **3.2 Study Area and Methods**

### **3.2.1 Big Creek Watershed**

Big Creek is a major tributary of the Middle Fork of the Salmon River in central Idaho and flows through the Frank Church-River of No Return Wilderness. At the confluence with the Middle Fork of the Salmon River, Big Creek watershed is 1540 km<sup>2</sup> with an elevation range from 1030 m to 2900 m (USGS, 2014). Basin-wide mean annual precipitation is 70 cm, which primarily falls as snow in wet winter months, resulting in peak runoff from late spring to midsummer (USGS, 2014; Knowles *et al.*, 2006; Stewart *et al.*, 2004).

Due to semi-arid conditions and wildfire activity, lower elevation hillslopes have patchy forest cover of primarily Douglas fir (*Pseudotsuga menziesii* var. *glauca*) and Ponderosa pine (*Pinus ponderosa*) with interspersed bunchgrasses, wildflowers, and occasionally sagebrush (*Artemisia*). Higher elevation slopes are increasingly forested with Douglas fir, and sub-alpine conifers at the highest elevations. Stands of Lodgepole pine (*Pinus contorta* var. *latifolia*) dominate some slopes recovering from wildfires.

The bedrock geology consists of the Mesoproterozoic Lemhi and Neoproterozoic Windemere Supergroups, the Eocene Challis Volcanic Group, and series of Neoproterozoic, Cretaceous, and Eocene intrusive rocks (Stewart *et al.*, 2013). Primarily northeast-southwest normal faulting is due to Neoproterozoic, Cretaceous, and Eocene

extension (Stewart *et al.*, 2013). Steep hillslopes and deeply incised river canyons result from significant Neogene uplift (~10 Ma) and the related capture of the Salmon River drainage by the Snake River (~2-4 Ma) (Sweetkind and Blackwell, 1989; Meyer and Leidecker, 1999; Kirchner *et al.*, 2001). Steep slopes (averaging ~ 25 degrees) result in thin or absent soil cover, and erosion processes are dominated by rock fall and debris flows initiated from deep-seated rotational slumps (Link *et al.*, 2014).

There is clear evidence of Pleistocene alpine glaciation in the mountains of central Idaho surrounding Big Creek (Thackray *et al.*, 2004; Colman and Pierce, 1984; Dingle and Breckenridge, 1982; Evenson *et al.*, 1982; Weis *et al.*, 1972), although there are no studies documenting the glacial history of Big Creek watershed. Approximately 50 km to the north, Weis *et al.* (1972) interpreted that north and northwest facing slopes higher than approximately 2440 m supported glaciers during late Pleistocene age. Just over 100 km to the south in the Sawtooth Mountains, Lundeen (2001) calculated glacial accumulation areas extending above approximately 2400 m. Additionally, Thackray *et al.* (2004) proposes late Pleistocene glacial advances in the Sawtooth Mountains at approximately 14,000 years before present (YBP), and the most extensive advance around 16,900 YBP.

This study focuses on four tributaries to the lower reaches of Big Creek: Pioneer, Cougar, Goat, and Dunce Creeks. Pioneer Creek has a predominantly north-facing aspect, while the other three tributaries are on the north side of Big Creek and have a predominantly south-facing aspect. Pioneer and Cougar watersheds are the largest (15.8 km<sup>2</sup> and 21.4 km<sup>2</sup>, respectively) and have the greatest elevation range (approximately 1200 to 2800 m, and 1200 to 2600 m, respectively). Goat and Dunce watersheds are 7.9

km<sup>2</sup> and 6.5 km<sup>2</sup>, respectively, and both span elevations from approximately 1100 to 2500 m (Table 3.2).

The Frank Church-River of No Return Wilderness is the largest designated wilderness in the contiguous United States and has undergone minimal human disturbance. Due to the lack of dams, irrigation, or manmade impermeable surfaces, this is an ideal setting to study catchment hydrology. Although its headwaters are remote, the Salmon River is a major tributary to the Snake and Columbia Rivers, which act together as a major waterway for inland transport of goods to the Pacific Northwest, as well as a significant source of water and electric power to the region. This research is based at Taylor Wilderness Research Station (“Taylor Ranch”), a small facility along Big Creek owned by the University of Idaho.

### **3.2.2 Surface network mapping**

We mapped the extent of visible surface flow within Pioneer, Cougar, Goat, and Dunce watersheds at three times within the late spring and summer field season: a high flow survey (5/28/14 – 6/15/14), intermediate flow survey (6/25/14 – 7/9/14), and low flow survey (7/18/14 – 8/3/14). These surveys of the watershed flow network determine the spatial distribution of surface water for a given discharge as measured at the stream outlet. While hiking throughout the respective watersheds, we used a Trimble 6000 GeoXH mapping-grade Global Positioning System (GPS) with sub-meter accuracy to manually track the locations along stream channels where surface flow begins or disappears beneath the subsurface. We required segments of stream flow and breaks in stream flow to be at least 20 m in length to be mapped. Pioneer and Cougar Creek watersheds span over 15 km<sup>2</sup> of rugged terrain and required at least three days to map,

over which time small precipitation events sometimes occurred that may have minimally affected mapping; mapping was not conducted during large precipitation events.

We processed the surface flow spatial data and maps using ESRI's ArcGIS 10.2 software. The raw dataset from mapping surface flow in the field consists of two sets of GPS points: one set represents the flowheads on 'start' points of initiation of surface flow in a stream channel and the other set represents the 'end' points where surface flow ceases downstream. We delineated the channel networks using a 10 m digital elevation model (DEM) of the watersheds and the flow accumulation tool with a threshold of 50,000 m<sup>2</sup>. We then used this channel network and used the start/stop points to map only the flowing channels to create the map of the surface flow networks. Because the 10 m DEM was locally not of a high enough resolution to delineate the actual channel network, especially in the headwaters where channels are not as developed, we manually shifted sections of the delineated channel network to follow areas where riparian vegetation was distinguishable with the National Agriculture Imagery Program (NAIP) aerial photography, and ensured that they intersected with mapped start and stop points.

We estimated the error associated with calculating the length of the surface flow network based on (1) differences of stream length based on the NAIP imagery and delineated stream network from the 10 m DEM, (2) an assumed 2 m uncertainty associated with each GPS point based on the scatter of points taken at a single location, and (3) an assumed 2% error due to our threshold of mapping stream segments and breaks greater than 20 m long. We used the following equation to propagate these errors for the total length of surface flow for a given watershed:

$$S_{T_f} = \left( \sqrt{8 * all_j + \sum_{allj} (L_j * 0.014)^2} \right) + 0.02 * T_f \quad \text{Equation 3.1}$$

where the number of stream segments in a watershed is  $all_j$ , the length of a segment is  $L_j$ , and the total surface network length is  $T_f$ . This calculation requires that the stream be parceled into segments that are bound by flow start and stop points, or a stream confluence.

### 3.2.2.1 Partitioning Active Stream Length Fluctuation

A flowhead is the first location from the top of a hillslope where surface flow initiates. Partitioning fluctuations in active stream length due to movement of the flowhead versus downstream fluctuations in continuity provides further insight about how stream length is changing and how water is interacting with the surface. We calculated stream length changes due to stream discontinuity by first measuring the distance between flowhead locations between each of the three surface flow surveys  $\Delta FH$ . The sum of the distances between flowheads subtracted from the total fluctuation in active stream length  $\Delta ASL$  provides total stream length changes due to stream discontinuity  $\Delta D$ .

$$\Delta D = (\sum \Delta FH) - \Delta ASL \quad \text{Equation 3.2}$$

### 3.2.2.2 Flowhead Stability

The spatial stability of flowheads depends in part on the origins and flowpaths of the water supporting the flowhead. We quantify individual flowhead stability by calculating the difference in the flowhead accumulation area (i.e., surface area that drains



to a point) between the high flow mapping survey in late May – early June 2014 and low flow survey in late July – early August. The difference in flowhead accumulation area ( $\Delta fhAA$ ) is then divided by the accumulation area of the stream network junction ( $jAA$ ) immediately downslope of the flowhead location from the low flow survey. This last step calculates the fractional gain in flowhead accumulation area, and normalizes flowhead stability to permit comparisons across different branches and watersheds.

$$\text{normalized flowhead stability} = \frac{\Delta fhAA}{jAA} \quad \text{Equation 3.3}$$

To determine flowhead accumulation area, we used the same flow accumulation tool and 10 m DEM as used for channel network delineation. As previously mentioned, mapped surface flow start and stop points did not always fall on the delineated stream network. To estimate flowhead accumulation area accurately, we manually shifted the flowheads to the closest line of higher accumulation area (i.e., the delineated channel network).

### 3.2.3 Measuring discharge

We measured discharge at the base of Pioneer, Cougar, Goat and Duncce Creeks using a SonTek Flowtracker Acoustic Doppler Velocimeter (ADV). Manual discharge measurements were used in conjunction with continuous gage height data from a pressure gage (In-Situ LevelTROLL 500) placed in a PVC well anchored at each stream edge in order to develop stage-discharge rating curves. This study site is in federally designated wilderness, and installing weirs for ideal gaging is not possible; thus, maintaining rating curves is critical for accurate hydrographs in these dynamic smaller mountain streams. Each year's spring peak runoff event typically alters the channel geometry. Due to the dynamic nature of these channels, the continuous gage height data will sometimes show

unrealistic shifts in gage height as a result of sedimentation events. Thus, shifting and cleaning the data is necessary to produce reasonable hydrographs. We followed the quality control processing of the stage data developed by Tennant (2011).

Pioneer Creek pressure gage data from the 2014 field season was unreliable due to instrument malfunction. Instead we modeled the 2014 Pioneer Creek hydrograph using the relationship between the Pioneer Creek hydrograph from the past four years and USGS records from five surrounding gaging stations: Thompson Creek (13297330), Blackbird Creek (13306336), Johnson Creek (13313000), Meadow Creek (13310850), and the Middle Fork Salmon (13310199). We used the SAS Institute's JMP 11 to develop a standard least squares multiple linear regression model with an  $R^2$  of 0.86 and AIC of -78006.3.

Equation 3.4

$$\text{Pioneer Ck. } Q \text{ (m}^3\text{/s)} = a + \text{Corrected Blackbird Ck.} + \text{Corrected Meadow Ck.} + \text{Corrected Johnson Ck.} + \text{Corrected Middle Fork Salmon} + \text{Corrected Thompson Ck.}$$

USGS Gage Location or Constant		Correction factor or constant
a (constant)		0.016
Blackbird Ck. (13306336)	If Intact	0.054*Q
	If Missing	0.0212
Meadow Ck. (13310850)	If Intact	-0.174*Q
	If Missing	-0.0144
Johnson Ck. (13313000)		0.003*Q
Middle Fork Salmon (13310199)		0.001*Q
Thompson Ck. (13297330)		-0.094*Q

Table 3.1: Correction factors for the Pioneer Creek multiple linear regression model. Q represents the daily flow measured at each of the stations. The numbers in parentheses refer to the USGS gage location.

Discharge associated with the surface flow surveys was measured one or two days before and after mapping and then averaged, and normalized by basin area for runoff calculations reported below.

### 3.3 Results and Discussion

#### 3.3.1 Stream length to discharge relationships

The average drainage density (km/km<sup>2</sup>) (Table 3.2) decreased by a factor of 1.16±0.06 the high flow surveys (5/28/14 – 6/15/14) and the low flow surveys (7/18/14 - 8/3/14) conducted at Pioneer, Cougar, Goat, and Dunce Creeks. These results reflect that

the active stream length fluctuated little between late May and early August 2014 (Figure 3.1). Stream discharge, however, decreased by a factor of approximately 3.18, 14.53, 2.28, and 2.80 at Pioneer, Cougar, Goat, and Duncce Creeks, respectively. We plot total stream length as power functions of runoff with log-log slopes,  $\beta$  (Figure 3.2). Previous studies of active network fluctuations with discharge have reported clear power-law relationships ( $\beta$ ) (e.g., Gregory and Walling, 1968; and other works summarized by Godsey and Kirchner, 2014).  $\beta$  values from the lower Big Creek tributaries are smaller than the average  $\beta$  of  $0.234 \pm 0.028$  from the studies summarized by Godsey and Kirchner (2014) (Figure 3.2). Only Pioneer watershed has a similar  $\beta$  value, for reasons we will discuss in Section 3.3.2.4.

Active stream lengths of the lower Big Creek tributaries are not as responsive to changes in discharge compared to the average stream, assuming past network studies are representative of global headwaters. However, the distribution of  $\beta$  across all sites is positively skewed, indicating that like the Big Creek tributaries studied here, many other streams previously studied are relatively unresponsive to changes in discharge (Figure 3.3).

Big Ck. Tributary	Watershed Area (km <sup>2</sup> )	Watershed Altitude (m)	Survey Date(s)	Average Discharge (m <sup>3</sup> /s)	ADN Length (km)	Drainage Density (km/km <sup>2</sup> )	$\beta$ (s.e.)
Pioneer	15.8	1200 - 2800	5/28 - 5/31	0.404±0.022	15.234±0.363	0.97	0.197±0.037
			6/25 - 6/27	0.163±0.008	13.129±0.320	0.83	
			7/18 - 7/20	0.127±0.006	11.960±0.296	0.76	
Cougar	21.4	1200 - 2600	6/6 - 6/10	0.462±0.016	39.177±0.879	1.83	0.083±0.10
			7/4 - 7/6	0.087±0.003	33.402±0.761	1.56	
			8/1 - 8/3	0.032±0.001	31.470±0.721	1.47	
Goat	7.9	1100 - 2500	6/19 - 6/20	0.018±0.001	8.319±0.219	1.06	0.055±0.024
			7/9	0.012±0.001	8.002±0.212	1.02	
			7/27	0.008±0.001	7.949±0.211	1.01	
Dunce	6.5	1100 - 2500	6/15	0.025±0.002	4.422±0.122	0.68	0.093±0.013
			7/8	0.013±0.001	4.117±0.116	0.64	
			7/26	0.009±0.001	4.028±0.113	0.62	

Table 3.2: Lower Big Creek tributary characteristics, including streamflow and active drainage network (ADN) data for calculating  $\beta$ . All mapping surveys were completed in 2014.

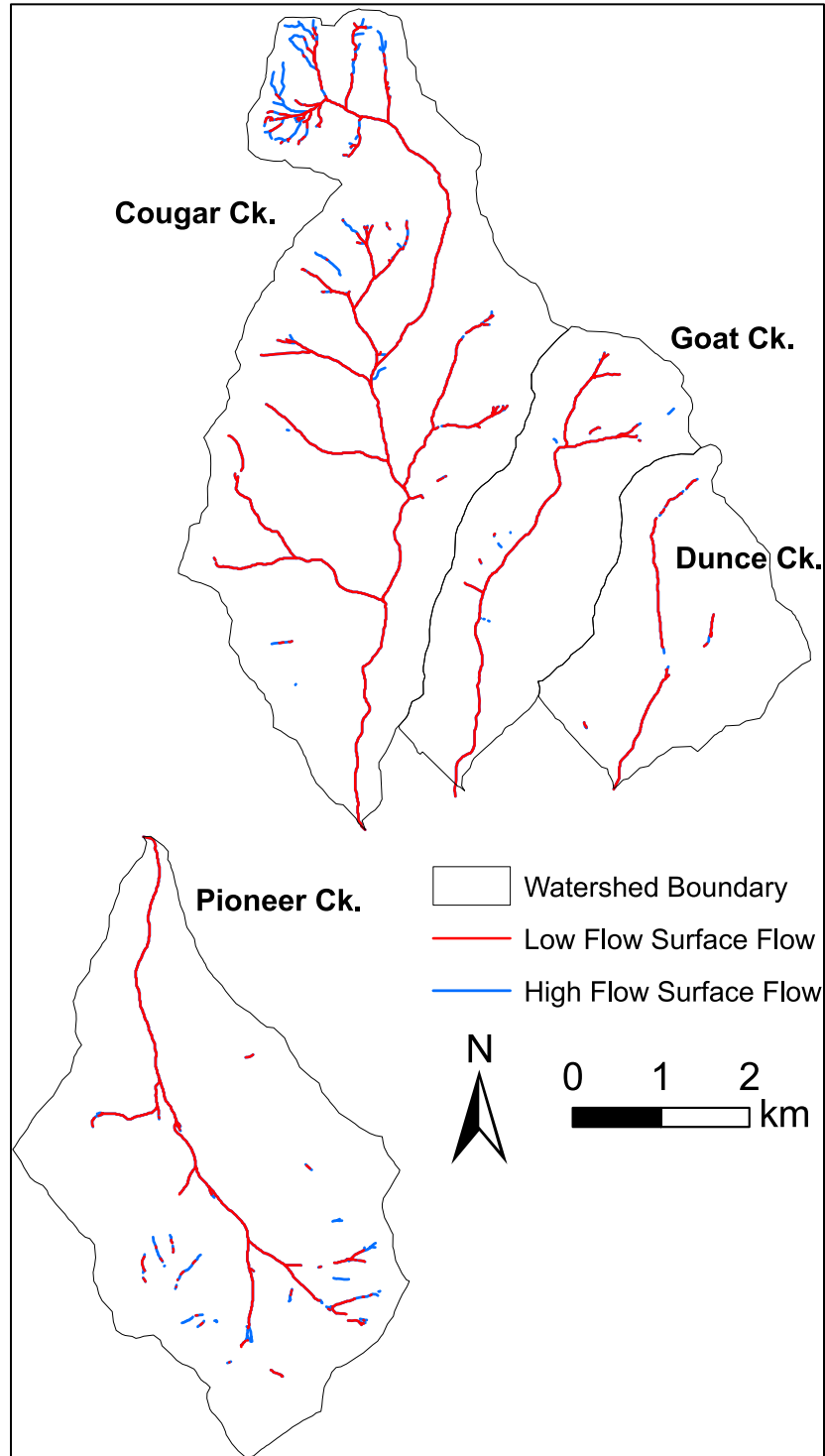


Figure 3.1: Surface flow mapped during the low flow surveys (7/18/14 – 8/3/14) in red overlies surface flow mapped during the high flow surveys (5/28/14 – 6/15/14) in blue. The lack of blue in the map indicates that the active stream length did not fluctuate much during late May – early August 2014.

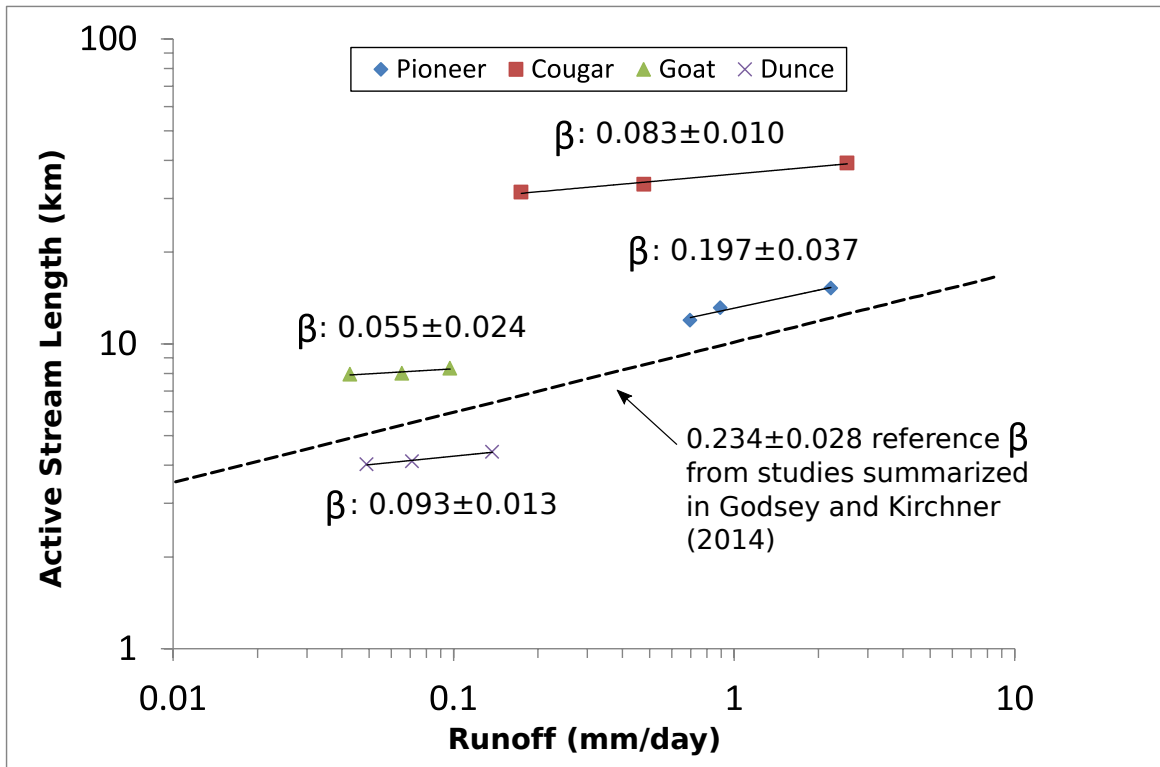


Figure 3.2: Active stream length (km) is plotted against runoff (mm/day) in log-log space.  $\beta$  (slope of the power law relationship) and standard error values for each of the lower Big Creek tributaries are labeled. All of the lower Big Creek tributaries have smaller  $\beta$  values than the average calculated from studies summarized in Godsey and Kirchner (2014). Active stream lengths at Big Creek are therefore less responsive to changes in runoff than the average. The error associated with each measurement of active stream length is about the same size, or smaller, than the size of the point plotted above.

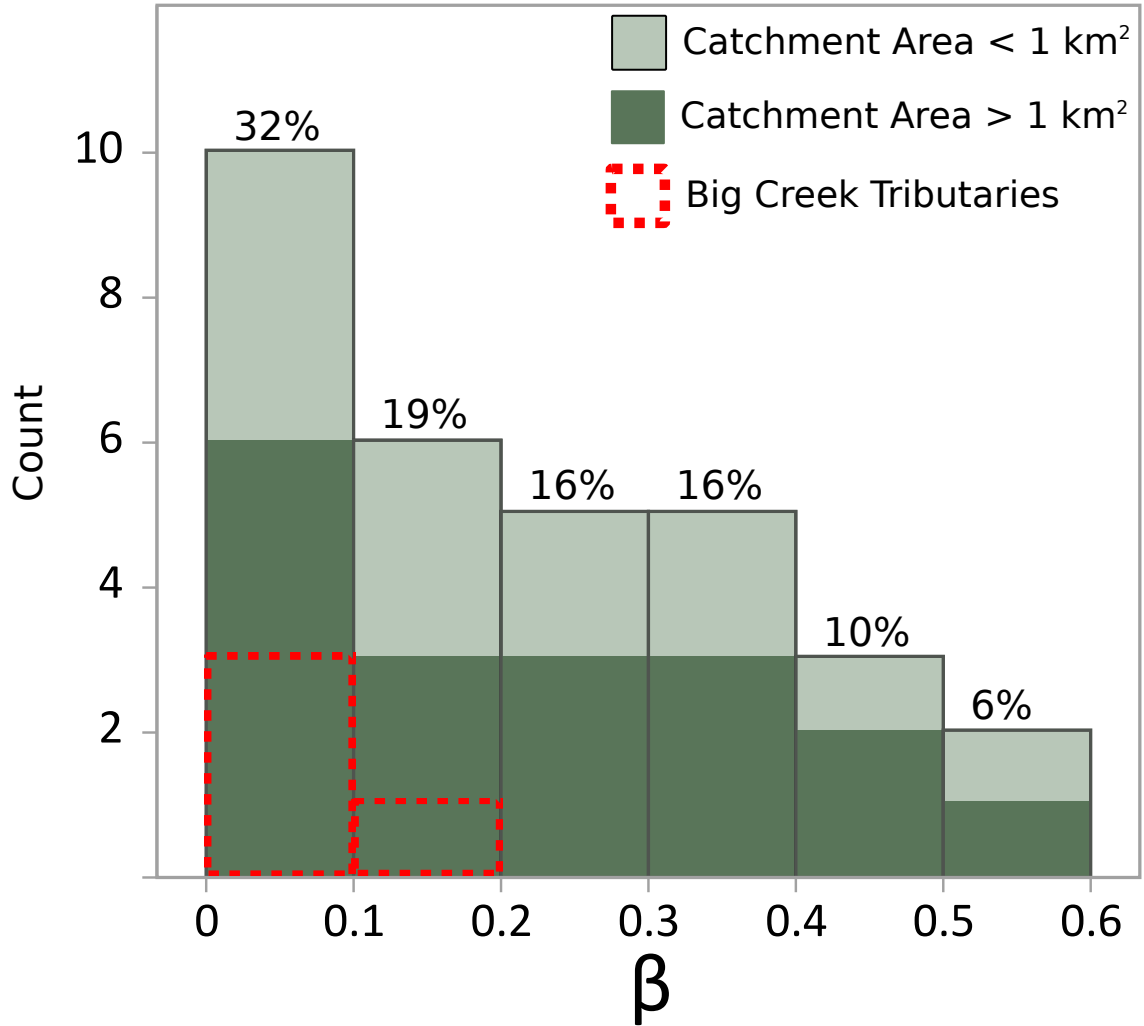


Figure 3.3: The distribution of  $\beta$  from the lower Big Creek tributaries of this study and the 27 other sites summarized in Godsey and Kirchner (2014). The studies from catchments less than 1 km<sup>2</sup> are colored light green, while the studies from catchments greater than 1 km<sup>2</sup> are colored dark green. Catchments greater than and less than 1 km<sup>2</sup> in area exhibit similar distributions of  $\beta$ . Additionally, the lower Big Creek tributaries plot on the positively skewed end of the histogram, meaning other streams are also relatively unresponsive to changes in runoff.



### **3.3.2 Geologic and Geomorphic Influence on Surface Flow Extent**

#### **3.3.2.1 Geology and Springs**

Active stream length might be insensitive to changes in discharge for a variety of reasons, including networks being primarily spring-fed. In the field, we observed and mapped many spatially stable spring locations where surface flow initiated. Spring discharge often became less vigorous throughout the season, but the spring location remained the same. Approximately 61%, 51%, 53%, and 91% of the changes in stream length between the high and low flow surveys were due to discontinuities in surface flow at Pioneer, Cougar, Goat and Duncce Creeks, as opposed to downslope migration of the initial surface flow expression (Figure 3.1).

It is likely that the locations of many springs within the lower Big Creek tributaries are primarily controlled by bedrock features (e.g., joints, faults, contacts, etc.) (Figure 3.4). For example, flowheads align approximately with geologic contacts of intrusive dikes in Cougar and Goat watersheds and mapped normal faults in Pioneer and Cougar watersheds (Figure 3.4). We present a conceptual model showing possible stream network end members: stable spring and alluvial/colluvial layer above less conductive bedrock would produce a more stable surface flow network than a stream network sourced primarily by shallow soil and regolith layers (Figure 3.5). In Figure 3.5A, the spring emerges at the approximate intersection of the controlling bedrock feature with the surface. Surface flow occurs where channel water depth is greater than the depth of the alluvial or colluvial layer overlying less conductive bedrock. In Figure 3.5B, surface flow begins only where the channel surface intersects the shallow

soil/colluvium layer that remains above field capacity and is subject to changing locations as this layer drains or fills.

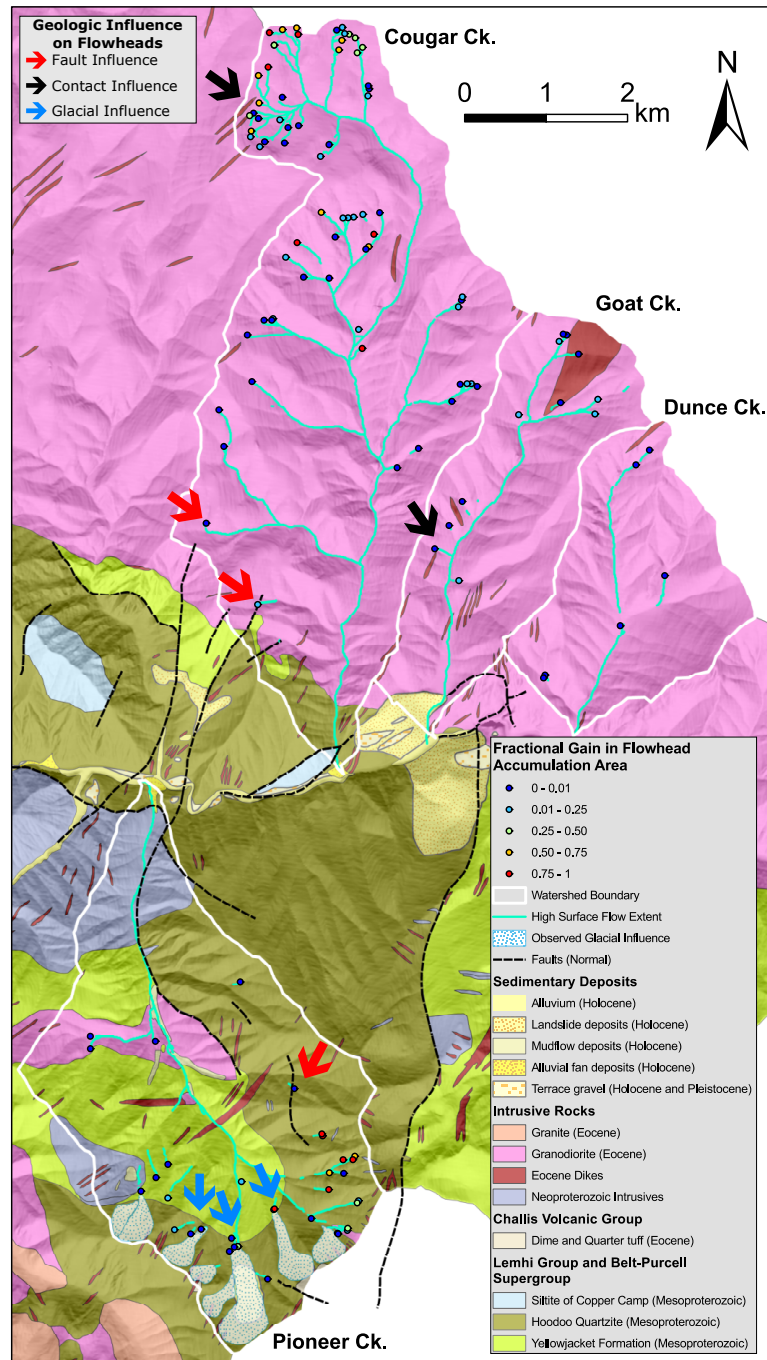


Figure 3.4: The bedrock geology of lower Big Creek by Stewart *et al.* (2013), overlain by locations with observed glacial influence, the high flow active stream network and flowheads. Flowheads are color-coded based on their spatial stability with more stable flowheads in blue and less stable in red. Arrows indicate examples of flowheads likely influenced by faulting, geologic contacts, or glacial geomorphology.

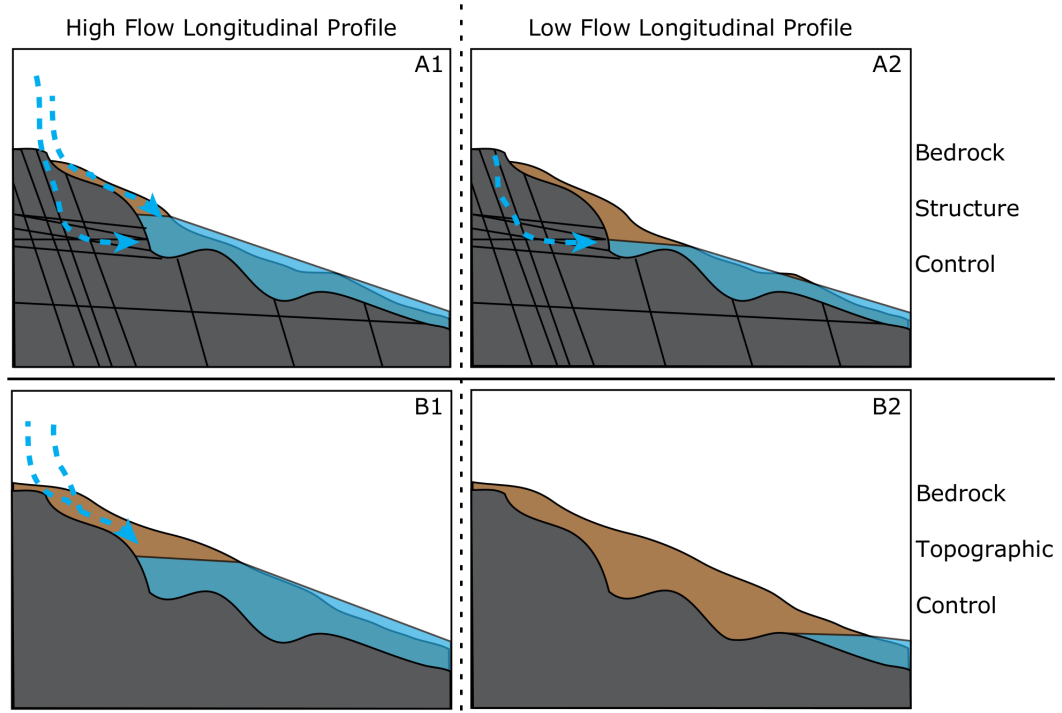


Figure 3.5: This conceptual model illustrates the two end-member controls on stream stability. (A) Streams are likely to be more stable when supplied by deeper bedrock aquifers via stable spring locations where conductive bedrock features (e.g., joints, faults, contacts, etc.) meet the surface. (B) Streams are likely to be less stable when supported primarily by shallow soil/colluvium layers.

### 3.3.2.2 Flowhead Stability and Accumulation Area

The two end-member controls on stream stability in Figure 3.5 could lead to distinct patterns of flow persistence: Figure 3.5A would be more stable than Figure 3.5B. We quantify the spatial stability of the initial surface flow expression, or flowheads, within the lower Big Creek tributaries. The stability of flowheads indicates the stability of the subsurface water source, and more stable sources are likely due to slow, long, and deep flowpaths (Figure 3.6A), potentially through saturated bedrock fracture networks (Figure 3.5A). We hypothesize that flowheads with larger accumulation areas (based on

surface topography) during the high flow survey will be more stable because longer, deeper, and slower flow paths support these locations from further upslope (i.e., at these locations there is more likely to be a larger bedrock aquifer contribution to flow than at flow heads with smaller accumulation area (Figure 3.6)).

Flowheads supported by large initial accumulation areas are reliably more stable than flowheads with smaller initial accumulation areas (Figure 3.7). However, there is considerable variability in the stability of flowheads with small high flow initiation accumulation areas (Figure 3.7). In some instances, small accumulation areas may result in a greater dependence of flow from more ephemeral, potentially shallow soil and regolith layers; in other instances, these locations may have more stable sources despite a small surface accumulation area. Thus, bedrock features controlling the spring location and flow may not be well reflected by surface topography. These findings are consistent with previous studies that suggest surface topography is not the best predictor of hillslope moisture conditions (Gannon *et al.*, 2014; Zimmer *et al.*, 2013; Tromp-van Meerveld and McDonnell, 2006; Buttle *et al.*, 2004; Freer *et al.*, 2002).

To further test whether flowhead stability can provide an accurate estimate of supporting flowpath characteristics we need to better assess the source aquifers of the springs and other flow initiation points throughout these watersheds. Isotopic analyses of water samples from these locations would provide valuable information on the water's origins, and flowpath similarly to studies like Mueller *et al.*, (2014), and Liu *et al.* (2013). Geophysical data similar to that collected by Daesslé *et al.* (2014) and Bièvre *et al.* (2012), would provide a more direct view of the subsurface and potential flowpaths, as

well as a network of wells penetrating into the bedrock immediately upslope of flow initiation points.

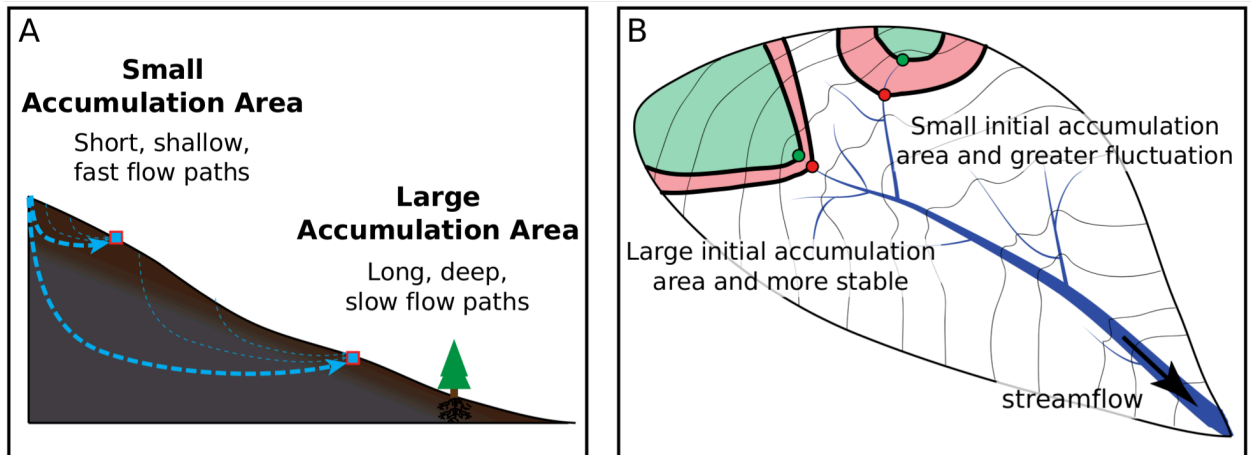


Figure 3.6: (A) Flowheads with small accumulation areas are supported by short, shallow, and fast flow paths, while flowheads with large accumulation areas are supported by long, deep, and slow flow paths. (B) Therefore, flowheads with large initial accumulation areas should be more spatially stable than those flowheads with small initial accumulation areas.

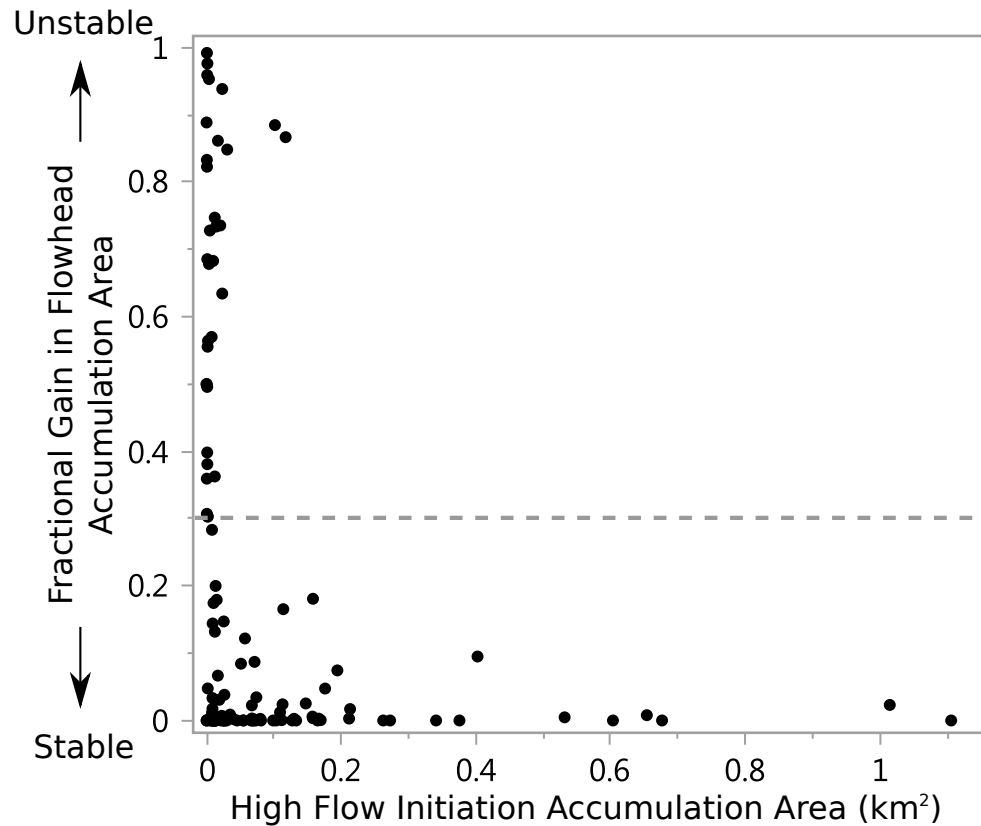


Figure 3.7: Fractional gain in flowhead accumulation area is a measure of flowhead stability. Flowheads that do not move will plot as zero on the Y-axis, while flowheads to stream branches that disappear completely will plot as one on the Y-axis. Flowheads with larger accumulation areas (i.e.,  $> 0.2 \text{ km}^2$ ) during the high flow surveys are fairly stable, while flowheads with smaller initial accumulation areas are more varied in stability. The error associated with each of the data points is smaller than the points themselves. The points above the dotted line represent those flowheads that are unstable (i.e.,  $> 0.25$  fractional change in flowhead accumulation area), which are the green, yellow, and red dots in Figure 3.4 and Figure 3.8.

### 3.3.2.3 Elevation and Aspect and Flowhead Stability

Flowhead stability also appears to be influenced by elevation and aspect. Flowhead stability depends on: (1) the timing of snowmelt, subsurface storage, and drainage throughout the watershed; and (2) geomorphology and near-surface hydrogeology, which impact the structure of aquifers and flow throughout the watershed. Approximately 88% of unstable flowheads ( $> 0.25$  fractional change) are above 2,200 m. This is probably due to the influence of snowmelt. During the beginning of the surveys in late May, the snowline was around 2000 m and quickly retreating upslope. Thus, flowheads may have been at higher locations during the short period when surrounding soils and colluvium were saturated, if watershed elevations extended above approximately 2000 m. Because snowpacks below approximately 2000 m are smaller and melt multiple times throughout the winter, spring snowmelt at lower elevations has a limited effect on flowhead extent. Less than 14 % of Goat and Dunce watersheds are above 2,200 m, compared to greater than 26% of Pioneer and Cougar watersheds, and thus exhibit much more stable flowheads compared to flowheads at higher elevations within Pioneer and Cougar watersheds. This is consistent with long-term isotopic analysis from springs suggesting that as snowpacks diminish water becomes increasingly older (Manning *et al.*, 2012; Rademacher *et al.*, 2005), and thus rain-dominated catchments should rely on long and deep flowpaths supporting stable flowheads.

In Pioneer watershed, the less stable flowheads are on the higher west-facing slopes, compared to the more stable flowheads on the high northeast facing slopes (Figure 3.4). In Pioneer watershed, aspect likely influenced the glacial history, and thus, present surface hydrology. High, northeast-facing slopes are the most sheltered from

solar radiation and therefore sustain larger and longer-lived snowpacks. In these locations, we observed glacial features like bowl-shaped cirques and moraines (Figure 3.4), which is consistent with studies describing glacial features in the mountains surrounding Big Creek (Thackray *et al.*, 2004; Colman and Pierce, 1984; Dingler and Breckenridge, 1982; Evenson *et al.*, 1982; Weis *et al.*, 1972). Bare rock on steep cirque walls does not support enough storage to sustain flow, and the highly conductive debris collected in the bottoms of these bowls allows for rapid infiltration of meltwater. This meltwater resurfaces downslope at more stable locations below likely terminal moraines, where the thickness of highly conductive debris diminishes. There is no evidence of glaciation on Pioneer watershed's steep west-facing slopes, likely a result of greater solar radiation exposure than the northeast-facing slopes at similar elevations. The lack of glacial cover on these slopes has allowed for the development of a more substantial, albeit thin, soil/colluvium layer. This thin layer supports ephemeral subsurface storage of snowmelt leading to less stable flowheads.

Considering the glacial evidence in Pioneer watershed is restricted to small cirque glaciers, it is likely that these glaciers belonged primarily to the locally more extensive advance at approximately 16,900 YBP suggested by Thackray *et al.* (2004) for the Sawtooth Mountains. The glacial history of Big Creek and classification of these features certainly deserve more attention because differences in flow permanence among watersheds may depend on a clearer understanding of their surficial geology.

In Cougar watershed, aspect also influences the timing of snowmelt and flowhead stability (Figure 3.8). In early June there was still snow at the highest elevations, with rapid melt observed on the south-facing slopes. By the mid June survey, snow was



melting rapidly throughout the upper Cougar watershed, and it was largely gone by the early August survey. The timing of these surveys may have led to the south-facing high-elevation flowheads to appear less stable than the north-facing high-elevation flowheads (Figure 3.8), simply because the north-facing slopes did not have as much time to drain following primary snowmelt. Aspect may additionally impact freeze-thaw conditions that can influence near-surface bedrock fracturing. Thus, decreased weathering on more south-facing slopes may result in a thinner and less developed soil/regolith layer which drains snowmelt faster (Hinckley *et al.*, 2014; Anderson *et al.*, 2013; Lifton *et al.*, 2009).

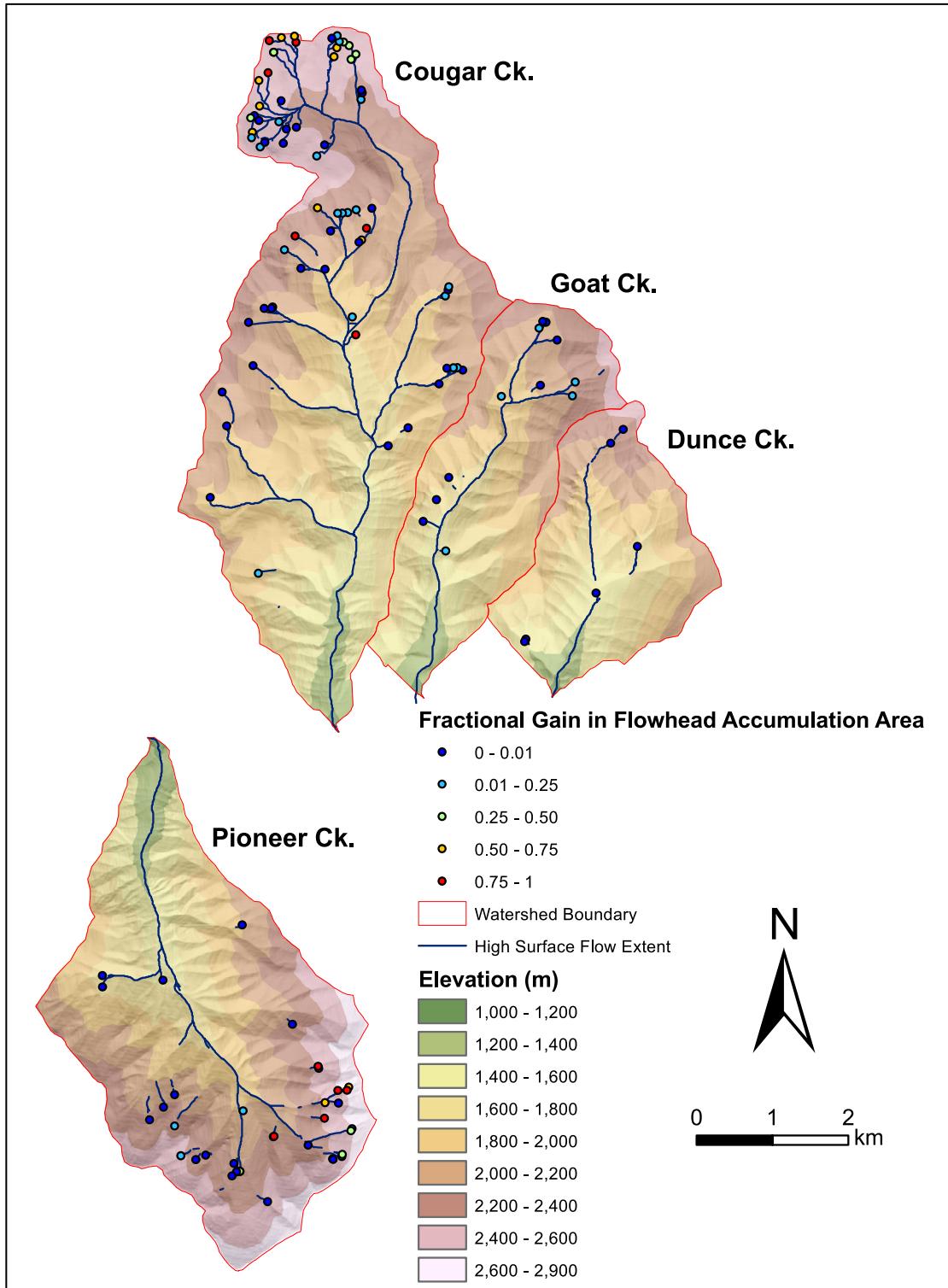


Figure 3.8: A topographic map of the studied watersheds, overlain by the high flow active stream network and flowheads. Flowheads are color-coded based on their spatial stability. Flowheads at lower elevations are generally more stable than those at higher elevations. High elevation flowheads on south or southwest-facing slopes tend to be less stable, than those on north-facing slopes.

### 3.3.2.4 Geology and Stream Length Fluctuations

Active stream length varies less with discharge at all the lower Big Creek tributaries compared with the average of other streams surveyed (Godsey and Kirchner, 2014). As discussed in Section 3.3.2.1, this is most likely due to the presence of stable springs controlled by fixed bedrock features, and the proportionately small influence of the thin, and highly conductive shallow soil layers that overlie bedrock on steep slopes. Among the lower Big Creek tributaries, only Pioneer watershed has a stream length - runoff power law exponent, or  $\beta$  value, similar to that of the  $0.234 \pm 0.028$  average of streams summarized in Godsey and Kirchner (2014) (Figure 3.2). This difference between Pioneer watershed, and the other tributaries may be largely geologic and geomorphic. All of the lower Big Creek tributaries have primarily stable spring locations throughout their watersheds; on average, 64% of stream length changes primarily reflect fluctuations in downstream surface flow continuity. Pioneer watershed exhibits surface flow at high elevation, small accumulation area locations. However, that surface flow then infiltrates into blocky, highly conductive colluvium and resurfaces in the mainstream or just before entering the mainstream. By contrast, once surface flow initiates along the channels of Cougar, Goat, or Dunce watersheds, it is more likely to remain at the surface. We hypothesize that these differences are primarily due to different weathering characteristics of Pioneer watershed's quartzite and metasedimentary rocks compared to the granodiorite that dominates the terrain north of Big Creek (i.e., Cougar, Goat, and Dunce watersheds) (Figure 3.9 and Figure 3.4). The quartzite and other metasedimentary rocks of Pioneer watershed break into highly conductive large blocks and cobbles that collect in valley bottoms (Figure 3.9A). Once flow encounters this thickening layer of

conductive blocky debris, it rapidly infiltrates until that layer shallows to a point less than the thickness of the saturated debris, or to a point when there is enough water to transport the debris. In Pioneer watershed, there are numerous locations where there is not enough water to clear a significant channel through the valley-bottom blocky debris until the main channel. Conversely, in Cougar, Goat and Duncce watersheds, the granodiorite generally weathers into a finer, sandy grus that is transported by comparatively much less flow, and thus stream channels are initiated and maintained throughout greater extents of these watersheds (Figure 3.9B).

It is also likely that fracture and joint geometries differ within granodiorite and the metasedimentary units. This would influence deeper flowpath and storage characteristics potentially resulting in differences in active drainage network response to discharge.

Suspended sediment and pebble transport analyses may help quantify the differences of bedrock weathering and channel development within metasedimentary versus granodioritic bedrock. Also, green LiDAR would allow for more detailed analysis of difference between channel geometries. It is likely that in granodiorite-dominated areas smaller fluvial channels will be detectable, while in areas underlain by metasedimentary rocks channel development will only occur at larger scales where flows are great enough to transport large debris.

### Longitudinal Stream Profiles

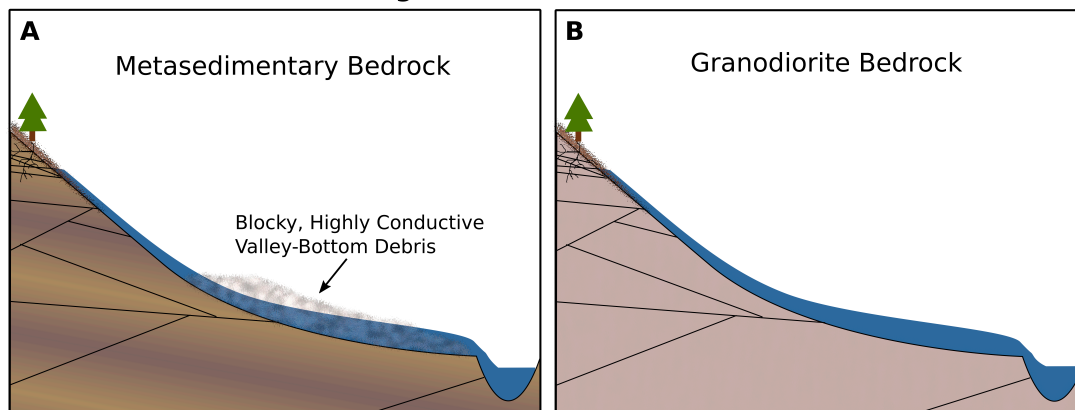


Figure 3.9: (A) The metasedimentary rock the predominantly underlies Pioneer watershed weathers into large blocks and cobbles that collects in valley bottoms. Streams will infiltrate into this highly conductive debris until water depth is greater than debris thickness. (B) The granodiorite that predominantly underlies Cougar, Goat, and Dunce watersheds weathers into a sandy grus, which smaller streams are more capable of transporting. Thus, streamflow through granodiorite is more continuous.

#### 3.3.2.5 Local Hillslope Geomorphology and Flowhead Stability

Local hillslope geomorphology should affect flowhead stability, and to some degree, flowhead stability will influence local geomorphology. We calculate curvature perpendicular (i.e., plan curvature) to the channel at each flowhead using the ArcGIS curvature tool and the 10 m DEM used for previous analyses. Because this calculation involves the DEM cell of the flowhead and the immediately adjacent cells, curvature perpendicular to the channel is measured across approximately 30 m. Thus curvature is measured over a distance greater than any channel width encountered, instead the channel and at least 10 m of hillslope on either side of the channel are incorporated. More concave slopes will have more negative curvature values, while convex features have

positive curvatures. Our initial hypothesis is that stable flowheads should be in more concave regions where flowpaths converge, while unstable flowheads will be on more planar slopes where flowpaths more likely parallel each other. When the curvature of the flowheads of the lower Big Creek tributaries is plotted against flowhead stability, we recognize four groupings of points for flowheads active during the relatively high flows of May 2014 (Figure 3.10). Two groups support our initial hypothesis: Group A consists of stable flowheads that are in within concave hillslopes and group B represents less stable flowheads that are in more planar hillslopes. We observe that group B flowheads are primarily on shallow gradients and supplied by unsaturated and highly conductive soil and debris layers largely fed by snowmelt, such as those flowheads in the most northern section of Cougar Watershed. Group C represents unstable flowheads that occur on concave hillslopes. This group directly contradicts the hypothesis; these flowheads are on steep slopes at high elevations, and are thus likely avalanche and rock fall paths. The small, high-elevation accumulation areas and the very thin soil and debris layers that support these flowheads rapidly release infiltrated snowmelt and are thus ephemeral. Group D consists of stable flowheads that are not on significantly concave slopes. We hypothesize that the group D flowheads are smaller, but persistent springs controlled by stable bedrock features that do not parallel surface topography.

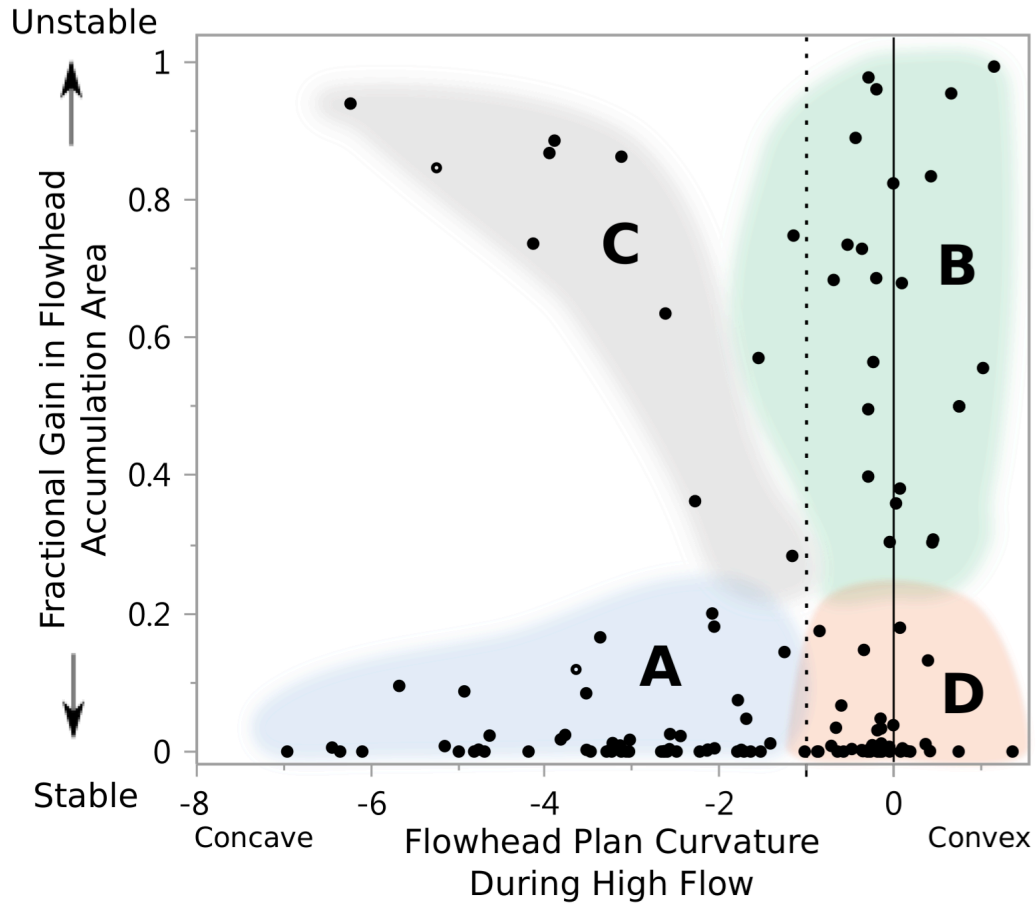


Figure 3.10: Fractional gain in flowhead accumulation area (i.e., flowhead stability), plotted against high flow flowhead plan curvature. This is curvature measured perpendicular to flow using a 10 m resolution DEM. Group A represents more stable flowheads on concave hillslopes. Group B represents less stable flowheads on planar hillslopes. Group C represents unstable flowheads in concavities likely carved by rockfall and avalanches with little surface storage. Group D represents stable flowheads on planar slopes. The open symbols represent data points that do not correspond with their respective group. The open symbol in group A is located within a rockfall/avalanche area, while the open symbol in group C is located just downslope of a moraine.

In addition to hillslope curvature, accumulation area explains some of the variation in the stability of flowheads supporting the surface flow of the lower Big Creek tributaries. Figure 3.7 and Figure 3.10 group B show that there are unstable flowheads with small accumulation areas located on planar hillslopes, which suggests they are fed by ephemeral, highly conductive, shallow aquifers that parallel surface topography. However, approximately 65% of the mapped flowheads are stable (i.e., less than 25% fractional gain in flowhead accumulation area). We hypothesize that stable flowheads are likely supplied by long, deep, and slow flowpaths via bedrock aquifers (Figure 3.6). Because so many flowheads within the lower Big Creek tributaries are stable, we expect that subsurface geometry and bedrock characteristics strongly control the active drainage network and a significant portion of the hydrograph.

### **3.3.3 Streamflow recession**

High elevation snowpacks in the lower Big Creek watersheds typically persist greater than 180 days in the average year (Tennant *et al.*, 2014). The mountains then shed this stored water during the spring and early summer melt. In 2014, after the snowmelt-induced peak flows, an approximately 28-day period of rapid recession at Pioneer Creek transitioned to an asymptotic recession (Figure 3.11). Pioneer watershed releases most of its water roughly six times faster than it accumulates as autumn and winter snowpacks; it releases the melt via short, fast, and shallow flow paths through thin soil and colluvium layers. The onset of the asymptotic flow recession at the beginning of July suggests the transition to deeper groundwater (bedrock aquifer) dependent baseflows with very little excess mobile water entering the stream from the highly conductive



shallow soil and debris layers. Low flow conditions initiate towards the beginning of July and persist until the end of the study period.

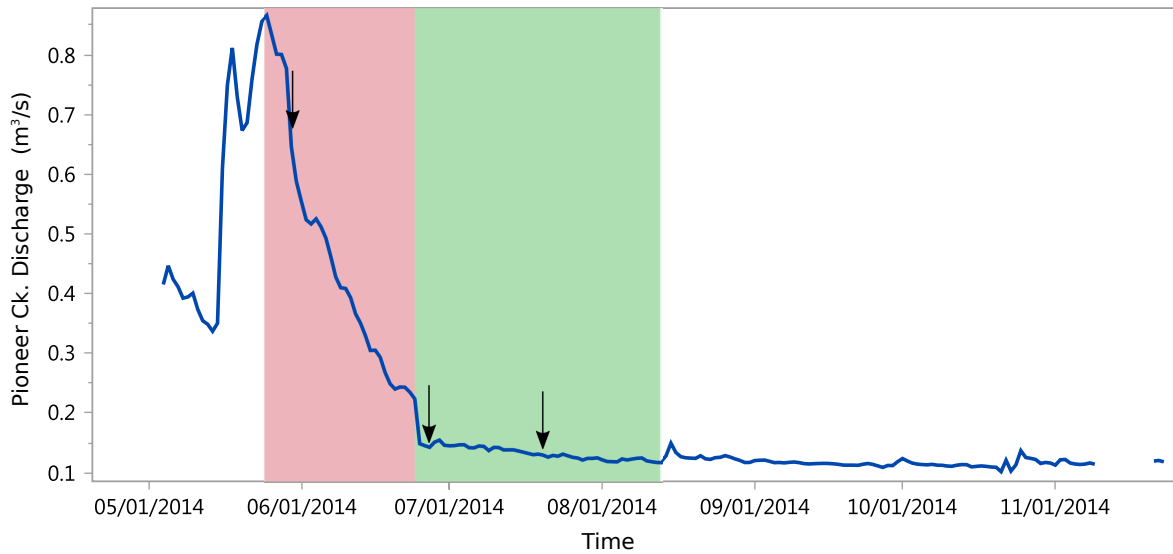


Figure 3.11: Pioneer Creek hydrograph. The rapid recession period (red) extends from 5/25/2014 to 6/24/2014, followed by a more gradual asymptotic recession. The rapid recession fits a log-log slope of  $-1.63$  ( $R^2 = 0.98$ ,  $p < 0.0001$ ), and the asymptotic recession from 6/25/2014 to 8/13/2014 (green) fits a log-log slope of  $-0.39$  ( $R^2 = 0.92$ ,  $p < 0.0001$ ). Arrows indicate the three active drainage network surveys of Pioneer Creek on 5/28/2014, 6/25/2014 – 6/27/2014, 7/18/2014 – 7/20/2014.

### 3.4 Conclusions

We determined that the extent of active drainage networks of the lower Big Creek tributaries were less responsive to changes in discharge than at many other locations during spring and summer 2014. Furthermore, downstream flowhead migration accounted for less than half of the changes in the active drainage network. This suggests that many extremities of the active network are anchored by springs.

Flowheads with large accumulation areas during the first survey in May were usually stable due to slow and deep flowpaths. Many flowheads with initially small

accumulation areas were also stable. Some flowpaths may not correspond with surficial topography, but instead are controlled by bedrock features unconnected to surface topography. Some stable flowheads were located on planar hillslopes, where we would normally expect to find non-converging, ephemeral flowpaths. Furthermore, flowheads at elevations below approximately 2000 m where snow persisted in late May 2014 were predominantly stable, suggesting that low elevation flowheads (i.e., less than 2000 m) relied on deep aquifers throughout the study period.

The Pioneer Creek hydrograph exhibits a steep recession from May through June 2014, followed by an asymptotic baseflow recession from June through September. We interpret this as an absence of fast-draining excess water from shallow, highly conductive aquifers. The gradual recession of flow from late June through September emphasizes the importance of perennial groundwater supporting streamflow during much of the growing season.

At high elevations, where the most substantial snowpacks develop, snowmelt controls the fluctuation of the active drainage networks during the late May through early August study. Flowheads on high-elevation south-facing slopes were typically less stable than flowheads on north-facing slopes, potentially due to thin, fast draining soil/regolith layers. Glacial geomorphology on the high-elevation north-facing slopes of Pioneer watershed resulted in stable flowheads at or downslope of potential moraine deposits. High-elevation north-facing slopes of Cougar watershed had stable flowheads, which we attribute to high rates of weathering and associated soil/regolith layers capable of storing melt waters.

Our survey of the active drainage network emphasizes a more complex reality than is often represented in models (e.g., Biswal and Marani, 2010; Kirchner 2009). Based on variations in flowhead stability with observed geomorphic characteristics, we suggest that deep, bedrock flowpaths in addition to shallow, ephemeral melt flow are important. Isotopic analyses, similar to that of Mueller *et al.* (2014) and Liu *et al.* (2013), of flowhead water from different elevations and different spatial stabilities would identify the length and rate of flowpaths supporting surface flow. Geophysical mapping, like that of Daesslé *et al.* (2014) and Bièvre *et al.* (2012), upslope of flowheads could provide imagery of bedrock topography and structure. These analyses would further test our hypotheses linking greater flowhead stability to long, slow, bedrock flowpaths.

Future work should continue to investigate streamflow and active drainage network dynamics of catchments across a variety of climates, spatial scales, geomorphology and underlying geology (e.g., Tague and Grant, 2009). A more diverse dataset of active drainage network studies could provide further insight into controls on network stability in a variety of settings. It is also uncertain how variable active drainage networks are beyond the seasonal scale. While streamflows have been changing due to the warming climate (Barnett *et al.*, 2005; Stewart *et al.*, 2004), the behavior of active drainage networks may also change in mountainous watersheds as more precipitation falls as rain. We may be able to deduce the susceptibility of stream networks to changes in climate by surveying active drainage networks across years with different amounts of rain and snow, and different ratios of rain and snow. Hydrograph patterns, flow connectivity, and drought susceptibility to climate change suggest the need for an improved understanding of the spatial distribution of flowpaths supporting streamflow.

## References

- Anderson, R. S., Anderson, S. P., & Tucker, G. E. (2013). Rock damage and regolith transport by frost: An example of climate modulation of the geomorphology of the critical zone. *Earth Surface Processes and Landforms*, 38(3), 299–316.
- Barnett, T. P., Adam, J. C., & Lettenmaier, D. P. (2005). Potential impacts of a warming climate on water availability in snow-dominated regions. *Nature*, 438(7066), 303–309.
- Bencala, K. E., Gooseff, M. N., & Kimball, B. A. (2011). Rethinking hyporheic flow and transient storage to advance understanding of stream-catchment connections. *Water Resources Research*, 47(3).
- Bièvre, G., Jongmans, D., Winiarski, T., & Zumbo, V. (2012). Application of geophysical measurements for assessing the role of fissures in water infiltration within a clay landslide (Trièves area, French Alps). *Hydrological Processes*, 26(14), 2128–2142.
- Bishop K, Buffam I, Erlandsson M, Laudon H, Seibert J, & Temnerud J. (2008). Aqua Incognita: the unknown headwaters. *Hydrological Processes*, 1–4.
- Biswal, B., & Marani, M. (2010). Geomorphological origin of recession curves. *Geophysical Research Letters*, 37(24).
- Biswal, B., & Nagesh Kumar, D. (2013). A general geomorphological recession flow model for river basins. *Water Resources Research*, 49(8), 4900–4906.
- Blyth K, & Rodda J. (1973). A Stream Length Study. *Water Resources Research*, 9(5): 1454-1461.
- Buttle, J. M., Dillon, P. J., & Eerkes, G. R. (2004). Hydrologic coupling of slopes, riparian zones and streams: An example from the Canadian Shield. *Journal of Hydrology*, 287(1-4), 161–177.
- Colman, S. M., & Pierce, K. L. (1986). Glacial sequence near McCall, Idaho: Weathering rinds, soil development, morphology, and other relative-age criteria. *Quaternary Research*, 25(1), 25–42.
- Daesslé, L. W., Pérez-Flores, M. A., Serrano-Ortiz, J., Mendoza-Espinosa, L., Manjarrez Masuda, E., Lugo-Ibarra, K. C., & Gómez-Treviño, E. (2014). A geochemical and 3D geometry geophysical survey to assess artificial groundwater recharge potential in the Pacific coast of Baja California, Mexico. *Environmental Earth Sciences*, 71(8), 3477-3490.
- Davis, J. M., Baxter, C. V., Minshall, G. W., Olson, N. F., Tang, C., & Crosby, B. T. (2013). Climate-induced shift in hydrological regime alters basal resource dynamics in a wilderness river ecosystem. *Freshwater Biology*, 58(2), 306–319.
- Day, D. (1978). Drainage density changes during rainfall. *Earth Surface Processes & Landforms*, 3, 319–326.
- Day, D. G. (1983). Drainage density variability and drainage basin outputs (New South Wales, Australia). *Journal of Hydrology: New Zealand*, 22, 3–17.
- Dingler, C. M., & Breckenridge, R. M. (1982). Glacial Reconnaissance of the Selway Bitterroot Wilderness Area, Idaho. In Bonnicksen, B., & Breckenridge, R. M. (eds.), *Cenozoic Geology of Idaho* (645 – 652). Moscow, Idaho: Idaho Bureau of Mines and Geology.

- Evenson, E. B., Cotter, J. F. P., & Clinch, J. M. (1982). Glaciation of the Pioneer Mountains: A Proposed Model for Idaho. In Bonnicksen, B., & Breckenridge, R. M. (eds.), *Cenozoic Geology of Idaho* (645 – 652). Moscow, Idaho: Idaho Bureau of Mines and Geology.
- Freer, J., J. J. McDonnell, K. J. Beven, N. E. Peters, D. A. Burns, R. P. Hooper, B. Aulenbach, and C. Kendall (2002). The role of bedrock topography on subsurface storm flow. *Water Resource Research*, 38(12), 1269.
- Gabrielli, C. P., McDonnell, J. J., & Jarvis, W. T. (2012). The role of bedrock groundwater in rainfall-runoff response at hillslope and catchment scales. *Journal of Hydrology*, 450-451, 117–133.
- Gannon, J., Bailey, S., & McGuire, K. (2014). Organizing groundwater regimes and response thresholds by soils: a framework for understanding runoff generation in a headwater catchment. *Water Resources Research*, 8403–8419.
- Godsey, S. E., & Kirchner, J. W. (2014). Dynamic, discontinuous stream networks: hydrologically driven variations in active drainage density, flowing channels and stream order. *Hydrological Processes*, 28(23), 5791–5803.
- Goyal, M. K., Madramootoo, C. A., & Richards, J. F. (2015) Simulation of the Streamflow for the Rio Nuevo Watershed of Jamaica for Use in Agriculture Water Scarcity Planning. *Journal of Irrigation and Drainage Engineering*, 141(3).
- Gregory, K. J., & Walling, D. E. (1968). The Variation of Drainage Density within a Catchment. *International Association of Scientific Hydrology Bulletin*, 13(2), 61–68.
- Hinckley, E.L. S., Ebel, B. A., Barnes, R. T., Anderson, R. S., Williams, M. W., & Anderson, S. P. (2014). Aspect control of water movement on hillslopes near the rain-snow transition of the Colorado Front Range. *Hydrological Processes*, 28(1), 74–85.
- Jaeger, K. L., Olden, J. D., & Pelland, N. A. (2014). Climate change poised to threaten hydrologic connectivity and endemic fishes in dryland streams. *Proceedings of the National Academy of Sciences of the United States of America*, 1–6.
- Kirchner, J. W. (2009). Catchments as simple dynamical systems: Catchment characterization, rainfall-runoff modeling, and doing hydrology backward. *Water Resources Research*, 45(2), 1–34.
- Kirchner, J. W., Finkel, R. C., Riebe, C. S., Granger, D. E., Clayton, J. L., King, J. G., & Megahan, W. F. (2001). Mountain erosion over 10 yr, 10 ky, and 10 my time scales. *Geology*, 29(7), 591-594.
- Knowles, N., Dettinger, M., & Cayan, D. (2006). Trends in snowfall versus rainfall in the western United States. *Journal of Climate*, 4545–4560.
- Leopold LB, Wolman MG, Miller JP. (1964). *Fluvial processes in geomorphology*. W.H. Freeman and Company: San Francisco; 522.
- Lifton, Z. M., Thackray, G. D., Van Kirk, R., & Glenn, N. F. (2009). Influence of rock strength on the valley morphometry of Big Creek, central Idaho, USA. *Geomorphology*, 111(3-4), 173–181.
- Link, P. K., Crosby, B. T., Lifton, Z. M., Eversole, E. A., & Rittenour, T. M. (2014). The late Pleistocene (17 ka) Soldier Bar landslide and Big Creek Lake , Frank Church

- River of No Return Wilderness , central Idaho, U.S.A. *Rocky Mountain Geology*, 4(1), 17–31.
- Liu, F., Hunsaker, C., & Bales, R. C. (2013). Controls of streamflow generation in small catchments across the snow-rain transition in the Southern Sierra Nevada, California. *Hydrological Processes*, 27(14), 1959–1972.
- Lundeen, K. A., (2001). Refined late Pleistocene glacial chronology for the eastern Sawtooth Mountains, central Idaho, [M.S. thesis], Idaho State University, 58.
- Manning, A. H., Clark, J. F., Diaz, S. H., Rademacher, L. K., Earman, S., & Niel Plummer, L. (2012). Evolution of groundwater age in a mountain watershed over a period of thirteen years. *Journal of Hydrology*, 460-461, 13–28.
- McNamara, J. P., Tetzlaff, D., Bishop, K., Soulsby, C., Seyfried, M., Peters, N. E., & Hooper, R. (2011). Storage as a Metric of Catchment Comparison. *Hydrological Processes*, 25(21), 3364–3371.
- Meyer, G.A., & Leidecker, M.E. (1999). Fluvial Terraces along the Middle fork Salmon River, Idaho, and their Relation to Glaciation, Landslide Dams, and Incision Rates: A Preliminary Analysis and River-mile Guide: A preliminary analysis and river-mile guide. In Hughes, S.S., and Thackray, G.D., (eds.), *Guidebook to the Geology of Eastern Idaho: Pocatello, Idaho Museum of Natural History*, 219-235.
- Mueller, M. H., Alaoui, A., Kuells, C., Leistert, H., Meusburger, K., Stumpp, C., Weiler, M., & Alewell, C. (2014). Tracking water pathways in steep hillslopes by  $\delta^{18}\text{O}$  depth profiles of soil water. *Journal of Hydrology*, 519, 340–352.
- Rademacher, L. K., Clark, J. F., Clow, D. W., & Hudson, G. B. (2005). Old groundwater influence on stream hydrochemistry and catchment response times in a small Sierra Nevada catchment: Sagehen Creek, California. *Water Resources Research*, 41(2), 1–10.
- Roberts, M.C., & Archibold, O.W. (1978). Variation of drainage density in a small British Columbia watershed. *AWRA Water Resources Bulletin* 14(2), 470–476.
- Roberts, M., & Klingeman, P. (1972). The relationship between drainage net fluctuation and discharge. International Geography, Proceedings of the 22nd International Geographical Congress, Canada, Adams and Helleiner (eds.), University of Toronto Press, 189–191.
- Stewart, D. E., Lewis, R. S., Stewart, E. D., & Link, P. K. (2013). *Geologic map of the central and lower Big Creek drainage, central Idaho*: Idaho Geological Survey Digital Web Map, scale 1:75,000.
- Stewart, I., Cayan, D., & Dettinger, M. (2004). Changes in snowmelt runoff timing in Western North America under a “business as usual” climate change scenario. *Climatic Change*, 217–232.
- Sweetkind, D.S., & Blackwell, D.D. (1989). Fission-track evidence of the Cenozoic thermal history of the Idaho Batholith. *Tectonophysics*, 157, 241 – 250.
- Tague, C., & Grant, G. E. (2009). Groundwater dynamics mediate low-flow response to global warming in snow-dominated alpine regions. *Water Resources Research*, 45(7), 1–12.
- Tennant, C. J. (2011). *The Influence of Precipitation Phase on Hydrograph Form : An Investigation of Twelve Tributaries to the Salmon River, Idaho*. Idaho State University.

- Tennant, C. J., Crosby, B. T., & Godsey, S. E. (2014). Elevation-dependent responses of streamflow to climate warming. *Hydrological Processes*, 29(2015), 991-1001.
- Thackray, G. D., Lundeen, K.A., & Borgert, J. A. (2004). Latest Pleistocene alpine glacier advances in the Sawtooth Mountains, Idaho, USA: Reflections of midlatitude moisture transport at the close of the last glaciation. *Geology*, 32(3), 225.
- Tromp-Van Meerveld, H. J., & McDonnell, J. J. (2006). Threshold relations in subsurface stormflow: 2. The fill and spill hypothesis. *Water Resources Research*, 42(2).
- U.S. Geological Survey (U.S.G.S), 2014, The StreamStats program for Idaho, online at <http://water.usgs.gov/osw/streamstats/idaho.html>.
- Wagner, M. J., Bladon, K. D., Silins, U., Williams, C. H. S., Martens, A. M., Boon, S., MacDonald, R. J., Stone, M., Emelko, M. B., & Anderson, A. (2014). Catchment-scale stream temperature response to land disturbance by wildfire governed by surface-subsurface energy exchange and atmospheric controls. *Journal of Hydrology*, 517, 328–338.
- Weis, P. L., Schmitt, L. J. J., & Tuckey, E. T. (1972). *Mineral Resources of the Salmon River Breaks Primitive Area, Idaho: 1353-C*. U. S. Geological Survey, Washington, D.C.
- Zimmer, M. A., Bailey, S. W., McGuire, K. J., & Bullen, T. D. (2013). Fine scale variations of surface water chemistry in an ephemeral to perennial drainage network. *Hydrological Processes*, 27(24), 3438–3451.

## **Chapter 4    Conclusions**

### **4.1    Summary of Thesis Work**

#### **4.1.1    Sap Flow Across the Snow-Rain Transition**

We sought to determine transpiration characteristics along a transect crossing the snow-rain transition using Granier sap flow sensors, and to explain the potential controls of observed transpiration using atmospheric and soil moisture data. We expected the differences in snow accumulation and timing of melt across this transect to result in differences in transpiration. Instead, we observed consistent sap flow patterns across all elevations. Sap flow peaked in early June and reached its minimum at the end of the study period in November. We observed correlations between sap flow and vapor pressure deficit (VPD) on short hourly-scales, and daily peak sap flows corresponded with shallow soil moisture data. The sap flow and VPD relationship throughout the spring and summer was bimodal across all elevations. In early July, sap flow responsiveness to changes in VPD markedly dropped, likely due to decreasing water availability as indicated by soil moisture data. We were surprised that this change in responsiveness occurred at approximately the same time across all elevations. Although snow quantity and melt timing differed across the transect, late spring rain events maintained similar soil moisture conditions at all elevations upon the onset of drier summer weather.

When occasional summer rain events temporarily ceased in early September, we observed differences in sap flow relationships between individual sites (e.g., sap flow at the snow-dominated site versus rain-dominated site) due to relative changes in water availability for transpiration between the sites. The observed change in sap flow



relationships between sites suggests water availability dropped the most at the mixed-precipitation site and least at the snow-dominated site during the 21-day rain-free period in September. We initially expected water availability would increase with elevation; however, the mixed precipitation site may have less access to water due to there being smaller trees at this site, which typically have less extensive and deep root networks. Orographic enhancement of precipitation was likely greater at the highest site (i.e., snow-dominated site). The rain-dominated site was much closer to the valley bottom and may have sustained transpiration via root access to deeper, more consistent water sources.

Water limitations dictated transpiration across all elevations. Occasional rains maintained shallow soil water across the watershed accounting for similar transpiration patterns in the spring and summer. When rains ceased, differences in rooting and site characteristics resulted in changes in water limitations. Therefore, we did not observe differences in Douglas fir transpiration at different elevations due to differences in snowpacks and melt timing.

#### **4.1.2 Active Drainage Network Summer Recession Dynamics**

We mapped the active drainage networks of four steep, semi-arid, mountain catchments in central Idaho during receding spring and summer flows as a way of observing catchment storage characteristics. We determined that the extent of active drainage networks of the lower Big Creek tributaries is less responsive to changes in discharge than at many other locations. Downstream flowhead migration accounted for less than half of the changes in the length of the active drainage network. The extremities of the active drainage network were predominantly anchored by springs. Flowheads with large accumulation areas during the first survey in May were likely to be stable due to

slow deep flowpaths. Many flowheads with small accumulation areas in May were also stable. Some of these stable flowheads were located on planar hillslopes, where one would normally expect to find ephemeral flowpaths because the landscape is not converging. Some flowpaths did not correspond with surficial topography, and we identified possible bedrock features controls that were not reflected by surface topography. The influence of slow and deep flow paths on active drainage networks was also apparent in the summer low flow period of Pioneer Creek. Starting in late June, a low flow recession, interrupted occasionally by summer storm events, dominated the hydrograph. Thus, we studied the influence of both long bedrock flowpaths, and climate and snow accumulation on active drainage networks.

Snowmelt controlled the observed active drainage network dynamics at high elevations where the most substantial snowpacks developed. Flowheads on high-elevation, south-facing slopes were typically less stable than flowheads on north-facing slopes, potentially due to thin, fast draining soil/regolith layers. Glacial geomorphology on the high-elevation north-facing slopes of Pioneer watershed resulted in stable flowheads at or downslope of potential moraine deposits. High-elevation north-facing slopes of Cougar watershed had stable flowheads, which we attributed to high rates of weathering and associated soil/regolith layers capable of storing melt waters.

The spatial distribution of flowhead stability across different topographic, geomorphic and geologic settings suggested two main flowpath controls on the stream network: a shallow, variably saturated layer and underlying fractured bedrock. As discussed in Section 3.1, the interpretation of field-mapped active drainage networks can help test and develop streamflow and catchment water balance models used to predict

and explain streamflow characteristics. For example, a model with a single storage-discharge relationship (e.g., Kirchner, 2009) may not be ideal for the watersheds studied here. Additionally, the general stability of the active drainage networks and observed discontinuities did not support the geomorphologic origins of streamflow recession proposed by Biswal and Marani (2010). Instead, efforts to model the streamflow of the lower Big Creek tributaries should account for the two primary flowpath controls described above.

#### **4.2 The Relationship between Trees and Streams**

The influence of transpiration on streamflow is evident from diel cycles of streamflow (e.g., Mutzner *et al.*, 2015; Graham *et al.*, 2013). Several models also include linkages between transpiration and streamflow (e.g., Godsey *et al.*, 2013; Lundquist and Loheide, 2011; Tague *et al.*, 2009). By monitoring sap flow along a transect of the western ridge of Pioneer watershed and mapping the active drainage network, we sought to quantify a relationship between the spatial distribution of transpiration and spatial distribution of streamflow (i.e., the active drainage network) throughout the spring and summer 2014. We surveyed the active drainage network surveys of four lower Big Creek tributaries from late May to early August. During this period, we recognized similarities in sap flow patterns across all elevations, and observed primarily stable active drainage networks with many stable flowheads despite changes in discharge. Therefore, we do not have strong evidence suggesting an influence between the observed spatial distributions of transpiration and streamflow extent.

Despite the stability of the network, observed significant temporal correlations between peak daily sap flow and Pioneer Creek discharge were found following the rapid

recession of streamflow in May and June ( $R^2 = 0.32, 0.66, \text{ and } 0.65$ ;  $p < 0.0001$  at the snow, mixed, and rain-dominated sites, respectively) (Figure 4.1 and Figure 4.2). The strong positive relationships between sap flow and discharge starting on 6/25/14 indicated water limitations to transpiration. Catchment-wide drying conditions following snowmelt led to both decreasing streamflow as well as decreasing sap flow. The beginning of low flow conditions on 6/25/2014 occurred just before the sharp decrease in sap flow sensitivity to changes in VPD on 7/1/2014 (discussed extensively in Chapter 2). Thus, the timing of water-limited conditions represented by a stronger sap flow and streamflow relationship corresponded with the timing of a shift in the sap flow – VPD relationship.

When we focused on low flow conditions from the end of June to the end of the study period in November (Figure 4.1B), we distinguished three periods with different sap flow and streamflow relationships: 6/25 to 8/5, 8/26 to 9/29, and 9/29 to 11/23/2014 (Figure 4.1 B and Figure 4.2 D, E and F). Sap flow correlated significantly with streamflow during the first two periods ( $R^2 > 0.6, p < 0.0001$ ), while they were decoupled during the third period ( $R^2 < 0.01, p > 0.5$ ). Precipitation increased and temperatures decreased at the start of the third period, which is consistent with energy-limited transpiration. The first two periods coincided with recessions in stream and sap flow following large precipitation events during the middle of June and August. These large precipitation events led to elevated streamflows and sap flow; however, the difference in the slope of streamflow-sap flow relationships following the two events suggests large precipitation events are able to restore water availability for sap flow more effectively than restore water sources for streamflow. Thus, sources of water contributing to

transpiration may be different than those for streamflow (e.g., Brooks *et al.*, 2010). Sap flow at the snow-dominated site was less strongly correlated with streamflow than at the mixed precipitation and rain-dominated site during the first two periods (Figure 4.2 D, E and F). Lower VPD values and more energy-limited conditions at the snow-dominated site influenced transpiration.

The correlations between sap flow and streamflow provide limited evidence of the influence of transpiration on streamflow. Both Douglas fir transpiration and streamflow react to water inputs from precipitation events, but what controls the partitioning of water between transpiration and streamflow? Given small intermittent snowpacks and little transpiration during the autumn and winter, Brooks *et al.* (2010) showed that autumn rains refill small pore spaces in soils which trees then access during the spring, following the primary drainage of winter precipitation. Infiltrating snowmelt and winter precipitation do not mix with the small pore spaces filled by autumn rains; instead, winter precipitation leads to a short period of flow through large pores and preferential flow paths, which contributes heavily to streamflow, but not transpiration (Brooks *et al.*, 2010). Based on this conceptual model, by Brooks *et al.* (2010), trees should not influence streamflow if transpiration does not occur during periods of preferential lateral flow of in the root zone. However, we observed peak transpiration corresponding with peak streamflow (Figure 4.1A), and thus it is likely that the trees studied here utilize mobile water during snowmelt. Once translatory flow has ceased in the unsaturated zone, transpiration depletes the remaining tightly bound pore water as suggested by Brooks *et al.* (2010) and modeled catchment transpiration by Emanuel *et al.* (2010). These small, connected, pore spaces with the lowest water potential should be the first to refill during

the next precipitation event, and thus transpiration can indirectly result in reduced contributions to streamflow. This is consistent with studies showing the influence of antecedent soil moisture conditions influencing streamflow (e.g., Brocca *et al.*, 2012; Aubert *et al.*, 2003). In section 4.3, we will discuss future possibilities for determining the influence of transpiration on streamflow.

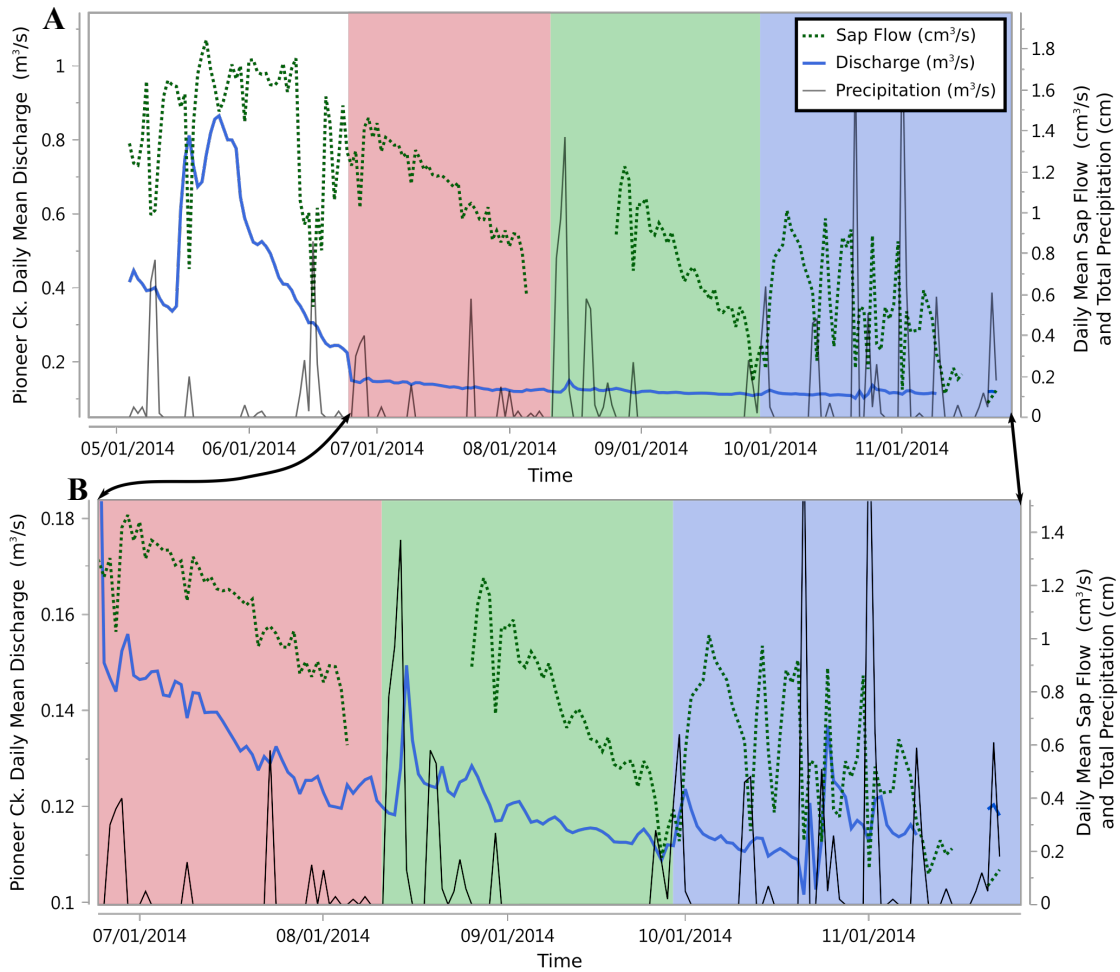


Figure 4.1: (A) Daily sap flow and stream discharge exhibited generally similar seasonal patterns with peak values in May. Background colors correspond with the data points and relationships in Figure 4.2 D, E and F. (B) The same discharge, sap flow, and precipitation time series for the post 6/24/2014 snowmelt period only. Here similarities in streamflow and sap flow recession following precipitation events in the middle of June (red zone) and August (green zone) are evident. After the end of September (blue zone) precipitation events increased, and streamflow and sap flow no longer exhibited similar recession characteristics.

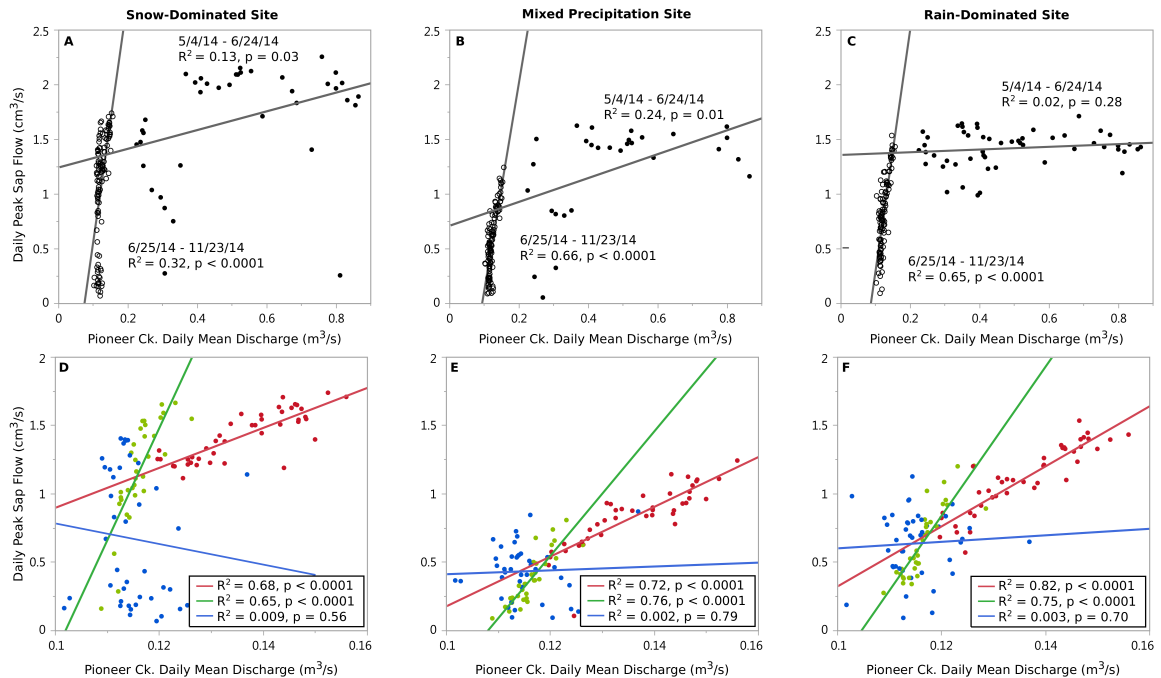


Figure 4.2: (A, B, and C) Daily peak sap flow at each elevation band is plotted against daily mean Pioneer Creek discharge. Daily sap flow correlated poorly with streamflow during the high flow period (open circles, prior to 6/25/14). Correlations improved markedly during low flow conditions following 6/24/14 (closed circles). (D, E, and F) These insets focus on the sap flow – streamflow relationships following 6/24/14 (closed symbols in A, B and C). The colors of the data points and best fit lines correspond with the background colors in Figure 4.1 A and B. The sap flow – streamflow correlations during spring melt recession period I (6/25/14 to 8/5/14 - red), and summer storm recession period II (8/26/14 to 9/29/14 - green), are the strongest, while there is very little correlation after the fall storm period III (9/29/14 to 11/23/14 - blue). The summer period two sap flow – streamflow relationship (green) is steeper than the spring melt relationship (red) because precipitation events increased transpiration more than streamflow during the summer.

### 4.3 Opportunities for Future Work

We measured Douglas fir sap flow, soil moisture, and VPD over an elevation gradient that crosses the snow-rain transition. Our results suggest that spring and summer rain events, instead of snowpack size and persistence control spatial patterns of soil moisture and thus transpiration. Controversy remains over whether trees and streams partition precipitation with little interaction between these fluxes. Thus, we need to know



the origins of plant water. Isotopic analyses of soil water and tree sap similar to those employed by Brooks *et al.* (2010) would provide valuable insight in our study area, where peak transpiration coincides with peak snowmelt and streamflow. Also a classification of soils and assessment of soil hydraulics in our study site would enable evaluation of the hypothesis that our sap flow sites maintained similar soil water availability during much of the study period.

Our study focused on the environmental, but not physiological, controls on transpiration patterns. Measuring water potentials and other plant hydraulic properties in leaves, branches, and trunks of trees across snowline may help explain how and why trees transpire similarly across the studied elevation transect (McDowell *et al.*, 2008).

We also chose to focus on Douglas fir. There are other tree and plant species transpiring throughout the watershed that may access different water sources at different times (Link *et al.*, 2014). Transpiration across snowline may depend more on the complete assemblage of species than Douglas fir alone, which could be tested via a network of eddy covariance towers added across an elevation gradient. These towers integrate the effects of multiple species (e.g., Goulden and Bales, 2014; Goulden *et al.*, 2012). Larger scale transpiration measurements may be better suited for determining the effect of transpiration on streamflow.

Determining the susceptibility of streamflow to changes in transpiration also depends on catchment flow and storage characteristics that likely extend beyond the root zone. Our survey of the active drainage network emphasizes a more complex reality than is often represented in models (e.g., Biswal and Marani, 2010; Kirchner 2009). Based on variations in flowhead stability with observed geomorphic characteristics, we suggest that

deep, bedrock flowpaths in addition to shallow, ephemeral melt flow are important. Isotopic analyses, similar to that of Mueller *et al.* (2014) and Liu *et al.* (2013), of flowhead water from different elevations and different spatial stabilities would identify the length and rate of flowpaths supporting surface flow. Also, geophysical mapping, like that of Daesslé *et al.* (2014) and Bièvre *et al.* (2012), upslope of flowheads could provide imagery of bedrock topography and structure. An improved understanding of the spatial distribution of flowpaths supporting streamflow remains important for determining the effects of increasing rainfall instead of snowmelt on both transpiration and streamflow.

## References

- Aubert, D., Loumagne, C., & Oudin, L. (2003). Sequential assimilation of soil moisture and streamflow data in a conceptual rainfall - Runoff model. *Journal of Hydrology*, 280(1-4), 145–161.
- Bièvre, G., Jongmans, D., Winiarski, T., & Zumbo, V. (2012). Application of geophysical measurements for assessing the role of fissures in water infiltration within a clay landslide (Trièves area, French Alps). *Hydrological Processes*, 26(14), 2128–2142.
- Biswal, B., & Marani, M. (2010). Geomorphological origin of recession curves. *Geophysical Research Letters*, 37(24).
- Brocca, L., Moramarco, T., Melone, F., Wagner, W., Hasenauer, S., & Hahn, S. (2012). Assimilation of surface- and root-zone ASCAT soil moisture products into rainfall-runoff modeling. *IEEE Transactions on Geoscience and Remote Sensing*, 50(7 PART1), 2542-2555.
- Brooks, J.R., Barnard, H. R., Coulombe, R., & McDonnell, J. J. (2010). Ecohydrologic separation of water between trees and streams in a Mediterranean climate. *Nature Geoscience*, 2, 100-104.
- Daesslé, L. W., Pérez-Flores, M. A., Serrano-Ortiz, J., Mendoza-Espinosa, L., Manjarrez Masuda, E., Lugo-Ibarra, K. C., & Gómez-Treviño, E. (2014). A geochemical and 3D geometry geophysical survey to assess artificial groundwater recharge potential in the Pacific coast of Baja California, Mexico. *Environmental Earth Sciences*, 71(8), 3477 -3490.
- Emanuel, R. E., Epstein, H. E., McGlynn, B. L., Welsch, D. L., Muth, D. J., & D’Odorico, P. (2010). Spatial and temporal controls on watershed ecohydrology in the northern Rocky Mountains. *Water Resources Research*, 46, 1–14.
- Godsey, S. E., Kirchner, J. W., & Tague, C. L. (2013). Effects of changes in winter snowpacks on summer low flows: case studies in the Sierra Nevada, California, USA. *Hydrological Processes*, 28(19), 5048-5064.
- Goulden, M. L., Anderson, R. G., Bales, R. C., Kelly, A. E., Meadows, M., & Winston, G. C. (2012). Evapotranspiration along an elevation gradient in California’s Sierra Nevada. *Journal of Geophysical Research: Biogeosciences*, 117(3).
- Goulden, M. L., & Bales, R. C. (2014). Mountain runoff vulnerability to increased evapotranspiration with vegetation expansion. *Proceedings of the National Academy of Sciences*.
- Graham, C. B., Barnard, H. R., Kavanagh, K. L., & McNamara, J. P. (2013). Catchment scale controls the temporal connection of transpiration and diel fluctuations in streamflow. *Hydrological Processes*, 27(18), 2541–2556.
- Granier, A. (1985). Une nouvelle méthode pour la mesure du flux de sève brute dans le tronc des arbres. *Annales des Sciences Forestières*.
- Kirchner, J. W. (2009). Catchments as simple dynamical systems: Catchment characterization, rainfall-runoff modeling, and doing hydrology backward. *Water Resources Research*, 45(2), 1–34.
- Liu, F., Hunsaker, C., & Bales, R. C. (2013). Controls of streamflow generation in small catchments across the snow-rain transition in the Southern Sierra Nevada, California. *Hydrological Processes*, 27(14), 1959–1972.

- Lundquist, J. D., & Loheide, S. P. (2011). How evaporative water losses vary between wet and dry water years as a function of elevation in the Sierra Nevada, California, and critical factors for modeling. *Water Resources Research*, *47*, 1–13.
- McDowell, N., White, S., & Pockman, W. (2008). Transpiration and stomatal conductance across a steep climate gradient in the southern Rocky Mountains. *Ecohydrology*, *204*, 193–204.
- Mueller, M. H., Alaoui, A., Kuells, C., Leistert, H., Meusbürger, K., Stumpp, C., Weiler, M., & Alewell, C. (2014). Tracking water pathways in steep hillslopes by  $\delta^{18}\text{O}$  depth profiles of soil water. *Journal of Hydrology*, *519*, 340–352.
- Mutzner, R., Weijs, S. V., Tarolli, P., Calaf, M., Oldroyd, H. J., & Parlange, M. B. (2015). Controls on the diurnal streamflow cycles in two subbasins of an alpine headwater catchment. *Water Resources Research*, *51*(5), 3403–3418.
- Tague, C., & Grant, G. E. (2009). Groundwater dynamics mediate low-flow response to global warming in snow-dominated alpine regions. *Water Resources Research*, *45*(7), 1–12.

## **Appendix A Suggestions for Similar Research**

### **A.1 Quantifying Transpiration with Sap Flow**

The dual-probe sap heat dissipation sap flow sensors (Granier, 1985) that I used to quantify transpiration are inexpensive, but time-consuming to construct. The construction process involves preparing and connecting very small wires. I summarize the approach I used in the assembly protocol included in Appendix B. However, it is far easier to build one or two sensors with someone who knows the process already and can demonstrate some of the more obscure techniques. While it can be frustrating at times, the construction process is simple.

I measured sap flow in Douglas fir trees. There are also some tips to installing these sensors into Douglas fir trees. The sap flow sensors need to be installed in the sapwood of the tree, so one first needs to remove the bark surrounding the sapwood. This can be done initially with a very large drill bit or hatchet, but in order not to drill too far into the sapwood a pocketknife is useful for making the final cuts into the moist red wood that marks the outer layer of sapwood (in Douglas fir trees). If you follow the probe design outlined in Appendix B, use 3/32" drill bit to make a horizontal hole towards the center of the tree. Make sure the hole is clean by drilling for several seconds and reinserting the drill at least twice until it removes cleanly. When inserting the sensor make sure you apply pressure aligned with the orientation of the drilled hole, otherwise the sensor will easily snap. After inserting the sensors and connecting wires, make sure to support the wires so that they are not pulling down on the sap flow probes. If these wires are left unsupported, the sensors will eventually be pulled out of the tree.

Regardless of the wiring layout for a given sap flow site, do not forget to label all wire ends in the lab, this will save time and confusion in the field.

In the Frank Church Wilderness, I also learned that bears are attracted to and rip apart shiny objects, especially the reflective bubble wrap I used to insulate the sap flow sensors. I camouflaged this insulation in a coating of black landscaping fabric and no longer encountered bear issues. Although the black fabric might reduce the effectiveness of reflective insulation, it is a better alternative than frequently having to replace sensors and deal with resulting data gaps. Camouflaging your sap flow sites is a priority.

When designing the power supply for sap flow sites, it is best to double or triple both the power supply (solar panel wattage) and the power storage (batteries) that you expect to need. It may be initially painful carrying heavy batteries and solar panels to the sites, but this will prevent you from having to replace these batteries. Also, all batteries are not the same. Car batteries are designed to provide an initial burst of energy required to start the car, as opposed to supplying the constant supply of energy required to power the Granier probes. Marine batteries are best suited for this purpose.

If you are working on hillslopes and ridges in Big Creek watershed, purchase a good pair of adjustable trekking poles. Poles will distribute some of the effort of carrying 40 lb. batteries up steep slopes from your legs to your upper body, and most importantly, distribute the pounding on your knees when you are going downhill.

## **A.2 Measuring Stream Discharge**

Gaging the lower tributaries of Big Creek is fairly simple using a Flowtracker ADV. The stream cross-section transect should include about twenty 40-second velocity readings. In the small tributaries of lower Big Creek, you will often have to redo velocity

readings due to a number of possible errors, so plan on taking an hour to gage each stream. A small piece of ribbon or flagging sometimes help align the sensor parallel to flow and avoid angle errors. There are some issues with using the Flowtracker for gaging the lower Big Creek tributaries. During low flows of the smaller tributaries (Goat and Dunces Creeks), the Flowtracker sensor is barely submerged. Although dilution gaging might be more appropriate for the stream size, salt tracers are potentially problematic in a wilderness setting. Additionally, during the winter months many sections of the creeks are frozen over or the edges have a lining of thick ice preventing a complete transect of velocity readings. Therefore, while we typically use the Flowtracker for discharge measurements, it might be worth the effort of writing a permit allowing the use of salt-slug dilution gaging.

Discharge measurements accompany continuous pressure transducer readings in order to develop a rating curve and then a hydrograph. In order to form a good rating curve, discharge measurements throughout the range of possible flows is important with a constant cross-sectional area, so take advantage of the typically short high flow period. Also, download and quality check the pressure transducer data relatively frequently to make sure that the sensor is working properly.

The locations of the pressure transducer and discharge transects are already set for the lower Big Creek tributaries. These locations are purposefully camouflaged because of their proximity to the Big Creek trail. Take a tour with someone who can locate these transects easily if stream gaging the lower Big Creek tributaries is a part of your project.

### **A.3 Surface Network Mapping**

For surface network mapping, I used a Trimble GeoXH GPS with ArcPad software. I mapped surface flow in the field using three point shapefiles for start points, stop points, and notes. The attribute table within each shapefile included the following fields: object ID, date, time, and notes. This information was helpful for remembering certain locations and conditions associated with a given point, which assisted me when creating the active drainage network maps (i.e., connecting the dots). I also recommend taking pictures of these points while in the field. Before mapping, load a line shapefile with a simple stream network to provide some orientation and an idea of how your points align with the overall channel network.

The process of surface network mapping lower Big Creek tributaries primarily requires off-trail walking over steep and rugged terrain. Use trails whenever possible, sometimes trail networks are not mapped, so ask people who are familiar with the area. Unmarked and unmapped trails are especially prominent in Big Creek where packing and outfitting were more widespread before wilderness designation, but since then the Forest Service has not maintained these trails.

Even with a widespread network of trails, off-trail work is still necessary for reaching most locations of flow initiation and discontinuity. Often traveling via ridges is far easier than trudging through riparian brush or side-hilling the slopes immediately lining the streams, although getting to the water requires traveling in these more difficult areas. Recent wildfires have left a number of fallen snags in the Big Creek watershed, making mapping a steeplechase or gymnastic experience, and therefore you want to be traveling as light as possible. Carrying a small daypack with the GPS, essential layers,



printed and laminated map (batteries on the GPS can die), small first aid kit, multitool, headlamp, notebook and modest water reservoir is recommended. Depending on the location you may chose to carry a water filter or treatment system, however in the lower Big Creek tributaries the water is clean and has yet to cause any issues to my knowledge. Also, in steep terrain, such as that along Big Creek, use adjustable trekking poles. Poles will help save your knees so you can map more, and maintain your balance so you don't fall as much and injure yourself. Minimizing risk of injury is smart no matter the conditions, but when in the Frank Church Wilderness a twisted ankle can cause a major hassle. Therefore, sturdy hiking boots and an emergency plan are a must. I recommend carrying a SPOT Gen3 satellite tracker (or any newer model available) to communicate with an emergency response network. This device allowed me to tell friends, family, advisors, and TWRS managers that I was 'OK' on a regular basis, and also alert the necessary people if I needed help or faced an emergency.

Mapping the lower Big Creek tributaries involved backpacking for mapping the larger tributaries, Pioneer and Cougar Creeks, as quickly and efficiently as possible. For both Pioneer and Cougar Creeks, a trail provides approximately central access to these watersheds. I set a basecamp at the pseudo-central locations and branched my mapping efforts from this basecamp. Although I would sometimes retrace my steps, this seemed more efficient than spending several hours packing up my campsite and carrying a heavy load to a new location. I also sited my basecamp near water sources and avoided snags (dead standing trees). Many of the snags in lower Big Creek are old enough so they fall in both windy and calm conditions. You do not want to be underneath a toppling snag, especially while in a sleeping bag. This is also important to remember when mapping.

## Appendix B Granier-Style Thermal Dissipation Probes Assembly Protocol

Provided by Keith Reinhardt, August 2013. Revised by John Whiting, September 2014

Note: An assembly-line method works best when making these probes. Repeat each step so that several pieces are prepared for the following step.

### Needle Preparation:

#### Materials

- 19 G X 1 ½” stainless steel hypodermic needles
  - (Excel Brand from DixieEMS.com)
- Dremel tool with cutting disc
- Safety glasses

- 1) Mark needles at the 1 and 2 cm from the base of the metal.
- 2) Cut needles using a Dremel tool to 2 cm in length from the base of the metal needle.
  - a. Try to avoid cutting the needle too short by cutting the needle on the point-side of the 2 cm mark you made in step 1.
- 3) Using the Dremel tool, cut a slight notch or hole in the side of the needle at the 1 cm mark.
  - a. Do not cut the notch too deeply as this will weaken the needle.
  - b. Use an uncut needle to punch a hole if a thin section of metal remains after the initial notch is formed with the Dremel.
- 4) Using an uncut needle, clean out the cut needle so that there are no metal flakes in the needle or hanging on rough edges. Try to smoothen sharp or rough edges at the end of the needle.
  - a. It is far easier to insert wires into the needles if they are clean and smooth.
- 5) Puncture a hole in the plastic ‘hub’ of the needle using an uncut needle that is angled to the open end of the hub (i.e., NOT towards the needle-end).
  - a. This allows for air to escape when filling the hub with epoxy later on.
  - b. For heated probes, this hole also allows the heating wire to re-enter the hub.

- c. Angling the hole towards the hub outlet makes threading the heating wire MUCH easier.

### **Aluminum Sheath Preparation:**

#### Materials

- Aluminum tube, round 3/32" OD, 0.014 nominal wall
    - (Aluminum 3003 Seamless Round Tubing, 3/32" OD, 0.0658" ID, 0.014" Wall, 36" Length from Amazon.com)
  - Single edge razor blade
  - 1/16" drill bit
  - Dremel tool
- 1) Mark aluminum tubing at 22 mm intervals.
    - a. The extra length of the sheath ensures the complete protection of the hypodermic needle core of the probe.
  - 2) Score the tubing at the 22 mm interval markings by placing the razor edge on the mark and rolling with slight pressure on a flat surface.
    - a. This is far more efficient than using the Dremel to cut the tubing.
  - 3) Carefully snap the scored tubing at each 22 mm section.
  - 4) Sheaths for heated probes should include a small notch (~2 mm) at one end for the heater wire.
    - a. This keeps the heater wire from being sheared by the aluminum sheath when it is inserted into the tree.
  - 5) Using both the 1/16" drill bit and the Dremel tool with cutting disk (or other tip of preference), lightly clean out the inside of the sheath and smoothen any rough edges at the ends.
    - a. A smooth sheath is critical for easily inserting the heating probe into the sheath.

## Wire Preparation:

### Materials

- Copper-constantan thermocouple wire, 0.019x0.030" (0.48x0.76 mm)
  - (Omega TT-T-36 Insulated T/C Wire)
- Constantan heating wire 0.005" (0.12 mm) diameter
  - (Omega TFCC-005 PFA covered wire)
- 22-4 g shielded gray stranded security cable
  - Southwire 56910544 500' 22-4 Gray Security Cable
- Wire cutters/strippers
- Single edge razor blade
- Solder
- Soldering flux
- Super glue gel
- Multi-meter
- Paper towel

### Thermocouple Wire (2 per Granier Sensor)

- 1) Cut thermocouple wire (paired copper-constantan wire) in 22 cm lengths.
- 2) Strip the clear, red, and blue insulation from about 1 to 2 cm from each end of the wire exposing both the bare copper wire and more silvery constantan wire.
  - a. Striping these fine wires takes a bit of a skill. It is easiest to first remove the clear insulation by cutting lengthwise between the red and blue wires with a razor blade. Remove the red and blue insulation by nicking and scraping or flicking with the blade perpendicular to the length of the wire.
  - b. It is alright if 3 to 5 cm of wire are removed from the initial 22 cm section in the process of stripping the thermocouple wire.
  - c. With a steady hand, it is possible to remove the clear insulation with wire strippers.
  - d. Try not to nick the actual metal of the wire during this step as this will reduce the integrity of the wire.
- 3) Twist the bare wires of *ONLY ONE END* tightly, evenly, and completely down to the shielding or insulation.
  - a. Hold the red and blue wire in one hand between thumb and pointer finger and twist with the other thumb and pointer finger.
  - b. A tight twist is essential to a good soldered connection and easy insertion into the hypodermic needle.
- 4) Dip the twisted wires into soldering flux and solder
  - a. Only a light and even coating of flux is necessary.

- b. Soldering is easiest by forming a small bead of solder on the soldering iron tip and then brush the thermocouple junction (twisted end) through the molten bead.
  - c. There should only be a thin and even coating of solder over the twisted wires, especially closer to the shielding.
- 5) Wipe excess solder flux from the wires with a paper towel.
  - 6) Clip off the extra length of twisted thermocouple so that the soldered connection is as short as possible (aka. A nub).
    - a. Make sure the connection is smooth, so that it will be easy to insert into the needle shaft.
  - 7) Dip the exposed metal nub in super glue so that the metal is coated with a thin film.
    - a. Let super glue dry before moving on.
  - 8) Strip the clear plastic coating from the rest of the wire.
    - a. Lay the wire flat and use a razor blade to lightly and carefully cutting the plastic coating between red and blue wires lengthwise without nicking the inner wires.
    - b. Be especially careful to remove all clear plastic from around the soldered end especially.
  - 9) Using a multi-meter, verify that the circuit is completed between the copper and constantan wires via the soldered junction.
    - a. The resistance should be between 3 to 50 ohms.

#### Heater Wire (1 per Granier Sensor)

- 1) Cut single-stranded constantan wire in 52 cm lengths.
- 2) Strip about 1 cm of each end.
  - a. The resistance should be between 16 to 17 ohms.

#### Gray Shielded Cable (1 per Granier Sensor)

This wire is used to connect the heated and reference probes in the lab for more efficient installation in the field.

- 1) Mark ~40 cm lengths of cable
- 2) Cut 40 cm lengths.

- 3) Strip gray casing and shielding for ~ 5 cm from both ends.
  - a. A twisted bare metal wire and/or white hair-like material within the gray casing can be pulled on for easy and efficient stripping of the gray casing.
- 4) Strip ~ 1 cm from both ends of the now exposed green, white, black, and red wires.
  - a. Wire strippers are useful for this step.

## Probe Assembly:

### Materials

- Prepared needles
- Prepared aluminum sheaths
- Prepared thermocouple wires
- Prepared heater wires
- Super glue
- Epoxy (Elmer's Wood Glue)
- 3 mL syringe
- Thermal conductivity paste (super glue gel)
- Multi-meter
- Permanent marker
- Recommended: Computer and Excel

### Reference Probe

- 1) Insert the connected end of a thermocouple wire into the hub end of the needle until the soldered nub is visible in the notch in the needle shaft.
  - a. Sometimes it is easiest to insert the soldered end in via the hub end, and other times to insert the stripped ends into the needle tip one at a time. It doesn't matter which as long as the soldered connection ends up at the notch with the ends exiting via the plastic hub.
- 2) With the multi-meter verify again that there IS a connection between the two ends of the thermocouple.
  - a. If there is no connection, then remove the thermocouple and try with another.
- 3) With the multi-meter verify that there IS NOT a connection between the thermocouple wires and the metal of the needle shaft.
  - a. If there is a connection, then remove the thermocouple wire and re-apply super glue at the soldered junction. While that wire dries, try another thermocouple wire.
- 4) Add a drop or two of superglue inside the notch in the needle holding the thermocouple's soldered junction in place, and a drop at the end of the needle.
  - a. Be careful with this set-up and in choosing a drying location, as the superglue does not do a very good job of holding the thermocouple in place on its own.
  - b. Let superglue dry until moving to the next step.
- 5) Recheck the thermocouple connection, and lack of connection between thermocouple and needle shaft.

- 6) Fill the hub of the needle with epoxy (wood glue).
  - a. It is easiest, and less messy to insert the wood glue using a 3 mL syringe.
  - b. Insert needle-end in Styrofoam or cardboard allowing the epoxy to dry without spilling.
  - c. Let glue dry overnight before moving on.
- 7) Place an aluminum sheath over the needle shaft and apply super glue to both ends of the sheath.
  - a. Let glue dry before moving on.

### Heater Probe

- 1) Insert the heater wire.
- 2) Insert the thermocouple wire so that the soldered junction is visible at the notch.
  - a. This is sometimes difficult with the heater wire in place, and generally takes some trial and error. Inserting the thermocouple wire while pulling the heater wire can help.
  - b. Sometimes using an uncut needle is necessary to clear the needle shaft of remaining debris/rough edges.
  - c. Be careful not to scrape off the superglue coating from the soldered junction.
- 3) Position the heater wire so that the end extending from the hub is roughly even with the thermocouple ends or 3 cm long. The end extending from the needle should be several times longer allowing for a complete wrap around the needle shaft.
- 4) With the multi-meter verify that there IS NOT a connection between the thermocouple wires, or the heater wire, and the metal of the needle shaft.
  - a. If there is a connection then remove the thermocouple wire and re-apply super glue at the soldered junction. While that wire dries, try another thermocouple wire.
- 5) Add a drop or two of superglue inside the notch in the needle holding the thermocouple's soldered junction in place, and a drop at the end of the needle.
  - a. Be careful with this set-up and in choosing a drying location, as the superglue does not do a very good job of holding the thermocouple in place on its own.
  - b. Let superglue dry until moving to the next step.
- 6) Recheck the thermocouple connection, and lack of connection between thermocouple and needle shaft, and heater wire and the needle shaft.



- 7) Take the long end of the constantan heating wire extending from the tip of the heating probe and evenly and gently but firmly wrap the wire around the needle shaft down to the connection between the metal shaft and plastic hub. Then place the working end of the heater wire through the hole in the side of the plastic needle hub so the end extends out of the plastic hub with the other wires. Continue holding the assembly so that the heater wire does not unravel
  - a. No section of the heating wire should overlap itself, or the sheath will not fit.
  - b. There should be no spaces between coils of the heating wire.
  - c. Be careful not to nick the wire on the needle.
  
- 8) Holding the assembly from above so that the heater wire doesn't uncoil, apply superglue to the hole in the needle's plastic hub and at the end of the needle shaft, then insert the needle shaft into an aluminum sheath carefully rotating the sheath until it covers the whole needle shaft. Make sure the heater wire extends from beneath the aluminum sheath at the small notch in the sheath. Then apply super glue to the tip of the aluminum sheath and where the sheath approaches the plastic hub.
  - a. Let glue dry overnight before moving on.
  
- 9) Select a heated probe and mark on the hub with permanent marker an identification number.
  - a. It is best if this information is entered into an Excel spreadsheet that is designed to calculate the coil resistance.
  
- 10) Measure in centimeters the lengths of the more opaque red heater wire leads (single-strand constantan wire) extending from the heated probe needle shaft and out through the plastic hub. Enter this data into the spreadsheet.
  
- 11) Measure the total resistance (in ohms) of the heater wire of the heated probe with a multi-meter. Enter this data into the spreadsheet.
  
- 12) In the spreadsheet, calculate the resistance of the heater wire leads (step 10) by multiplying the length of the heater wire leads (cm) by 0.4 (ohms/cm).
  - a. The 0.4 ohms/cm constant may want to be confirmed with a multi-meter, although this is what has been used so far.
  
- 13) Also in the spreadsheet, calculate the heater wire coil resistance by subtracting the lead resistance (step 12) by the total resistance (step 11).
  - a. This is critical to know later in the field so that power requirements can be calculated.

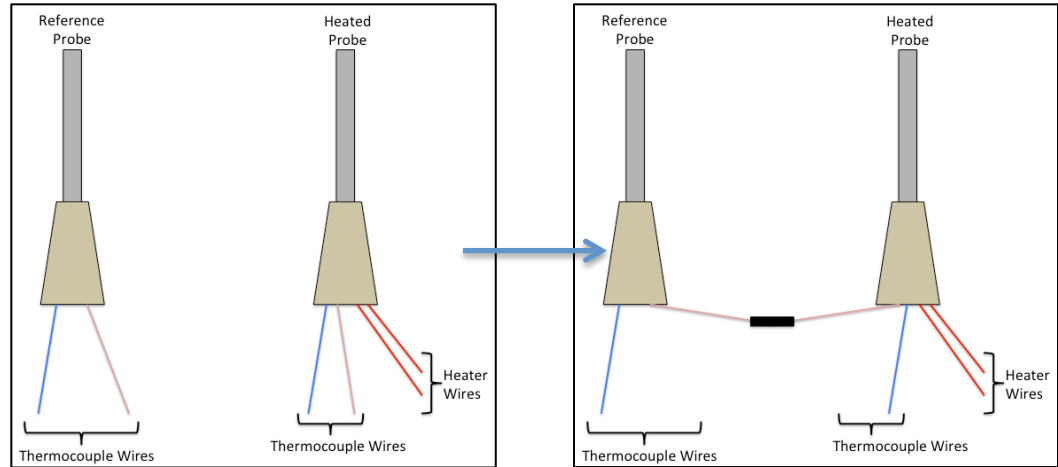
Example Spreadsheet Entry:

Sensor ID #	Rtotal (ohms)	lead length (cm)	Rcoil (ohms)
1	22.2	20.75	13.9

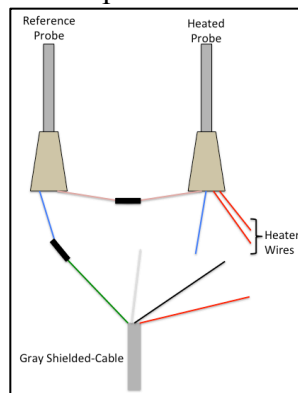
## Connecting the Heated and Reference Probes – Completing the Grainer Sensor

### Materials

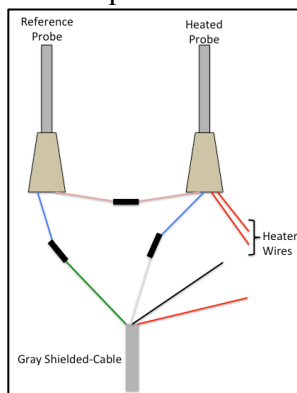
- Prepared gray shielded cable
  - Prepared reference probe
  - Prepared heated probe
  - Heat shrink
    - Buyheatshrink.com – Clear, 3:1 Ratio Polyolefin
      - 6 mm – (HS3-025-CL)
      - 9 mm – (HS3-0375-CL)
  - Electrical tape
  - Silicon gel
  - Permanent marker
  - White electric tape or duct tape
  - Quart plastic bag
- 1) Cut a length of the smaller heat shrink for a selected reference probe so that the heat shrink will cover about half of the plastic hub (covering the punctured hole in the hub) and leaves about 1.5 to 2 cm of thermocouple wire uncovered.
  - 2) Position the heat shrink as described above and shrink with a heat gun.
    - a. If the heat shrink does not fit snugly around the needle hub then create a more waterproof seal with the silicon glue after the heat shrink has cooled.
    - b. Let glue dry before moving on.
  - 3) Connect the red thermocouple wires of the heated and reference probes.
    - a. Connect wires tightly, evenly, and completely using the same twisting technique as used to prepare the thermocouple wire junction prior to soldering.
    - b. Once the wires are twisted together fold them back on one of the wires and wrap the connection with a small piece of electrical tape for insulation.



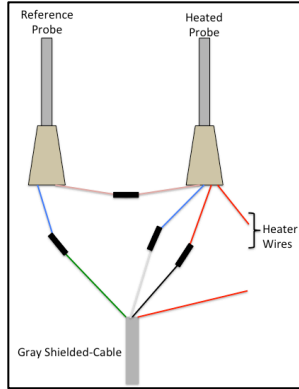
- 4) Connect the blue thermocouple wire from the reference probe to the green wire from the gray-shielded cable.
  - a. Use the previous connecting and insulating technique.



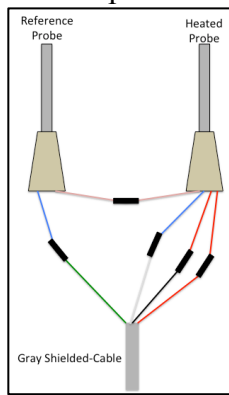
- 5) Connect the blue thermocouple wire from the heated probe to the white wire from the gray-shielded cable.
  - a. Use the previous connecting and insulating technique.



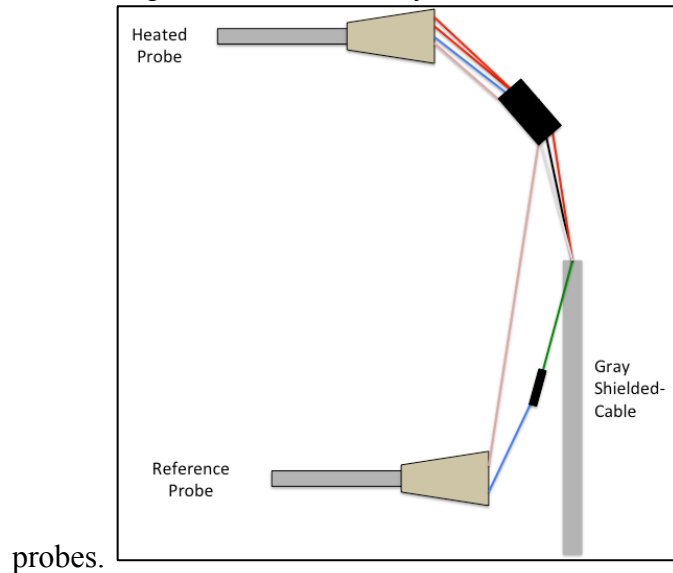
- 6) Connect one heater wire to the black wire from the gray-shielded cable.
  - a. Use the previous connecting and insulating technique.



- 7) Connect the remaining heater wire to the red wire from the gray-shielded cable.  
 a. Use the previous connecting and insulating technique.



- 8) The distance between the two red thermocouple wires determines the maximum length between the two probes. Extending the green wire as much as the red thermocouple wires comfortably allows maximizes the distance between the



- 9) Check the green to white, and red to black connections using a multi-meter.

- 10) Wrap the wires extending from the heated probe with some electrical tape.
- 11) Secure the very end of the heat shrink of the reference probe to the gray cable with electrical tape.
- 12) Mark the identification number of the heated probe somewhere on the gray cable that will not be covered by heat shrink.
- 13) Cut a section of the larger heat shrink so it will be long enough to cover at least half of the plastic hub of the heated probe and the tape securing the end of the reference probe heat shrink to the gray-cable.
- 14) Gently push the heated probe through the larger heat shrink and heat once in place.
  - a. Move on when heat shrink is cool.
- 15) Apply silicon glue to the both ends of the larger heat shrink filling any gaps that might permit moisture.
  - a. Allow glue to dry before moving on.
- 16) Using the identification number find the coil resistance of the complete sensor. Mark this number on the gray cable and on a tab of white tape ( $R_c = ??$  ohms).
- 17) Place the sensor in a small plastic bag marked with the coil resistance.
- 18) Sort bags by  $R_c$  because the sensors should be grouped by similar coil resistances for best results.